Interplay between LV Grids and EVs' Charging Flexibility

A Smart Charging Approach

F. Verbist

Master of Science Thesis

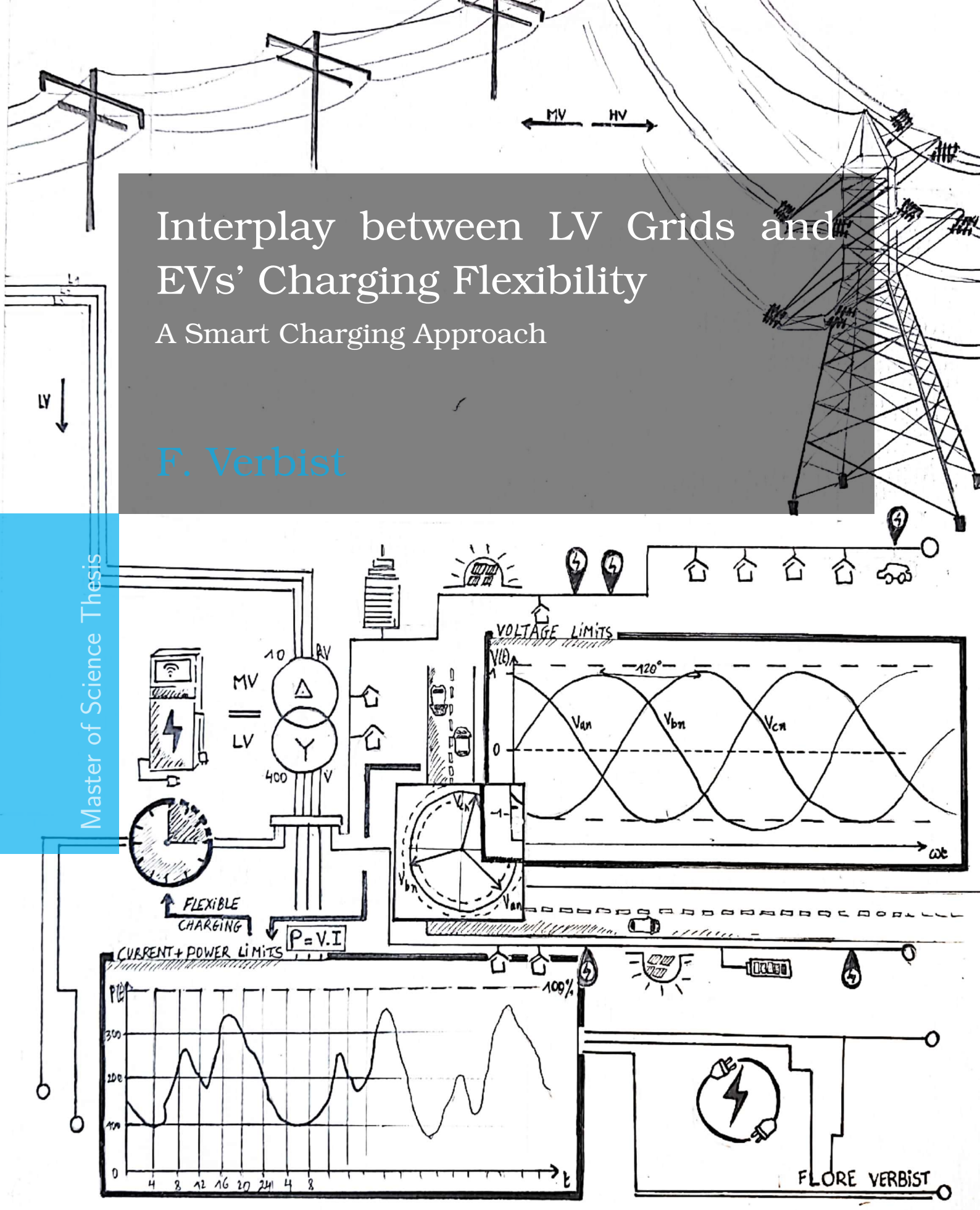

TU Delft Delft University of Technology

MSc Sustainable Energy Technology

Interplay between LV Grids and EVs' Charging Flexibility

A Smart Charging Approach

Master of Science Thesis

For the degree of Master of Science in Sustainable Energy Technology at Delft University of Technology

F. Verbist

July 19, 2022

Student number:	5369835
Project duration:	January 10, 2022 - July 27, 2022
Thesis committee:	Dr. P.P. (Pedro) Vergara Barrios - supervisor, EEMCS
	MSc. N.K. (Nanda) Panda - daily supervisor, EEMCS
	Dr.ir. JL (Jose) Rueda Torres - chair committee, EEMCS
	Dr. S. (Stefan) Pfenninger - committee member, TPM

Faculty of Electrical Engineering, Mathematics & Computer Science
Delft University of Technology

The work in this thesis was partly fulfilled in the context of the ROBUST project. For more information, visit their webpage at: https://tki-robust.nl/. ROBUST received funding from the *MOOI 2020* Top Sector Energy subsidy programme by the Ministry of Economic Affairs and Climate Policy, executed by the Netherlands Enterprise Agency.

" If there is any one secret of success, it lies in the ability to get the other person's point of view and see things from that person's angle as well as from your own."

— *H. Ford*

Samenvatting

De elektrificatie van alle sectoren is vandaag de dag onmisbaar om koolstofneutraliteit te bereiken tegen 2050. Wat mobiliteit betreft, streven veel landen in de wereld naar een emissievrij wagenpark door massaal in te zetten op elektrische voertuigen. Dit gaat echter gepaard met een aantal uitdagingen in verband met congestie- en spanningsproblemen in de elektriciteitsnetten als gevolg van een ontoereikende netcapaciteit. Wanneer de netversterking de toenemende vraag naar elektriciteit niet kan bijbenen, zowel qua planning als financiële middelen, moet een slimmere, efficiëntere oplossing het probleem verhelpen.

Dit proefschrift beoogt een optimale manier van flexibiliteitsverdeling uit te werken door het slim opladen van elektrische voertuigen in laagspanningsnetten. Op die manier kan netversterking tot het minimum worden herleid. De belangrijkste bijdrage van dit werk bestaat in de ontwikkeling van een slim, optimaal laadalgoritme dat tracht te voldoen aan de netbeperkingen, zoals spannings- en congestiegrenzen. Het werk van dit proefschrift heeft betrekking op een typisch stedelijk laagspanningsnet in Nederland.

Allereerst wordt het vereiste niveau van netversterking onderzocht door middel van het kwantificeren van de spannings- en congestieproblemen in het laagspanningsnet. Dit wordt gedaan door ongecontroleerde oplaadscenario's toe te passen tot 2050 voor zowel winter als zomer. Vanaf 2030 zou een versterking van de transformatoren moeten worden overwogen wanneer geen slimme heffingsmethodologie wordt toegepast. Congestie op de lijnen doet zich ook voor in 2030, maar wordt duidelijker in 2050 wanneer ook lokale congestie op de lijnen onafhankelijk van transformator overbelasting optreedt. Zonder slim laden zou dat een zorgvuldigere selectie van oplaadpunten en versterking van de stroomafwaartse lijnen vergen.

Na onderzoek van de ongecontroleerde scenario's werd de behoefte aan een optimale slimme laadstrategie duidelijk. Deze werd vervolgens ontwikkeld. Uit de resultaten bleek dat in 2050, 94.5% van de congestie op de lijnen en 100% van de transformatorcongestie en spanningsproblemen kunnen worden omzeild met slim laden alleen. Dit werd bereikt door de invoering van netbeperkingen op de meest kwetsbare plaatsen in het elektriciteitsnet. Bijgevolg kon de behoefte aan netversterking bijna volledig worden vermeden tot ten minste 2050.

Dit werk onderscheidt zich van andere studies door uitgebreid stil te staan bij de integratie van drie concepten: een nieuwe tariefstructuur, bidirectioneel laden en de noodzaak aan netbeperkingen in een slim laad model. Dit maakt het mogelijk de voordelen voor alle belanghebbenden samen te vatten, waaronder: de netbeheerder, de laadpaalbeheerder en de eigenaars van de elektrische wagen. De eindconclusie houdt in dat de integratie van deze drie concepten resulteert in één van de meest gunstige onderzochte strategieën voor alle drie de partijen tezamen.

Abstract

The electrification of all sectors is essential to achieve carbon neutrality by 2050. In terms of mobility, many nations around the globe envisage a zero-emission fleet resulting in a massive deployment of Electric Vehicles (EV). Nevertheless, this goes hand-in-hand with some challenges related to congestion and voltage problems in power grids caused by inadequate grid capacity. When grid reinforcement cannot keep up with the increasing demand for electricity, both in terms of planning and excessive financial means, smarter, more efficient solutions should solve the problem.

This thesis aims at providing an optimal strategy for consumers' flexibility distribution by smartly charging EVs in Low-Voltage (LV) grids. In that way, grid reinforcement should be reduced to a minimum. In order to do so, the main contribution of this work is covered by the development of a smart, optimal charging model that tries to comply with grid constraints including voltage and congestion boundaries. The work of this thesis relates to a typical urban LV grid in the Netherlands.

First of all, the required level of grid reinforcement is investigated by means of quantifying the voltage and congestion problems in the LV grid. This is done by applying uncontrolled charging scenarios up to 2050 for both winter and summer. The results showed that from 2030 onwards, transformer reinforcement would need to be considered when no smart charging methodology is applied. Line congestion occurs as well in 2030, but becomes more apparent in 2050 when also local congestion in the lines takes place independent of transformer congestion. Without smart charging that would involve a more careful selection of charging points and reinforcement of downstream lines.

After investigating the uncontrolled scenarios, the need for an optimal smart charging strategy became apparent. This was developed afterwards. The results showed that in 2050, 94.5% of line congestion and 100% of transformer congestion and voltage problems could be bypassed with smart charging only. This was achieved by implementing grid constraints at the most vulnerable locations in the power grid. Consequently, the need for grid reinforcement could be almost completely avoided till at least 2050.

Lastly, this work distinguishes itself from others by extensively reflecting on the integration of three concepts: a novel recently developed tariff structure [1], the effect of bidirectional charging, as well as the necessity for grid constraints. This allows summarising the benefits for all stakeholders including the Distribution System Operator (DSO), the Charge Point Operator (CPO) and EV owners. The final conclusion was made that including these three concepts results in one of the most favourable investigated strategies for all three parties together.

Table of Contents

Acknowledgements

It has been quite a journey doing my Master in Sustainable Energy Technology. During the corona period, I experienced a severe lack of motivation and challenges in my study. However, that turned 180 degrees while doing my master thesis. Overall, it has been a very smooth and positive experience that gave me a lot of motivation with only minor difficulties. Therefore, I want to express my gratitude to a variety of people.

First of all, I would like to thank my parents and my sister for their continuous support and willingness to listen during both positive, but also very difficult periods. Besides, I appreciate the faith they put into my work and me as a person, often much more than I did myself. The same holds for my dearest housemates, Patricija, Aurora and Paula. I am so grateful for the past two years in which they truly formed a new family to me sharing all kinds of common interests.

Secondly, I would like to express my deepest gratitude to my two supervisors, Prof. P.P. Vergara and N.K. Panda. They gave me the opportunity to chase my own ambitions and interests. Thank you both for your eye for detail and constructive and valuable feedback. In addition, thanks for always sharing an honest opinion, for being clear and for not shying away my stubbornness. Besides, I would like to thank Prof. J.L. Rueda Torres and Prof. S. Pfenninger for completing my thesis committee.

Thirdly, my gratitude goes as well to the people from the ROBUST consortium, with special attention and admiration to Nico Brinkel from Utrecht University: thank you Nico for your valuable advice, continuous support and foremost, for sharing your genius ideas with me.

Lastly, my acknowledgements go to the numerous people from TU Delft that were willing to talk with me before and during my thesis about different interesting concepts and research projects. Especially, thanks to the study advisor to say: 'Go.For.It!'. So indeed, let's go for it...

Enjoy reading!

Delft, University of Technology F. Verbist
July 19, 2022

List of Figures

List of Tables

Glossary

List of Acronyms

AC	Alternating current
ACM	Authoriteit Consument en Markt
ADMM	Automated Direction Method of Multipliers
aFRR	Automatic Frequency Restoration Reserves
BEV	Battery Electric Vehicle
CPO	Charge Point Operator
DC	Direct current
DA	Day-Ahead
DSM	Demand Side Management
DER	Distributed Energy Resources
DG	Distributed Generators
DR	Demand Responsiveness
DSO	Distribution System Operator
EHV	Extra High-Voltage
EMS	Energy Management Systems
EN	European Norms
EV	Electric Vehicles
FCEV	Fuel-Cell Electric Vehicles
GA	Genetic Algorithm
GPLK	Gepanserd Papier Lood Kabels
HV	High-Voltage
ICE	internal combustion engines
IRENA	International Renewable ENergy Association
L	Lines
LT	Line of the Transformer
LV	Low-Voltage
MV	Medium-Voltage
MILP	Mixed-Integer Linear Programming
ML	Machine Learning
MPC	Model Predictive Control
NEDU	Dutch Energy Data Exchange
NREL	National Renewable Energy Laboratories
OBC	On-Board Charger
OPF	Optimal Power Flow
PEI	Power Electonic Interfaces
PF	Power Factor
PHEV	Plug-in Hybrid Electric Vehicles
PILC	Paper Insulated Lead-covered Cables
PSO	Particle-Swarm Optimisation
PV	Photovoltaics
p.u.	per-unit
RES	Renewable Energy Sources
RHO	Receding Horizon Optimisation
RMS	Root-Mean-Square

SOC	State Of Charge
s.t.	subject to
ST	Stacked Tariffs
T	Transformer
TOU	Time-Of-Use
TSO	Transmission System Operators
UFC	Ultra-Fast Charging
V1X	Unidirectional Charging
V2B	Vehicle-to-Building
V1G	Vehicle-on-Grid
V2G	Vehicle-to-Grid
V2H	Vehicle-to-Home
V2X	Vehicle-to-everything
X/R	Reactance/Resistance

List of Symbols

γ	Frequency of occurrence
γ_A	Absolute Concurrency
γ_R	Relative Concurrency
V_0	Nominal Voltage
$\mathrm{V}_{\mathsf{RMS}}$	RMS-Voltage
ρ_{L}	Penetration level
c/h	Fraction cars per household
n_{EV}	Total number of EVs
n_{hh}	Total number of households
Δ_{I_ϕ}	Current Error
$\mathsf{I}^{\mathsf{PF}}_{t,\phi}$	Phase current at time t and phase ϕ in PowerFactory

Remark: This list only contains the symbols that are used outside the optimisation algorithm. For the list of symbols related to the optimisation, please refer to Table 4-2.

Chapter 1

Introduction

The rise of Electric Vehicles (EV) in the present world is ubiquitous as many nations around the globe are setting out plans to move towards greener mobility. This forms an essential aspect of achieving the climate goals set out in the Paris Agreement. In order to stay below the agreed 2°C temperature rise, all nations are indicating their own targets in various sectors [12]. In the Netherlands, the objective is to reduce carbon emissions by 49% in 2030 and 95% by 2050, as imposed in its climate agreement of 2019. One-fifth of these emissions is currently related to road traffic. As a result, in terms of mobility, the objective towards 2030 is to ban the sale of passenger cars with internal combustion engines (ICE) and to commit to 100% emission-free cars. In 2050, the entire mobility fleet should be decarbonised using green electricity, green hydrogen, other renewable fuels (Power-to-X, e.g. NH3) and biofuels [13]. Certainly, with the emergence of renewable energy technologies like wind and solar energy, the switch to electric mobility is a logical step to take.

Nevertheless, these targets bring challenges on several fronts. When looking at electric vehicles, enough green electricity and charging stations must be available at all times. However, the rapid influx of EVs imposes also many challenges related to the electricity network, which should be examined in great detail. One may wonder if the current electricity grid can cope with a large influx of EVs. In that regard, smart charging strategies and grid reinforcement may be needed to alleviate risks and wear in the electricity network.

This study aims to quantify and locate bottlenecks in a typical Dutch Low-Voltage (LV) grid related to congestion and voltage problems. Afterwards, an optimal smart charging model is developed to mitigate these problems. The purpose of this research is to make full use of EVs' flexibility in order to deal with the perceived bottlenecks in a targeted way. This leads to the main intention to delay grid reinforcement as much as possible.

An introductory research overview is presented as follows. Section 1-1 provides an overview of the LV grid characteristics and requirements. Subsequently, trends of EVs and their implementation in the LV network are explained in Section 1-2. The research objectives and thesis outline can be found in Sections 1-3 and 1-4 respectively. Last but not least, this introductory chapter is finalised with the thesis contribution and motivation in Section 1-5.

1-1 The Dutch Low Voltage Network

1-1-1 Network Characteristics

It is essential to consider the network topology and related characteristics when studying the effect of EVs' charging on LV grids. The power grid topology in the Netherlands can be classified on a geographical scale (national-, regional-, local grid) or specified by voltage level (Extra High-Voltage (EHV), High-Voltage (HV), Medium-Voltage (MV) and LV level) [14]. An overview of the latter classification with its corresponding characteristics is provided in Table 1-1. This table indicates the vast amount of cables belonging to the LV network maintained and operated by the Distribution System Operator (DSO). The Transmission System Operators (TSO), Tennet, is in charge of the higher voltage levels [5]. As one can conclude from Table 1-1, the LV grid contains the largest amount of cables and connections in the Netherlands.

Table 1-1: Overview of the Dutch power grid [5].

	Operator	Voltage [kV]	Total Length [km]	Total Connections
Extra High Voltage (EHV)	TSO	220/380	± 2900	111
High Voltage (HV)	TSO/DSO	50/110/150	± 8800	136
Medium Voltage (MV)	DSO	3-5/6-12.5/20/25-30	± 105700	± 33 000
Low Voltage (LV)	DSO	0.4	± 441300	± 8 170 00

These LV networks mostly have a radial topology and connect many small consumers, mainly households (± 95%) and small businesses (± 5%) [15]. A radial topology eases the estimation of the power flow direction, especially with the introduction of distributed Photovoltaics (PV) and emerging bidirectional EVs. Nevertheless, some old Dutch LV grids can still have a meshed topology. These have better voltage management and lower power losses but are less safe when faults occur [16]. The latter is another reason to transform LV grids into a radial configuration involving less safety equipment.

1-1-2 LV Network Requirements

Electrification plays a significant role in enabling a sustainable energy transition. However, the implementation of many EVs, distributed PV and heat pumps puts pressure on the grid. At all times, the electricity network should provide adequacy of electricity, adequacy of grid capacity and compliance with power quality standards [17]. These three aspects are addressed below. EVs can exacerbate the pressure on all three criteria when charged in a conventional, uncontrolled way. Contrarily, smart charging using EVs as flexible assets should aim to mitigate these problems in the power grid.

First, looking at power adequacy, power should be available at any time. With increased penetration of electrical appliances such as EVs and the increased implementation of variable Renewable Energy Sources (RES), a continuous electricity supply with a reduced carbon content is less straightforward. Allowing affordable adequacy would require suitable storage solutions and consumer demand flexibility. When EVs are charged in a smart way, they can provide both storage and flexibility to the grid using unidirectional or bidirectional charging methods.

Besides adequacy of the energy commodity, also network congestion related to inadequate transmission and line capacity is an essential factor to consider in the electrification process. Electrification leads to higher currents

flowing through cables and transformers. This can lead to a violation of thermal limits when the maximum current rating of the infrastructure is reached. As a consequence, physical components of the power network can be damaged due to unacceptable temperature rises [17]. If the current exceeds its limits, the power losses will also increase, resulting in higher operational costs for the DSO. Grid reinforcement or reconfiguration can overcome these issues. Nevertheless, in practice, grid reinforcement is not always the most economically favoured and feasible option as this would lead to significant investments such as breaking up streets for new cables. Besides, also LV/MV transformers with a higher rated power up to 630 kVA are sometimes needed to be installed [16]. Measures to delay and reduce grid reinforcement include curtailment of PV inverters, storage solutions and Demand Side Management (DSM) [18]. The latter two measures again apply to smartly (dis)charging EVs by using their flexibility in an optimal way.

Lastly, the smart operation of EVs can improve the power quality in the LV network. Power quality standards are established to ensure electricity is of sufficient quality such that electronic equipment will not be damaged. When power quality standards on the LV level are violated, the DSO will call on the aggregators to supply ancillary services to restore the nominal operation conditions [19]. An overview of the power quality standards is provided in Table A-1, as included in Appendix A. The most critical voltage phenomena related to EVs are explained below (1-1-3).

1-1-3 Voltage Quality Standards

The voltage quality is the primary indicator of the power quality of the (LV) network. European Norms (EN) are developed to standardise and regulate the related power quality in the electricity grid. Country-specific alterations can be applied to the EN standards. In that case, one should speak of NEN-EN when specifying the Dutch standards [20]. The *EN 50160* applies to voltage characteristics in public electricity networks. This standard discusses both continuous voltage phenomena and voltage events. The former is mainly related to changes in the nominal voltage signal due to load patterns, non-linear loads or changes in loads. The latter is related to deviations from the desired voltage waveform due to unpredictable or external events such as faults and weather conditions. For the continuous phenomena, the limits related to each event are mostly quantified on a statistical basis. That means that the 10 minutes average $\mathrm{V_{RMS}}$ should stay bound for 95% of all measurements in a week.

According to the supply voltage standard, the voltage variation over the LV and MV part of the grid should stay between the limits of $\mathrm{V}_0 = 1 \pm 0.1$ [per-unit (p.u.)] with V_0 the nominal voltage. However, that is not always self-evident, certainly not at the end of the feeder lines. In general, with conventional distribution feeders (meaning low Distributed Energy Resources (DER)), the voltage at the end of the feeder line can drop significantly in distribution networks due to the line's internal resistance. Higher voltage drops are often perceived in sub-urban or rural areas compared to urban areas which use much shorter power cables [18]. Nevertheless, if the buses with the largest loads are located close to the MV/LV substation, the voltage drop at the end of the feeder will be less, due to a lower path resistance [21]. In contrast, with the integration of more DER such as PV, a voltage rise can also occur when a large amount of PV power is connected at the end of the feeder lines. This voltage rise is caused by active power injections and small Reactance/Resistance (X/R)-ratios of the PV power in LV feeders. Measures to (partly) mitigate voltage rises and drops include grid reinforcement, transformer tap change, demand-side management, energy storage, active power control and reactive power curtailment [22].

Another continuous voltage phenomenon that gains importance is harmonic distortion caused by non-linear loads such as the On-Board Charger (OBC) of EV. Harmonics can cause supplementary power losses or damage to electrical appliances due to overheating [23]. The reader is referred to Table A-1 for a schematic overview of all voltage phenomena in distribution grids.

1-2 Electric Vehicles: Burden or Blessing?

1-2-1 EV characteristics

Figure 1-1 displays the expected increase of EVs and charging points towards 2050 (ELAAD) [2]. As can be deducted from this graph, an exponential EV increase needs to occur till 2030, followed by a linear increase till 2050. That is due to the climate target to reach 100% EV sales by 2030 and a complete carbon neutral fleet by 2050 [13]. Likewise, also charging stations should increase. As can be concluded from Figure 1-1, this will occur at a rather logarithmic pace. Nevertheless, the Netherlands is currently leading in Europe in terms of the absolute amount of charging stations installed [24].

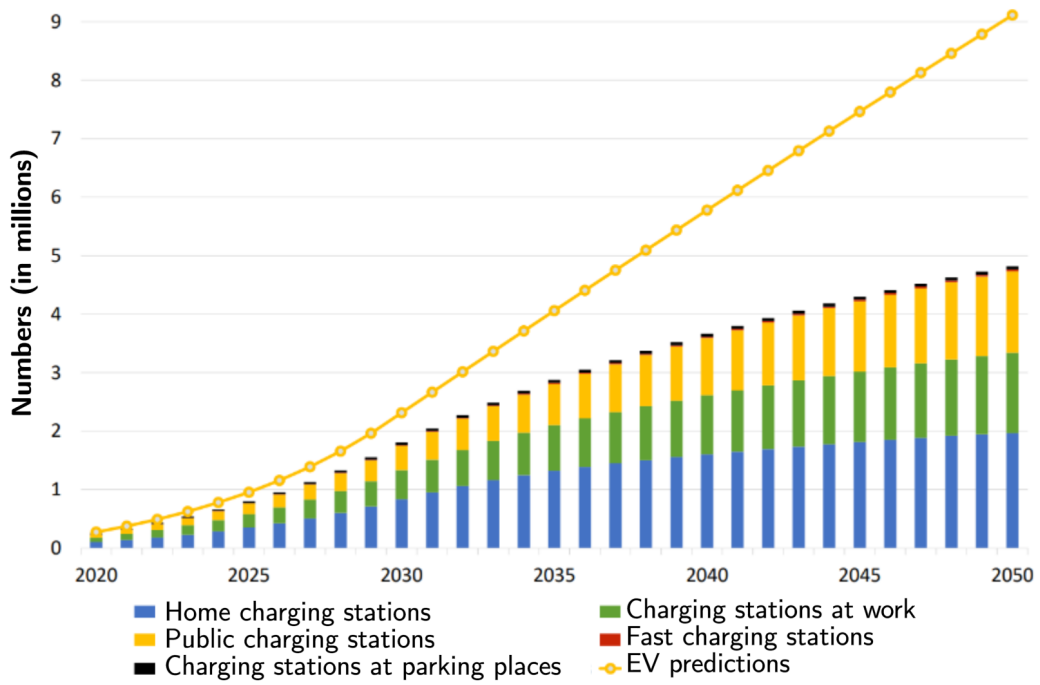

Figure 1-1: Trends of the estimated EVs's adoption rate together with the expected amount of charging points in the Netherlands till 2050 (data derived from [2]).

In general, EVs can be divided into two main technologies: Plug-in Hybrid Electric Vehicles (PHEV) and Battery Electric Vehicle (BEV). The former uses next to an electric motor connected to a rechargeable battery pack, also an ICE. In terms of the energy transition, these types of EVs are expected to phase out. Besides, also

Fuel-Cell Electric Vehicles (FCEV) have an electric motor, but these EVs do not draw electricity directly from the grid as they use hydrogen instead. BEV work on Direct current (DC) and thus have mostly an OBC embedded in the EV that can convert Alternating current (AC) to DC.

Different charging regimes can be identified as well, depending on the charge power. The term *slow charging* is applied to charge powers up to 22 kW with AC. Charging on a single-phase results in 3.7 kW power using 16 A, which is mostly the rated current in households. For households with a three-phase connection and three-phase chargers on board the EV, the charge power is increased to 11 kW (3 x 3.7 kW). When charging at 22 kW, more current is required, which is not very common for households, but can still occur at LV level, for example at public charging stations. Remark that the charge power is not necessarily limited by the charging station, but can also be limited by the OBC of the EV [25], [3].

Fast charging applies to charge powers higher than 22 kW. Some charging stations can still deliver up to 43 kW with only AC. However, from 50 kW onwards, DC flows to the battery. This is achieved by the conversion of AC to DC 'off-board' by off-board chargers. The advantage besides faster charging is that the charge power is not restricted by the onboard chargers. Mostly one speaks from Ultra-Fast Charging (UFC) for charge powers of more than 150 kW. This can be highly useful for larger vehicles. These fast-charging stations are not deployed at the LV grid and can be found mostly at highways and sometimes in cities [3]. In general, it holds that: the longer the EV is connected, the higher its flexibility.

Up to this point, EVs and the LV grid are mainly treated separately. However, when disregarding the interaction between EVs and the grid considering their potential charging flexibility, many opportunities for all market participants are omitted. In this regard, controlled (smart) charging can be an attractive solution in contrast to uncontrolled charging when considering the related challenges as addressed below.

1-2-2 Smart charging: Opportunities & Challenges

Electric vehicles are parked for 95% of the day, meaning that using EVs as a flexible asset would be attractive for balancing the grid [3]. This could reduce possible grid reinforcement related to uncontrolled charging strategies. In fact, several studies have proven that uncontrolled charging would be detrimental to existing LV grids. For instance, Yu et al. investigated the effect of uncontrolled charging on different LV distribution grids in the Netherlands, Germany and Austria, with an EV penetration of up to 80%. The conclusion was made that more problems occur in sub-urban grids compared to rural and urban grids due to long cables and many grid connections [26]. Furthermore, in [27], Berlin's DSO looked at the effect of uncontrolled charging with only 20% EV penetration. The results indicated that, especially on the LV-level structural extensions are needed when EV charging flexibility is disregarded. Updates on the MV and HV levels were less critical [27].

The above results are explained by the fact that with uncontrolled charging, most EVs are charged when the EV owner arrives at home on weekdays. Charging mostly takes till the battery is full. However, at that moment, the residential load will also be increased related to heating, cooking, lights and the use of other electrical appliances, which results in increased peak demand and extra stresses on the LV power grid [3]. In that regard, smart charging strategies are becoming more and more important in mitigating low power quality and capital expenditures alleviated by the vast amount of EVs [28]. According to the International Renewable ENergy Association (IRENA) [3, p. 2], smart charging is defined as the adaptation of - *[...] the charging cycle of EVs to both the conditions of the power system and the needs of vehicle users.* Consequently, smart

charging strategies are a key element in the energy transition, delivering flexible services to the system operators. Especially with a lot of variable RES, extra storage is required for balancing and thus stabilising the grid. Nevertheless, although many smart charging approaches exist nowadays, their practical implementation is still in its infancy. That is because both technical and organisational constraints must be overcome. Besides, a new dimension is given to smart charging by the emergence of more advanced bidirectional smart charging strategies and technology: Vehicle-to-everything (V2X), including Vehicle-to-Grid (V2G), Vehicle-to-Home (V2H) and Vehicle-to-Building (V2B). Both V2H and V2B are used to increase self-consumption of own-produced energy and avoid energy curtailment. V2G can be used to provide ancillary services and active power support to the system operators.

The benefits of EVs used as a flexible asset are schematised in Figure 1-2. The work of this thesis focuses on the local level operated by the DSO. At this level, an aggregator or CPO mostly serves as the intermediate between the DSO and EVs. Flexibility of EVs is used at the LV level to provide active power support by shifting their demands to off-peak periods. A more detailed explanation of these charging practices is provided in Chapter 2. Besides, vehicle owners with a private charging station combined with home-generated energy can increase their self-consumption.

As opposed to the local level, for more system-wide services, EVs should be aggregated under a Virtual Power Plant (VPP). That allows EVs to provide ancillary services such as frequency regulation, load balancing and spinning reserves beyond the LV network and national scales [3], [19]. Recently, a Dutch pilot project investigated the use of V2G for delivering secondary control reserves (Automatic Frequency Restoration Reserves (aFRR)) when aggregated under a VPP called *Next Kraftwerke*. This VPP contains more than 10,000 decentralised consumers who adds the flexibility of more than 1,500 MW for participating in both wholesale and balancing power markets [29]. EV data is centrally exchanged between TSO, VPP and the aggregator named *Jedlix*. Nevertheless, to fully optimise frequency regulation, information about the entire electricity network, considering HV, MV and LV should be taken into account as frequency is not regulated on a LV level only [29].

At present day, only a few home and public charging stations enable smart charging strategies. Besides, many EV are not capable of delivering V2X services due to technical constraints. However, Unidirectional Charging (V1X) such as Vehicle-on-Grid (V1G) can still provide smart charging opportunities by delaying the charging cycle [3]. Proper policies and frameworks should be implemented to provide the right incentives for the EV to deliver the requested services. These include proper pricing schemes, a 'DSO role-change', policies related to smart metering and related privacy issues, amongst other.

First of all, **proper pricing schemes** are needed to provide the right incentive to EV owners to unlock Demand Responsiveness (DR). Time-invariant pricing will not be effective in that case. Besides, pricing should be adapted to bidirectional charging practices as well. In fact, it should be possible for an EV owner to **participate in different markets** providing maximum flexibility, which would need to allow for *staggered* tariffs [3]. Real-time pricing in the Netherlands is currently not a common practice in the residential sector and mostly applies to larger consumers (e.g. greenhouses) only [30]. Nevertheless, a public Charge Point Operator (CPO) could use day-ahead based energy contracts.

Next to pricing, **software and hardware requirements** are needed involving smart meters, Energy Management Systems (EMS) and appropriate chargers equipped with effective communication protocols. Advanced smart metering using an EMS is required for communication between the aggregator and EV owner. In that way, scheduling (dis)charging activities is made possible [6]. Shared information with the aggregator can include estimated State Of Charge (SOC), user preferences, vehicle ID and charging station ID. The latter two can

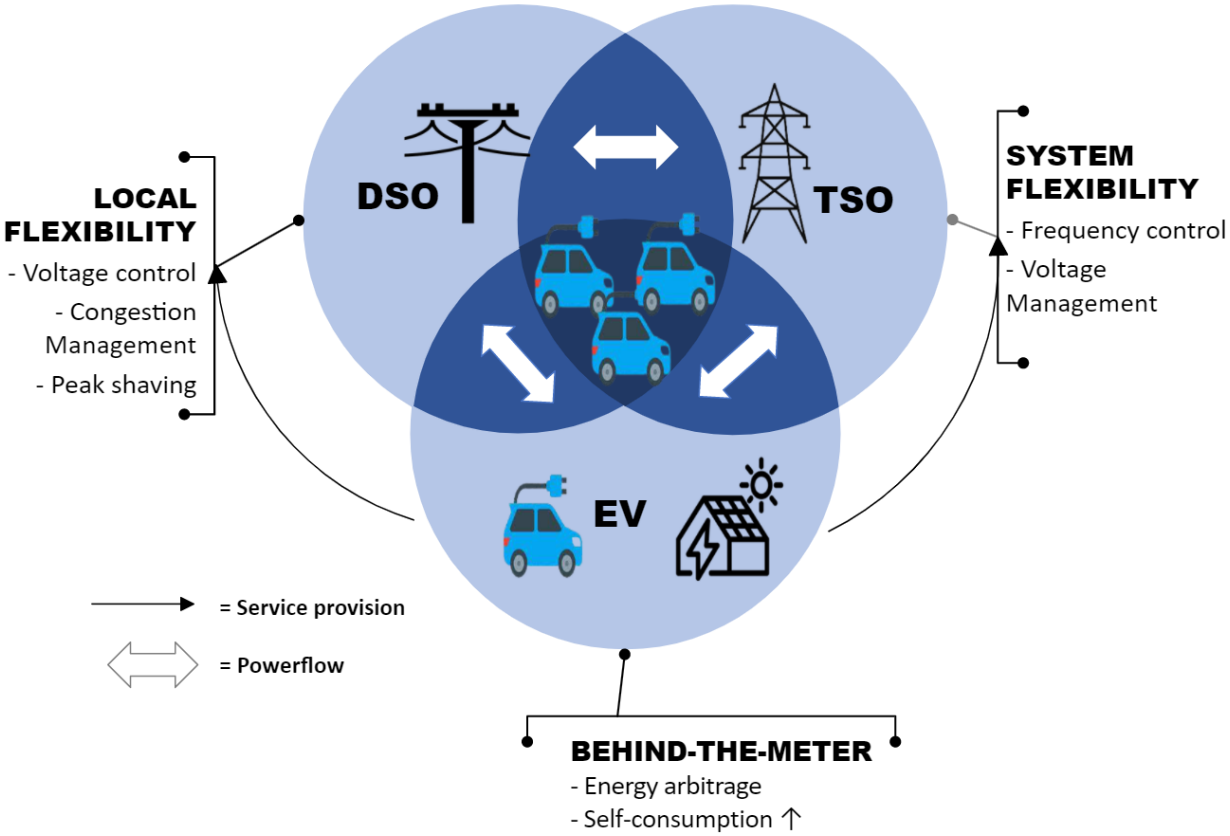

Figure 1-2: Benefits of (bidirectional) smart charging using EV (based on [3]).

give access to more data via a database, such as battery capacity, location and charging station capacity. Nevertheless, **privacy issues** can exist when data containing EV user's behaviour is shared with a third party [28]. The right protocols should be established to ensure the EV user's privacy.

Lastly, smart charging on a LV level requires a **DSO role-change** in the Dutch LV network. Although flexibility is well introduced at the system level by TSOs, this is not the case on local grid levels operated by DSO. A DSO often does not have the authority and thus also not the incentive to manage congestion using smart grid applications. They are legally obligated to comply with the needs of all customers. Consequently, when a charging fleet aggregator is restricted by grid capacity, financial compensation should be provided when providing flexibility to the DSO [31, 30]. Furthermore, a lack of regulation prevents the DSO from actively intervening in electricity markets by using flexible assets such as EVs.

1-3 Research Objectives

The objectives related to this thesis are addressed in this section. A concise answers to the research questions can be found in the final chapter, Chapter 6.

1-3-1 Main Research Question

The main objective of this thesis relates to the following research question:

*How can **EVs' charging flexibility** be **used optimally, to avoid possible grid congestion and voltage problems on a LV grid** due to inflexible loads and non-optimised charging?*

To be able to formulate the answer, some sub-objectives are defined in the section below (1-3-2). This research question applies to a specific LV grid in the Netherlands for scenarios up to the year 2050 involving V2G and V1G, two different pricing schemes and different levels of grid constraint modelling. Although one should always reflect on the generalisation of the results, the adopted methodologies can be applied to other case studies as well.

1-3-2 Sub-Research Questions

Several sub-research questions are defined. They are key elements in completing the answer to the main research question.

1. *To what extent do **voltage and congestion problems** manifest in a typical Dutch **LV** grid when **uncontrolled charging** is applied both in winter and summer till 2050?*

   This research question is addressed in Section 5-1. The question relates to the frequency of occurrence of under-/overvoltage and congestion problems. This allows for validation of the need for EV flexibility allocation by a smart charging model. Besides, the interplay between these grid problems and network components is also discussed, which relates partly to sub-question 3.

2. *What are **good features of existing optimised charging models** applicable to the studied LV grid to help mitigate grid issues such as congestion and voltage problems?*

   For this research question, a literature study on existing smart charging models is conducted first (see Chapter 2). Afterwards, an optimised charging model is developed based on the state-of-the-art. The focus is on reducing voltage and congestion problems in the LV grid while allowing for bidirectional charging.

3. *In which case is the **integration of grid constraints and power flow modelling relevant** in the optimised charging model?*

   This research question discusses how grid constraints can be introduced in a smart charging model. Furthermore, it discusses the performance of the modelled power flow in terms of precision and computational time. Cases are investigated in which the model might or might not benefit from the implementation of these constraints. That includes varying the charging technology (V2G and V1G), the level of grid constraints (no limits, transformer limitation and feeder constraints) and the tariff structure (day-ahead or stacked tariffs). A discussion on this sub-objective can be found in sections 5-1 and 5-2.

4. *To what extent does the developed **optimised charging model** help in mitigating **voltage and congestion** issues in the **LV** grid?*

   This research question looks into the remaining congestion and voltage problems (if any) after implementing grid constraints. Different case studies are ran of which the results can be found in Chapter 5.

5. *To what extent does the stacked tariff scheme, V2G and grid constraints affect the **interests of the involved stakeholders** (DSO, CPO and EV owner)*?

This research question concludes this thesis. The optimally of the model is assessed in the broader sense of the word by looking to the interests of all involved parties. A table assessing on the benefits of these stakeholders is included at the end of Chapter 5 as well.

1-4 Thesis Outline & Methodology

In order to answer the aforementioned research questions, a certain methodology was adopted. Figure 1-3 gives an overview of the applied steps in this thesis together with the related chapters. After this introduction, a literature study is conducted about state-of-the-art smart charging methods (see Chapter 2). In Chapter 3, the used LV grid is discussed together with the inputs and assumptions that were adopted for the different scenarios. Besides, Chapter 3 also contains more information about the EV charge simulator tool that was developed based on [32]. With this tool, appropriate charging transaction data was created, which could be used in Chapter 4. In the same chapter, an appropriate smart charging model was developed to create optimised charging using EV flexibility. The loading by flexible assets together with inflexible assets was analysed in PowerFactory (2022) in terms of congestion and voltage events [33].

The used PowerFactory file contained a model of the discussed LV grid. The software is able to simulate (un)balanced (three-phase or single-phase) loads and electricity sources in the modelled LV grid. With the Newton-Raphson method, the software calculates the three-phase voltage and current characteristics in all nodes and lines of the modelled grid. Furthermore, a script was made in python to change data in Power-Factory according to the scenario choice automatically. The results of the analyses can be found in Chapter 5. All the simulations ran on a Windows computer with an Intel(R) Dual-Core(TM) i5-7200U CPU @2.70GHz processor containing 16.0 GB RAM. All python scripts including the smart charging model together with the documentation files can be found on `https://github.com/ROBUST-NL/Interplay_EVs-LV_grid` once the project is made publicly accessible. An overview of the python structure considering main files, sub-files and file interdependencies is provided in Appendix C.

The conclusion can be found in Chapter 6 and gives the final answer to the sub- and main research questions. Furthermore, recommendations are made to improve the current study in further research.

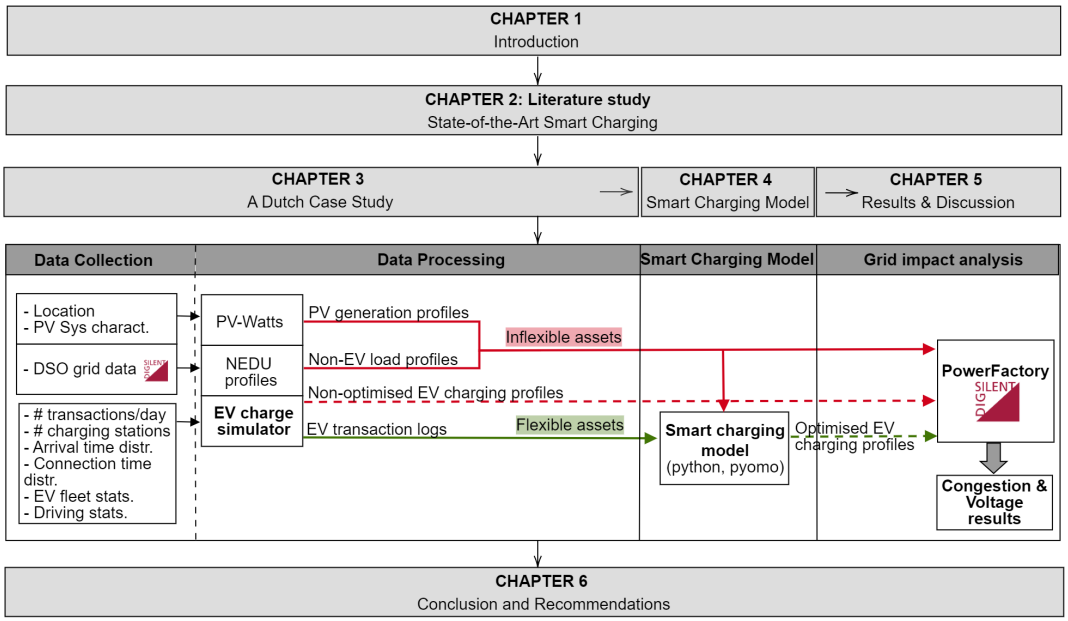

Figure 1-3: Schematic showing the thesis outline and applied methodologies.

1-5 Thesis Contribution & Motivation

The importance of this research relates to the fact that LV grids are experiencing congestion and voltage problems due to distributed PV, EVs and electric heating. In order to effectively apply grid reinforcement with sufficient pace, EV flexibility should be used to the full extent. In that way, grid reinforcement can be delayed and voltage and congestion problems can be mitigated. This study tries to make these grid problems quantifiable. In its turn, it gives insights to policymakers to allow certain smart charging strategies. Additionally, by investigating bottlenecks in the grid, the DSO gets a more transparent overview of the level and location of reinforcement that should take place. Not only delayed, but also efficiently planned grid reinforcement is important to keep track of these bottlenecks. Early detection of bottlenecks at specific locations in the grid might also notify stakeholders in time such that an informed decision about the placement of new chargers can be made.

Furthermore, there exists a lack of research that investigates the relevance of implementing grid constraints in optimised charging models. Currently, some chargers in the investigated LV grid are already equipped with a existing smart charging model. However, that does not involve power flow modelling downstream the LV/MV transformer station. This study tries to reflect on the relevance of adding these power flow constraints using a power flow model for an existing LV grid.

Another interesting feature of the developed smart charging model is the implementation of both EVs with and without V2G capability. Most smart charging developers disregard V2G into their model. However, it allows giving more insight into the benefits and drawbacks of this developing technology.

Overall, after applying the methodologies in this study, a DSO should get a clear overview of possible weaknesses in his LV grid and how EVs' flexibility allocation might solve these issues effectively.

Chapter 2

State-of-the-Art Smart Charging

This chapter gives a literature overview to determine good features of existing smart charging models applicable to this study. First, a general overview of smart charging objectives and methods is presented in Section 2-1. Afterwards state-of-the-art centralised smart charging methods are discussed in Section 2-2. Table 2-2 gives a literature overview in order to compare the different existing smart charging implementations in literature.

2-1 Smart Charging Approaches

2-1-1 EVs' Best Charging Practices at LV Level

When developing a smart charging approach for distribution networks, it is important to consider the objective of the developed model. Considering the aforementioned definition, smart charging should meet vehicle owner's requirements but should also comply with the grid code, potentially reducing system operator costs [3]. Therefore at the LV level, the most natural smart charging approach is to accomplish valley-filling by peak reduction of the electricity demand. Valley-filling is an active power control strategy which can be implemented thanks to the extended parking time of most EVs. Besides, when considering V2G technology, EVs can also discharge a part of their battery capacity at peak hours, providing added flexibility. Nevertheless, the detrimental effects on battery degradation should be considered [34].

From the DSO perspective, the benefits of valley-filling are twofold. The first benefit of this peak-reduction strategy is the reduced power loss in the cables, in its turn reducing monetary losses of the DSO. Besides, it allows the grid operator to comply more easily with the grid code. In that sense, the grid can host more capacity such that network infrastructure reinforcement can be postponed. On the generator side, valley-filling will decrease ramping requirements of conventional power generators, which eases the transition to more variable

RES like wind and solar energy. Additionally, this also reduces starting and stopping costs for conventional power producers due to a more balanced load profile. Consequently, the load factor of these generators can be higher [27].

On the other hand, the total operational cost of charging should be as low as possible from the perspective of the EV owner and aggregator. Therefore, most charging models implement a financial objective to accomplish user satisfaction. Time-varying pricing strategies are usually adopted, which provokes charging flexibility. Most studies make use of Time-Of-Use (TOU) pricing. This mechanism implements different predefined charging prices during the day, mostly for two or three fixed time blocks. In that regard, the off-peak period will always contain a lower price than the mid- or on-peak time blocks [27, 35]. More advanced pricing strategies make use of dynamic pricing. This dynamic pricing should reflect the network operating conditions and abundant renewable energy production. Nevertheless, they mostly only reflect production cost and not the network operating conditions which can lead to the so-called *avalanche effect* if no charging constraints are invoked [35]. This phenomenon shifts the load peak in time instead of reducing it.

Unconventional approaches in smart charging literature include, for instance, flicker reduction and reactive power control. The former strategy was implemented by Brinkel et al. [19] using V2G technology. However, that requires charging patterns to change with a very high frequency, which is not practical to implement and should be assessed in terms of battery degradation. Leemput et al. [36] implemented three local rule-based charging methodologies, each with different active power charging strategies and objectives: high comfort (uncontrolled charging), low charging cost (off-peak charging) and low grid impact (EV peak shaving). They investigate the impact of these strategies combined with reactive power provision of EVs when a capacitive Power Factor (PF) is implemented in their charger. This should provide voltage support. Nevertheless, LV cables have a low Reactance/Resistance (X/R) ratio, which makes reactive power control less effective in addressing voltage disturbances compared to active power control methods. Besides, increasing the reactive power will increase power losses and requires larger sizing of charging equipment [28, 36].

2-1-2 EV Charging Methodology

Considering smart charging methods, (nearly) all EV charging models can be classified under optimisation or rule-based control. The latter involves mostly a modelling environment. The rules can be generic, based on the queuing approach or fuzzy logic. However, compared to optimisation approaches, the solution is often not optimal [37]. Considering optimisation methods, a subdivision is made in classic mathematical optimisation and optimisation using meta-heuristic methods. The latter is not always able to find the global optimal solution; however mostly a near-optimal solution can be found in a reasonable time span [37].

Furthermore, two distinct control approaches exist in EV charging: centralised and decentralised charging, both requiring an EV aggregator. A comparison of these two approaches is schematised in Table 2-1 and explained below.

Centralised control can provide a globally optimal solution respecting network and customer constraints using a master control engine. The aggregator is the controlling agent, adjusting charge schedules according to network and EV information. With a centralised approach, it is possible to fully support the system operator for balancing and ancillary services by using EV as a flexible asset [6]. Nevertheless, the computational complexity can grow significantly with the number of grid connections. Besides, in terms of communication, numerous

messages will need to be communicated in a limited amount of time [38].

In contrast to centralised charging, with decentralised/distributed charging, vehicle owners are the decision-making entity about their charge patterns. They choose their desired charging pattern (time and rate) and send that to the aggregator. The charging pattern can be guided by appropriate electricity tariffs. Although there is no guarantee that network constraints will be met, most decentralised charging models comply more with user preferences. Nevertheless, with price-based strategies, the risk exists that many EV owners charge at the same time based on attractive low tariffs, leading to an avalanche effect in which a new load peak occurs. There exist also studies such as [39], for which EVs can provide ancillary services, but for which the primary user-interests are not fulfilled. User-satisfaction, regarding obtaining a desired SOC level should always get highest priority. Furthermore, de Hoog et al. [40] proved that implementing a centralised charging model might allow the LV grid to host more EVs than a decentralised model. Nevertheless, decentralised charging is in most cases beneficial in terms of computational and communication requirements, which allows for a more practical real-time implementation. Nimalsiri et al. [41] compared their decentralised approach using the Automated Direction Method of Multipliers (ADMM) [41] with a centralised approach using quadratic Receding Horizon Optimisation (RHO) developed by the same authors [42]. The results show an increased calculation efficiency, where the decentralised charging is 60 times faster. Besides, the distributed approach does not need a central controller or aggregator, but uses peer-to-peer communication to determine the charged energy [41]. Remark that the computation time is case-specific and depends on the optimisation method or iterations needed to get to an optimal solution [38, 6, 7].

Real-world projects are indicated in Table 2-1 as well. The *FLEET* project is an example of centralised charging applied in Utrecht, a city in the Netherlands. It is a pilot project in which they test various pricing schemes. They try to avoid congestion on the transformer level, stimulate valley-filling and increase renewable energy consumption. Existing decentralised charging applies to EV owners, who are aggregated under *Jedlix* [3].

Although decentralised charging is mainly seen as a more practical smart charging approach, centralised charging can be applicable when charging stations are publicly owned compared to private charging stations. This applies to charging in cities and charging at work [35]. In that case, a Charge Point Operator (CPO) can serve as an aggregator himself, buying energy and controlling the charging stations [43].

Table 2-1: Comparison of decentral and central EV-charging [6, 7].

Characteristics	**Charge Control Strategies**	
	Centralised	**Decentralised**
Charge Decision	Aggregator	EV owner
Control Factor	Direct control	Mainly price-based
Ancillary service Provision	More	Less
Grid security risk	Very low	Potential
Optimality	Global	Local
Computational Requirements	More	Less
Communication Requirements	More	Less
User Charging Authority	Less	More
Privacy Concerns	More	Less
Scalability	Less	More
Real-world Example	FLEET[1]	Jedlix[43]

2-2 State-of-the-Art Centralised Charging Strategies

This dissertation focuses on the flexibility potential of EVs in a LV grid to improve and maintain acceptable voltage and congestion levels. However, with decentralised charging, compliance with favourable congestion and voltage levels are not always guaranteed. Besides, load peaks can often occur due to uncertainty in the final result of the decentralised model. In contrast, centralised charging can offer better utilisation of the network capacity and the provision of ancillary services [28]. Therefore, a centralised control model is more desired in the scope of this work, especially due to the fact that only one CPO is regarded. Furthermore, the focus in the discussion below, was given to models that give a real-time solution and include power flow modelling or comply somehow with grid congestion and voltage problems.

Many centralised smart charging strategies exist in literature. Most of them are purely based on optimisation. However, it is essential to assess their usefulness and application potential in a practical setting. Some of the most applicable models are listed in Table 2-2 and explained below. The models are assessed based on: their control strategy, objective functions, implemented constraints, computational requirements, case study, PV or V2G implementation and model requirements in terms of EV inputs.

First of all, an algorithm having **low calculation time** is a key requirement when it is being used in a practical setting. Therefore a good model should be able to provide a real-time solution. The choice of the optimisation method is a crucial factor in computational cost reduction. Using non-linear methods, especially non-convex or mixed-integer problems, will result in a substantial computational burden. Methods like Genetic Algorithm (GA) or Particle-Swarm Optimisation (PSO) and other meta-heuristic approaches can be deployed but often still lead to significant computation times. Formulating a linear problem by avoiding non-linear objectives and linearising constraints is a common approach to avoid computation issues. At least three different approaches for linearisation exist in the smart charging literature. First of all, Goldoust and Masoud Esmaili [44] conducted a sensitivity analysis on the network parameters in power flow simulations to linearise them. Nevertheless, when linearising non-linear dynamics, the solution can deviate from the global optimal solution. Secondly, also Nimalsiri et al. [42] used a linearisation strategy. Power flow constraints were linearised using linear Distflow equations. The Distflow equations were developed by Baran and Wu [45] for network power flows and voltage modelling. Although the model itself was quadratic due to a non-linear objective function, a (near-) real-time solution was still obtained. A third approach to obtain a linear formulation was used by de Hoog et al. [46]. The authors suggested Direct current (DC)-equivalent network constraints by using representation of the power system. Especially for the voltage drop, this approximation seemed to be validated with only minor errors compared to power flow simulations.

One remarkable difference between [44] and [42, 46] is the use of **static and dynamic methods**, respectively. With a static method, the optimisation is performed for the EV at the moment the EV is connected and will not be updated when new information comes in. A forecast is mostly made for the day ahead. In contrast, dynamic simulations will update the charge pattern after each time step for the coming period using the new information introduced at each new point in time. In fact, dynamic optimisation finds the same optimal solution as the static optimisation procedure. However, it will only implement it for the first time step and it repeats this procedure for the next time steps when time moves forward. In that way, it uses only forecasted values near real-time. Such approach is mostly referred to in literature as sliding window, rolling horizon or RHO inspired by Model Predictive Control (MPC).

Sabillon et al. [47] also used **RHO for dynamic scheduling of Electric Vehicles (EV)** in residential networks

with Mixed-Integer Linear Programming (MILP). To reduce the computational cost of this approach, the authors refined only the implementation time step, and took more giant time steps for the predictions of the consecutive charging period. This is validated by the fact that the consecutive steps are not implemented. Besides, also integer relaxation for the non-applied time steps was used, a technique also used in an earlier publication of the same authors [48].

Yi et al. [49] used a **two-stage hierarchical optimisation** method with RHO to obtain a real-time solution. Such algorithm is extremely fast and can solve the EV charging schedules in a matter of seconds. In principle, hierarchical optimisation in the context of smart charging means that a central controller will control different EV groups. Afterwards, a local controller manages the power distribution on a smaller scale [38, 49]. Chen et al. [50] used a similar concept. By using a multi-level online charging model, both papers are able to combine the benefits of decentralised and centralised charging.

Another interesting real-time centralised smart charging approach was developed by Zhan et al. [51]. The authors implement **rule-based optimisation strategy**. In fact, for each time step, a static power flow simulation is executed in PandaPower [52]. When thermal or voltage limits of the network are violated, the optimisation kicks in to coordinate the charging of EV. Accordingly, active and reactive power setpoints of the DER are adjusted based on cost optimisation, restricted by grid constraints and penalising a low SOC near departure. The latter is needed because the model only optimises one step ahead. The effectiveness of this approach lies in the fact that the static power flow yields a faster output than the single-step optimisation, which is only performed when a threshold in the flow simulation is exceeded. Nevertheless, the charging flexibility of the EV is used to a limited extent, by charging the battery as fast as possible and only deviating from the schedule when grid code violation occurs [51].

Instead of combining a rule-based and optimisation approach, Quiros-Tortos et al. [53] compared both. First, they developed a centralised rule-based charging mechanism using a P-controller. The algorithm was tested in nine British residential Low-Voltage (LV) networks. Afterwards, they compared it with an optimisation-based approach using the same voltage and thermal constraints. The optimisation showed a better performance in terms of power quality and congestion management. However, it also required much more inputs compared to the controller (rule-based) model such as the SOC of the battery [53].

To refer back to Table 2-2, one can conclude that the implemented **optimisation objectives are mostly economically-inspired**. One of the advantages is that a cost-based objective function is mostly linear, allowing for a linear optimisation strategy. Besides, **all the models in Table 2-2 require information about the SOC**, which is not always easily obtained in practice. An overview of existing SOC estimation methods with the focus on control theory methods is provided by [54].

Table 2-2: Literature table considering (real-time) centralised charging techniques.

Source	Method	Objective	Constraints	Computation (assuming normal PC)	Scale	PV	V2G	EV Input
de Hoog et al., 2015 [46]	Linear RHO with DC equivalent model	* Greedy Charging: max.. stored energy * Min. charging cost with dynamic spot price	* 3P thermal limits * 3P voltage limits * Max bat capacity * Max currents * Target SOC >95%	MATLAB Near-real time	*57 EVs * 5 min over 8 h period	No	No	* SOC * Battery capacity * Expected departure time
Yi et al., 2020 [49]	Quadratic hierarchical RHO	Min. load deviations to obtain valley filling	* Boundaries on aggregated energy allocation, based on: - feeder capacity - SOC requirements	PYTHON, CVXOPT One-stage: 312 sec (50 EVs) Two-stages: 1 sec (50 EVs) Two-stages: 4 sec (500 K EVs)	* 50 EVs - * Each 15 min over 24 h period	No	No	*SOC arrival and departure * Time departure * Forecasted EVs and non-EV load
Nimalsiri et al., 2021 [42]	Quadratic RHO with LinDistFlow	Min. charging cost based on TOU	* SOC limits * Battery power constraints * Voltage constraints * Energy requirement to reach SOC	PYTHON, CVXPY 48 sec	* 600 EVs on MV with IEEE 13 *Each 30 min over 24h	No	Yes	* desired SOC * Time departure, arrival * Forecast day-ahead (non-)EV load
Goldoust and Masoud Esmaili, 2015 [44]	Multi-Objective Linear Programming with use of sensitivity factors and fuzzy members	Energy losses and aggregator cost based on TOU	* SOC limits * Battery power constraints * Limits on high variations on charging * Thermal limits	GAMS, CPLEX 0.266 sec	* 67 EVs	No	No	* Desired, arrival SOC * Arrival, departure time
Sabillon et al., 2018 [47]	Mixed integer linear RHO with integer relaxation and different window lengths	Min. overall system cost	* Max. allowable energy * 3P voltage limits * 3P thermal limits	AMPL, CPLEX Time limit of 120 sec	* 107 nodes * 1x 15 min and 24 x 1 hour	Yes	No	* SOC * Arrival, departure time * Forecast of loads and PV
Zhan et al., 2021 [51]	Power flow based one-step ahead optimisation with second-order cone relaxation	Min. cost related to losses, PV, user dissatisfaction, heat pump	* Thermal limits * Voltage limits * Battery and PV power constraints	Pandapower: 1 sec PYTHON, GUROBI: 4 sec	* 67 households (100% EVs)	Yes	No	* SOC * departure time
Brinkel et al., 2020 [19]	Linear optimisation	Min. EV cost based on historical aFRR prices	* Battery power constraints * Restricting residual load to reduce flicker	PYTHON, GUROBI with supercomputing service	* 99 EVs * 20 seconds resolution needs supercomputing	Yes	Yes	* SOC * uncontrolled/ controlled charging * Expected departure time
Quiros-Tortos et al., 2016 [53]	*Hierarchical controller * NLP with binary relaxation	*Min. EV disconnections	* 3P thermal limits * 3P voltage limits	* Real P-controllers * AIMSS with CONOPT * Validation with OpenDSS	* 86 EVs * 1, 5, 10 and 30 min	No	No	* SOC (only for the optimisation)

Chapter 3

A Dutch Case Study

3-1 Modelled LV Grid

A real-world modelled LV power grid was investigated in PowerFactory, to test the developed smart charging model and corresponding scenarios. The selected LV case study is located in a dense city area in The Netherlands. The LV grid itself hosts one MV/LV transformer with a rated capacity of 400 kVA. At this transformer station, 11 feeders are connected with a total of 344 connections. The total number of feeders increases downstream the network due to the integration of several distribution substations without a transformer. At these substations, the network can be switched to different configurations: radial or meshed. In this study, the topology was kept in radial operation. This configuration is most preferred by the DSO due to easier monitoring of power flows. That is especially needed with the expansion of the (bidirectional) EV fleet and distributed PV. The cable types and their corresponding loading in normal operations are listed in the appendix in Table A-2. Most of the cables belong to the class Gepanserd Papier Lood Kabels (GPLK), in English called Paper Insulated Lead-covered Cables (PILC). The GPLK is a very old cable type, installed more than 60 years ago (1954). Since 1980, these cables have not been installed anymore in the Netherlands. The other cable type: VVMvKhas/Alk 4x6, is installed more recently and allows higher current ratings [16]. Therefore, these cables are located closer to the MV/LV transformer station.

The phase voltage magnitude maximum deviations were regarded as $\pm$ 0.05 p.u. from unity. Although the EN-50160 consider a larger margin of $\pm$ 0.1 p.u. (see Appendix Table A-1 [10]), a smaller margin was considered due to two reasons. First, the DSO of the discussed LV network works with this number. Second, the MV fluctuations are not modelled in PowerFactory, which would normally enlarge the fluctuation on the LV level. This adoption was justified by other papers [17] and also by actually measurements at the LV/MV transformer reported by N. B. G. Brinkel [1]. Furthermore, the tap position was changed and fixed to the minimum possible position, leading to the highest obtainable voltage at the transformer node. Consequently, the tap position is already in its most favourable position in terms of avoiding undervoltage problems further down the feeders.

3-2 Data Collection

3-2-1 Non-EV Load

Non-EV load, also referred to as baseload in this study, corresponds to the electricity consumption of households, small businesses and public lighting. This includes consumption related to electrical appliances and heating by heat pumps if applicable. The electricity usage patterns are derived from Dutch Energy Data Exchange (NEDU) which makes typical energy consumption profiles in the Netherlands freely available [55]. Regular household's baseload consumption corresponds to the E1B profile with a double meter for night and weekend tariffs. For the larger consumers, small businesses and schools, the E2B was applied. Both profiles are averaged out over more than 1000 energy meters in the Netherlands and measured for the year 2021. For public lighting, a square wave profile, corresponding to E4A was applied. The standardised profiles were interpolated to 15-minute time intervals and multiplied by the individual yearly electricity consumption of each connection.

Figure 3-1 and Figure 3-2 show the result of the aggregation of all the derived NEDU profiles. As one can see, the aggregated power closely matches the actual measured consumption at MV/LV transformer level (blue). This is the case for both winter (Figure 3-1) and summer (Figure 3-2). It justifies the disaggregation with the use of NEDU profiles. Furthermore, it proves that the aggregated transformer loading is quite predictable. A strong evening peak is related to people arriving home from work, using all kinds of electrical appliances and heating.

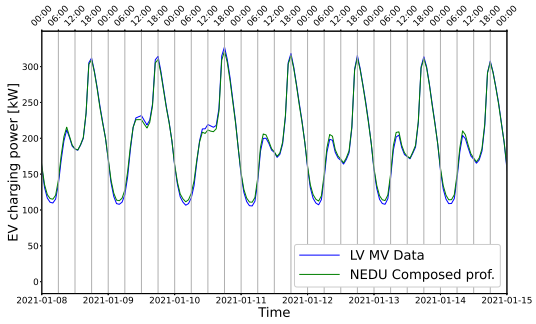

Figure 3-1: Comparison of NEDU profiles and actual measured power at MV/LV substation transformer for week 2.

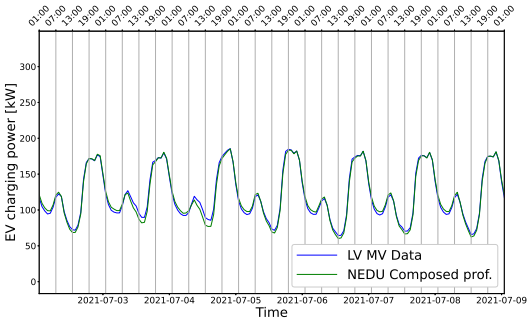

Figure 3-2: Comparison of NEDU profiles and actual measured power at MV/LV substation transformer for week 27.

Furthermore, the Dutch climate agreement states that all houses should move away from natural gas for heating and cooking by 2050. Green(er) alternatives such as (hybrid) heat pumps, hydrogen heating and district heating networks will need to be put to full use [13]. Practically, that would mean that yearly 180,000 (hybrid) heat pumps should be installed across the Netherlands. Nevertheless, the houses in the studied LV grid are quite old and built in the interwar period. That means that they are less suitable for (all-electric) heat pumps. District heating might be a more suitable option for most of them, although a decision by the municipality about the most suitable heating method in this area is not yet forthcoming [56, 57]. Based on this information, a moderate heat pump adoption rate of 8%, 15% and 40% (2025, 2030 and 2050) was applied relative to the 2021 scenario. This resulted in an estimated yearly load increase of 4.15%, 7.79% and 20.76 %. These values were multiplied

with the load profiles of the 2021 scenario. Remark that this practice is a simplification. The actual heating profiles depend on several parameters such as demand responsiveness based on the implemented (financial) incentives, weather conditions, building characteristics etc. Nevertheless, a heat pump electricity profile would not deviate much from the current consumption pattern according to the consumption profiles in [58, 59].

3-2-2 PV Data

In 2021, the PV capacity in the discussed LV grid amounted to 83.6 kWp spread across 18 different installations. In Table 3-1 the predictions towards 2050 regarding this capacity are made based on internal data from a Dutch DSO. Note that these PV adoption rates are relatively low compared to the actual rooftop potential of the area. Higher adoption rates might be applicable depending on the assumed scenario.

Table 3-1: Assumed projections of the PV installations in the LV grid.

Year	PV capacity [kWp]	Nr. Installations	Average [kWp]
2021	83.6	18	4.64
2025	99.8	21	4.75
2030	110.8	25	4.43
2050	145.0	34	4.26

Hourly standardised data was derived from the National Renewable Energy Laboratories (NREL) PVWatt calculator to establish the production profiles of the PV installation [60]. Although the used weather data applies to Amsterdam, it resembles a typical Dutch PV power profile. The hourly data was interpolated on a 15-min basis to fit with the other collected data sets.

3-2-3 EV Data

This section discusses the EV data collection and future predictions for the concerned LV grid. The information in the following section discusses how the collected data is used for simulating uncontrolled charging scenarios.

Currently, the discussed district hosts six public charging stations, each with one pair of charging poles. These charging stations are maintained and operated by one CPO and have a total capacity of 22 kW AC power each. Besides, the same CPO also hosts an additional eight chargers (charging points) used for their own shared EVs spread across four charging locations (charging stations). The privately-owned charging stations are assumed to be negligible in this dense city area as, on average, 7 out of 10 cars in the Netherlands rely on public parking. That means that in an urban area, almost all cars will need to be stationed publicly [61]. According to charging data from 2019-2020 related to the six public charging stations, the public chargers are mostly used by visiting cars. The amount of cars that charge more than once a week is equal to 10. These cars are regarded as local EVs. Their weekly average charging sessions were used to calculate the amount of accountable visiting EVs, which resulted in 14 vehicles. Eventually, the total amount of accountable EVs (n_{EV}) hosted by the LV network was estimated to be 32: 14 visiting EVs, 10 local EVs and 8 shared EVs. It reflects a total of 1.6 cars per charger, which is regular in the Netherlands. However, compared to the European directive that indicates a maximum of ten EVs per charger, this number is quite low. In fact, compared to the rest of Europe, the

Netherlands leads in the number of chargers even in absolute number [62]. That leads to faster integration and transition towards electric mobility. However, future-wise, it is expected that the amount of chargers will not linearly scale with the amount of EVs. That was also deducted from Figure 3-3. Instead, a charge simulator was used to derive an appropriate density of EV chargers. More details about this charge simulator can be found in Section 3-3. It turned out that with 5 EVs per charger 111 of the 33,631 transactions were unsuccessful. That means that all chargers are fully occupied for 0.33% of all transactions. This number was seen as acceptable. In case of full occupancy, a car can still search for a charger in a neighbouring LV grid.

Based on the average number of cars per household (c/h = 0.4) in the LV grid and the number of households (n_{hh}) in the district, a penetration level (ρ_{L}) of 5.57% was achieved (including local and shared EVs) [63]. This number is slightly higher than the average share of EVs in the Netherlands (3.96%), probably due to the active involvement of the CPO for charging equipment and shared EVs [8]. The following formula (3-1) was used to obtain this penetration level:

$$\rho_L = \frac{n_{\mathsf{EV}}}{n_{\mathsf{cars}}} = \frac{n_{\mathsf{EV}}}{n_{\mathsf{hh}}\mathsf{c/h}} \tag{3-1}$$

According to the Dutch ambition regarding EV sales, penetration scenarios were established for 2025, 2030 as well as 2050 as indicated in Table 3-2. The 100% penetration in 2050 reflects the decarbonisation of the entire passenger vehicle fleet as stated by the Dutch climate agreement. The resulting EVs and the total amount of transactions are obtained from these penetration levels. An average of 107 transactions per year for one EV was used, based on the 2029-2020 EV data.

The final results related to each scenario can be found in Table 3-2. A complete overview of the derivation of these numbers is schematised in Figure 3-3.

Table 3-2: Assumed projections of the electric car fleet in the discussed LV grid [8].

Year Information: Dutch ambition	Penetration Level [%]	Total EVs	Charging points	EV / Charger	Total annual transactions
2021 10% of all new passenger cars sold with electric powertrain and a plug	5.57	32	20	1.61	3462
2025. 50% of all new passenger cars sold with electric powertrain and a plug, at least 30% of the EVs should be BEV or FCEV (zero emission).	30	94	27	2.18	10,089
2030 100% of all new passenger cars sold should be BEV or FCEV (zero emission).	50	157	34	2.74	16,815
2050 Car fleet 100% zero emission.	100	313	63	5.00	33,631

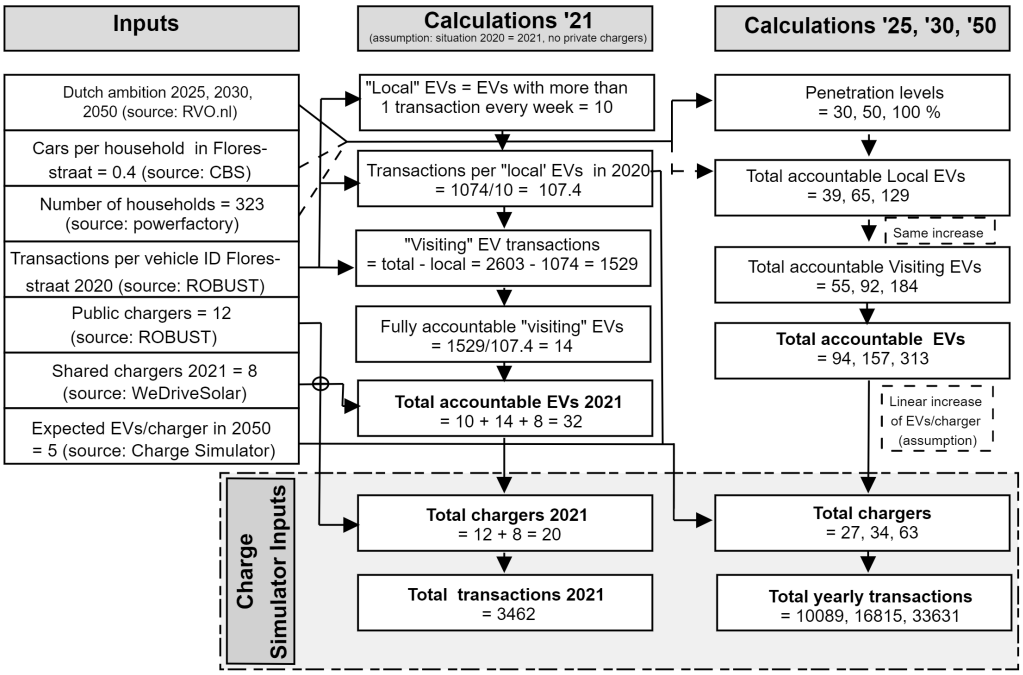

Figure 3-3: Flow diagram of the EV prediction scenarios. The output of this diagram contains the total chargers and yearly transactions for the years 2021, 2025, 2030 and 2050.

3-3 EV Charge Simulator

To simulate the **uncontrolled** charging scenarios and create charge transaction logs at the LV grid, two approaches can be regarded: using existing real-world data or synthetic data. Although the availability of charging data for one year, the choice was made to extend a pre-existing script: *EV-charge simulator*, from the Aalto University [64, 32]. This EV-charge simulator was programmed in python using object-oriented programming. It is capable of creating realistic charging patterns based on statistical inputs as well as the predicted amount of chargers and transactions. The tool is very versatile, which allows adapting the charging patterns automatically to new prediction scenarios. In that way, inconveniences of incorrectly logged transactions can be avoided as well as future estimates of charging density and V2G adoption rates can be more easily integrated. Besides that, it allows for a more automated way of assigning charging profiles to charging stations in the power flow model (PowerFactory).

The output of the charge simulator is twofold. It contains a table with the transaction logs and the 15-minutes data of the charging power at each charging point. The transaction logs include EV maximum charging power, battery capacity, arrival SOC, arrival time, duration time, maximum charging power, V2G capability and charger

ID. For the 15-minute charging profiles, the principle *charge-on-arrival* at maximum power is used.

The adaptations to the existing script of [64] include:

- Transformation of building-related chargers to network-integrated chargers.
- Possibility to simulate over multiple days on a 15-minute basis instead of single-day simulations.
- Inter-day dependency: continued charging if charging-time spans more than one day
- Inclusion and update of statistical parameters such as the hourly probability of arrival times for each weekday separately, the inclusion of the probability distribution for the charging duration, statistics related to the SOC, the average driving distance and car fleet parameters.
- Implementation of SOC and duration dependency: when SOC of 80% is reached, the script reduces the power to zero but keeps the EV connected.
- Improvement of the script to distribute EVs over available chargers also in case more than one EV arrives at the same time.

As indicated by the last bullet point, the script can search for free chargers and indicates the number of unsuccessful events, which gives an indication of the shortage or redundancy of EV chargers. Besides, the script can also reduce the power of charging whenever the rated power of the connected EV is lower than the one of the charging station.

Statistics were derived from the 2019-2020 data provided by the ROBUST project, to customize the simulator to the investigated district. A normal distribution was used to simulate the average driving distance between two charging sessions. A value of 2x21.7 km on average with a standard deviation of 20 km was obtained based on data from the discussed area [65]. Afterwards, the arrival time and charge duration time distributions were collected and inserted in the simulator. The simulation output statistics of these implementations were compared with the input statistics from ROBUST. The results are visualised in Figure 3-4 and Figure 3-5. It becomes clear that the distributions are comparable. The difference between the two is ought to be related due to randomisation used in the charge simulator. Furthermore, the connection time in the charge simulator was set to a maximum of 48 hours, which explains the larger range in connection hours for the actual data.

More statistics implemented in the charge simulator relate to the EV fleet. Based on data from [9] and [8], a hypothetical and simplified EV fleet was created. These EV parameters are shown in Figure 3-3 and kept constant for the four different scenarios. The car model types and their distribution are mainly based on the current EV fleet of the Netherlands [8] and future expectations found in [9]. The latter contains car models that will be out in a few years. Based on their price and driving range, the most interesting EVs were selected and a plausible distribution was assigned accordingly. Remark that the last row of Table 3-3 indicates the V2G capability. A rather high adoption rate of V2G functionality was adopted, to better understand the effect of this technology on the LV grid.

The EV uncontrolled charging profiles generated with the charge simulator and the adoptions as explained above, are displayed in Figure 3-6. This figure contains the aggregated EV load profiles. The EVs are charged on arrival at maximum charge power. Besides, also the weekly average charging power is plotted. As one can see, a clear charging peak can be observed in the late afternoon, mainly after 6 pm. Nevertheless, the charging statistics are derived from public charging points, meaning that the load peaks are assumed to be more irregular

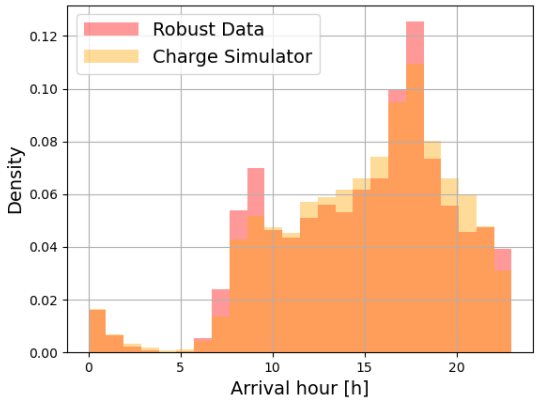

Figure 3-4: Comparison of ROBUST data with Charge Simulator output in terms of arrival hour.

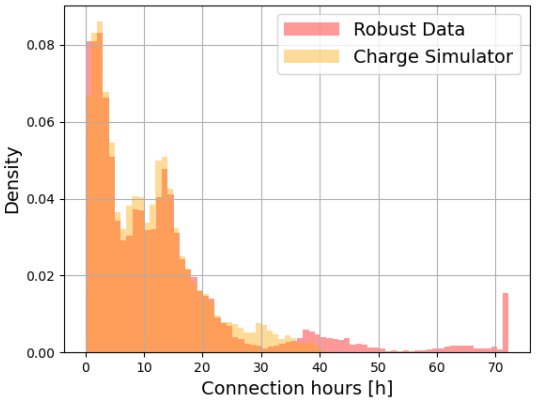

Figure 3-5: Comparison of ROBUST data with Charge Simulator output in terms of connection time.

Table 3-3: Car parameter input to the charge simulator [9, 8].

Car ID number	**1**	**2**	**3**	**4**	**5**	**6**	**7**	**8**
Reference model	Tesla Model 3	Kia Niro	Volkswagen ID.5 Pro Performance	Tesla Model S Long Range	Sono Sion	Renault ZOE - R110	Hyundai Kona	Mitsubishi Outlander
EV Type	BEV	BEV	BEV	BEV	BEV	BEV	BEV	PHEV
Range (km)	380	370	430	585	260	315	395	50
Milage (km/kWh)	6.6	7.1	5.6	6.2	5.5	6.0	6.2	3.7
Battery (kWh)	57.5	64.0	82.0	95.0	47.0	52.0	64.0	11.0
Charge Power(kW)	11	7.2	11	16.5	11	22	11	3.7
Distribution (%)	0.3	0.1	0.1	0.1	0.1	0.1	0.1	0.1
V2G (1=yes, 0=no)	1	0	0	1	1	1	1	1

compared to private charge profiles. Around 5 am no charging takes place because no new EVs arrive and all connected EVs are fully charged. In the weekend, that gap extend to 8 am in the morning considering the 2050 scenario.

Furthermore, Figure 3-7 shows a filled-area plot for which the colours indicate the level of flexibility provision for scenario week 2, 2050. Flexibility is defined as the number of hours the EV is connected with a full battery. The vertical axis of Figure 3-7 indicates the charging power that can be displaced and used in a later time period. As can be seen, some EVs (dark red) would not be able to provided flexibility due to a short connection time. This corresponds to 14.6% of all transactions of that week. Others provide a lot of flex due to longer connection times. Their flexibility can be provided by delayed charging or by discharging when equipped with V2G technology. Slightly more than one-third, 34.5%, of the EVs can even provide more than 10 hours of flexibility. Consequently, a lot of EVs flexibility can be used to comply with certain smart charging objectives. This will be addressed in the next chapter.

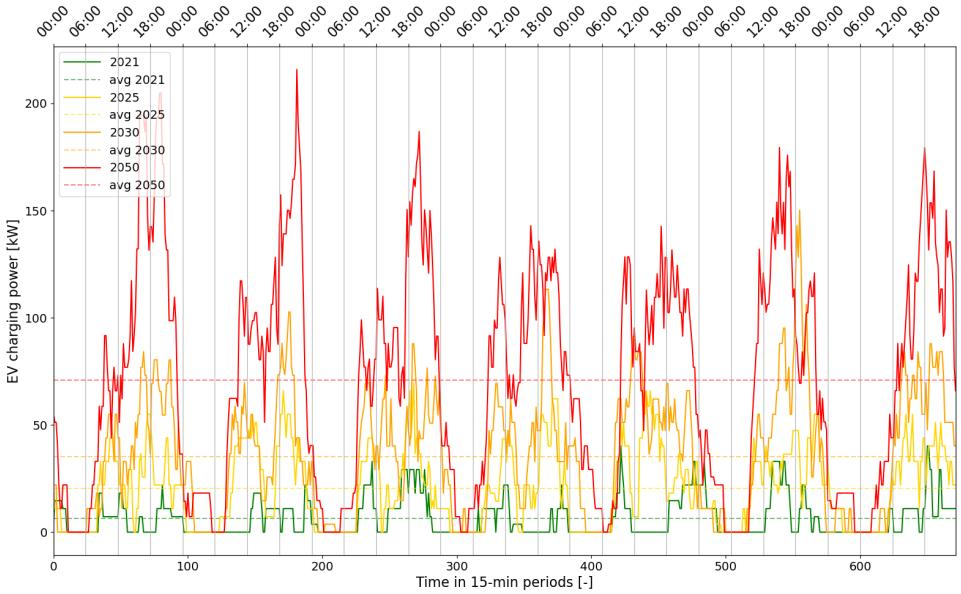

Figure 3-6: Aggregated charging power of charge simulator for week 2 and four different scenarios (year: 2021, 2025, 2030, 2050).

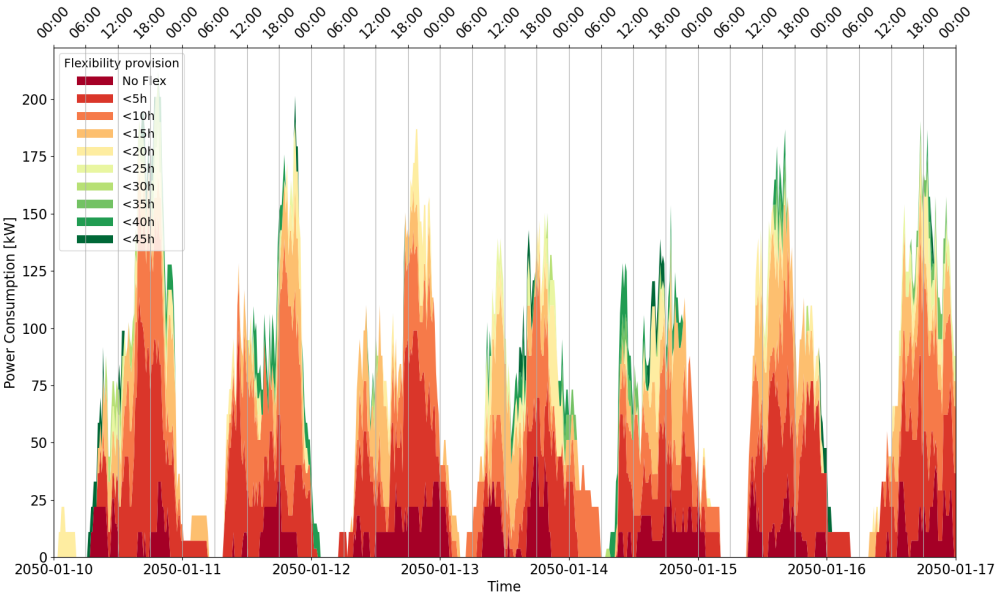

Figure 3-7: Aggregated flexibility of the connected cars week 2, 2050. The colours indicate the flexibility level which is the connection time left with full battery. The vertical axis indicates the amount of charging power that can be redistributed at that time.

Chapter 4

Smart Charging Model

A smart charging model has been developed that aims to comply with CPO benefits, DSO interests and the EV-owner satisfaction. This chapter contains the applied concepts in Section 4-1. It explains the principles used in the developed smart charging model. These principles are based on the knowledge gained after the literature study that was conducted in Chapter 2. Afterwards, Section 4-2 converts these principles into the mathematical optimisation formulation applied in this study. The Pyomo optimisation language in python was adopted to realise a working smart charging model.

4-1 Applied Concepts

A mathematical optimisation model was developed, to be able to optimally control the charging of an electric vehicle fleet. First of all, the model works in a **centralised way**. Although this has some disadvantages, as discussed in section 2-1-2, a centralised formulation can be appropriate in an urban context with a high number of charging stations. Especially with only one CPO that operates in the LV grid, a centralised model might be a suitable approach.

Second, the model makes use of the aforementioned **RHO concept**. That allows adjusting the charging of connected EVs based on foresight in electricity consumption and generation on the LV level. Furthermore, it ensures the desired SOC level. In MPC terminology, this desired SOC is regarded as the equilibrium or steady-state at the end of the EV connection period. This connection period can be seen as the **control horizon which is vehicle dependent**. The overall control horizon during a particular time step can be associated with the EV with the longest connection time at that time step.

Besides that, the **prediction horizon**, which includes predictions for the non-EV load, PV-generation and incentive data for charging, spans **24 hours or 96-time intervals**. That corresponds to discrete time steps of

15-minutes. In that way, charging can be delayed when there is enough flexibility meaning that the connection time is longer than the actual required time to charge. Predictions related to non-EV loads can be derived from historical records as applied in this work. However, a combination of historical data and weather data, amongst others can be used as well as input to an appropriate Machine Learning (ML) model to better predict the consumption behaviour and renewable generation on the LV level. This was regarded to be out of scope for this work. Similarly, for the weather data, instead of using historical weather data, actual weather forecasts and price forecasts for a 24-hour period would be more applicable in a real-life scenario.

Besides production or consumption data of the inflexible loads, also information related to the charging station should be provided. In general, the **model requires the initial SOC at arrival, V2G capability, the battery capacity and maximum charging power of the connected EVs and information about the maximum charging power and location of the charging station**. Most of this information can be related to the EV and charger ID; however, derivation of the SOC is less straightforward. In this work, it was assumed to be a known parameter, but in practice, this SOC should be estimated using ML related to the EV driving and charging patterns or other estimation methods provided by [54]. Most traffic is related to work and grocery shopping, which both show predictable patterns, meaning that the SOC can be estimated to some extent. A good estimation is crucial when charging gets delayed till the very last moment.

Transaction data for the optimisation was derived from the charge simulator and imported into the optimisation. An example of these transaction logs is displayed in Table 4-1. The charger ID indicates to which charging point the EV is connected. Data related to a particular car ID can be found in columns: V2G, initial SOC, car maximum power and maximum charging capacity. There are two columns that indicate the time: arrival time and departure time. They start counting on the first day of the week in 15 minutes time intervals. For instance, an arrival time of 4 in week 2 of 2050, would mean that the car starts charging on Jan 10 at 1:00 am.

When the time of the optimisation loop is equal to the arrival time of one of the EVs, the transaction constraints will be activated until the vehicle leaves. Until that moment, the desired SOC, V2G functionality, departure time, maximum capacity and maximum charging power is memorised by the model. Note that again two time indications are used in the optimisation: one for the actual time ($t^{\text{actual}} \in [0, 672[$ when regarding one week) and one for the horizon time ($t \in [0, 96]$). These times are also indicated in Figure 4-1 in *black* and *red*, respectively.

Figure 4-1 gives a schematic overview of the RHO principle applied in the optimisation model. It contains two example optimisation periods. These are also highlighted in *grey* in Table 4-1. Both periods contain 96-time intervals for which the constraints need to satisfy. In the first example, a vehicle enters the charging point with ID 0 at time $t = 4$. The expected connection time will be 20 hours, meaning 80-time steps. In that regard, the battery should be charged till the maximum obtainable SOC bounded by the upper level of 80%. Besides that, Table 4-1 indicates V2G $= 0$, meaning that only charging can take place. For the second example, discharging can take place because V2G $= 1$. Nevertheless, the control horizon equals only 18-time steps or 4.5 hours, which reduces the flexibility provision. The SOC profiles of both examples are indicated with dashed lines; however, a full line is used for the first time step. That is because only the solution of the first time step will be implemented. The solution of the other time steps can change when time proceeds due to new collected information.

Table 4-1: Charging transactions for part of week 2 (2050) at charging points 0 and 1.

Charger ID	V2G	Arrival Time	Departure Time	Initial SOC [%]	Desired SOC [%]	Max. Power EV [kW]	Max. Energy Capacity EV [kWh]
0	0	4	84	37.0	80.0	11.0	82.0
1	0	67	127	20.0	80.0	7.2	64.0
0	1	86	131	73.0	80.0	16.5	95.0
1	1	129	147	33.0	80.0	11.0	57.5
0	0	134	135	49.0	80.0	11.0	82.0
0	0	139	172	47.0	80.0	7.2	64.0
1	1	166	194	20.0	80.0	3.7	11.0
0	1	179	198	46.0	80.0	11.0	57.5
0	1	230	246	30.0	80.0	11.0	47.0
0	1	253	288	34.0	80.0	11.0	57.5
1	1	265	278	20.0	80.0	22.0	52.0
1	0	279	324	70.0	80.0	11.0	82.0
0	0	321	383	36.0	80.0	11.0	82.0
1	1	326	388	20.0	80.0	11.0	57.5
...	...	...	...	...	...	...	...

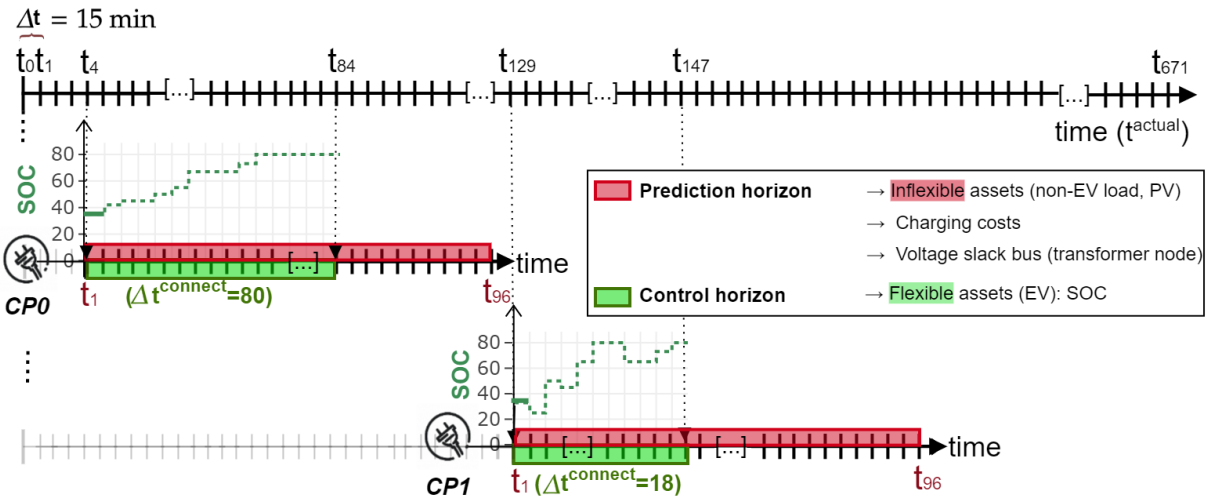

Figure 4-1: Receding horizon principle applied in the smart charging model.

An example of the actual optimised charging profiles at the first two charging points is displayed in Figure 4-2, together with the SOC of the connected car. All corresponding transactions are again provided by Table 4-1 to be able to verify the outputs of the charging profiles. The transactions are ordered in terms of arrival time (3rd column of Table 4-1). A SOC of zero in the bottom plot means that no EV is connected to the charging point, this can be cross-checked with Table 4-1.

Finally, it is important to specify the premise of the model to be able to justify the mechanisms and objectives behind it. **The model is developed from the viewpoint of CPO or aggregator (sometimes the same party). Their goal is to make maximum profits by still complying with the interests of the DSO. In the**

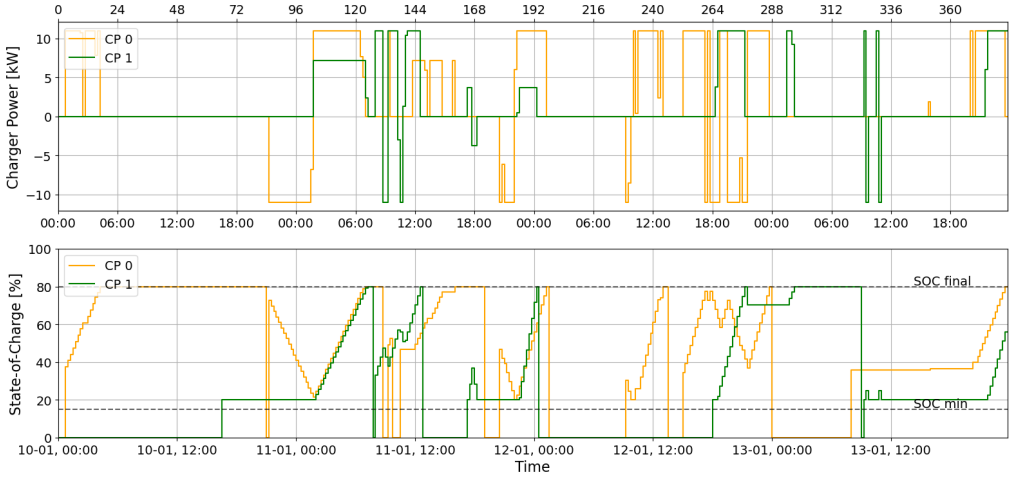

Figure 4-2: Charging profiles at charging points 0 and 1 during week 2, 2050.

long term, that relates to delaying grid reinforcement of the LV grid. In the short term, they provide services such that curtailment by the DSO can be avoided. In this regard, the charging of EVs will need to happen as much as possible during off-peak moments, resulting in valley-filling. In principle, the following concept holds: the flatter the transformer load; the lower the power losses, the more capacity the grid can host and the longer the delay of infrastructural updates. It is far-most important that no additional load peaks are created by using an inappropriate objective function and a lack of constraints. Furthermore, **the needs of the EV owners are to be fulfilled, meaning that their desired SOC should be reachable**. If the model fails to comply with these criteria on a regular basis, the DSO should be stimulated to reinforce the grid where needed. Of course, this only holds when the model is able to use the EVs' charging flexibility to full extent and in a proper way. Further details about the optimisation formulation are given below in Section 4-2.

4-2 Optimisation Formulation

Mathematical optimisation contains three distinct components: an objective function, decision variables and constraints. On top of that, parameters and state-variables can be defined as well. The generic formulation of the optimisation problem is shown in (4-1):

$$\begin{cases} \min & f(\mathbf{x}, \mathbf{y}) \\ \text{s.t.} & h(\mathbf{x}, \mathbf{y}) = 0 \\ & g(\mathbf{x}, \mathbf{y}) \leq 0 \end{cases} \tag{4-1}$$

In this formulation, f represents the objective functions, which should be minimised. The constraints to this problem can either be equality (h) or inequality constraints (g). The corresponding variables and parameters as well as the sets to which they belong are described below.

4-2-1 List of Optimisation Symbols

Table 4-2 below contains a list of all symbols related to the optimisation formulation. They are classified in terms of sets, decision variables, state variables and parameters related to charging transactions and power flow modelling. The symbols are used in the equations contained in this Section.

Table 4-2: Symbols related to the optimisation model.

Symbol	Definition	Set(s)
Sets		
Ω_{T}	Set of time periods (horizon length) $\{t \in \mathbb{N} \mid 1 \leq t \leq 96\}$	
Ω_{C}	Set of charging points entire grid $\{c \in \mathbb{N} \mid 1 \leq c \leq 64\}$	
Ω_{S}	Set of charging points sub-grid $\{s \in \mathbb{N} \mid s \in \Omega_{\mathrm{C}}\}$	
Ω_{B}	Set of nodes $\{b \in \mathbb{N}_0 \mid 0 \leq b \leq 504\}$	
Ω_{P}	Set of nodes with a charger connected $\{p \in \Omega_{\mathrm{B}}\}$	
Ω_{L}	Set of lines $\{l \in \mathbb{N}_0 \times \mathbb{N}_0 \mid l = (i,j) \in \Omega_{\mathrm{B}} \times \Omega_{\mathrm{B}} \wedge i \neq j \wedge i, j$ = binding nodes $\}$	
Ω_{Φ}	Set of phases $\{a, b, c\}$	
Ω_n	Set of cutting planes $\{n \in \mathbb{N} \mid 1 \leq n \leq N\}$	
Decision variables		
$\mathrm{P}_{t,c}$	Three-phase active (dis)charging power at time t, charging point c [p.u.]	$\forall t \in \Omega_{\mathrm{T}}, c \in \Omega_{\mathrm{C}}$
State variables related to charging transactions		
$\mathrm{P}_t^{\mathsf{ll}}$	Low-cost charging power at time t [p.u.]	$\forall t \in \Omega_{\mathrm{T}}$
$\mathrm{P}_t^{\mathsf{ml}}$	Medium-cost charging power at time t [p.u.]	$\forall t \in \Omega_{\mathrm{T}}$
$\mathrm{P}_t^{\mathsf{hl}}$	High-cost charging power at time t [p.u.]	$\forall t \in \Omega_{\mathrm{T}}$
$\mathrm{P}_t^{\mathsf{Dis}}$	Discharged power at time t [p.u.]	$\forall t \in \Omega_{\mathrm{T}}$
$\mathrm{SOC}_{t,c}$	State-of-charge for car at charging point c and time $t \in$ [0,1]	$\forall t \in \Omega_{\mathrm{T}}, c \in \Omega_{\mathrm{C}}$
α_c	Fraction of the desired SOC ($\overline{\mathrm{SOC}}_c^*$) obtained at departure time (t_c^{dep}) $\in [0,1]$	$\forall c \in \Omega_{\mathrm{C}}$
State variables related to power flow modelling		
$\Gamma_{t,l,\phi,n}$	Approximated current magnitude at time t, line l, phase ϕ, intersecting plane n [p.u.]	$\forall\, t \in \Omega_{\mathrm{T}},\, l \in \Omega_{\mathrm{L}},\, \phi \in \Omega_{\phi},\, n \in \Omega_{\mathrm{n}}$
$\Psi(z)$	Approximated Euclidean norm of vector z	
$\mathbf{I}_{t,l}$	Vector of three-phase currents at line l, time t [p.u.]	$\forall t \in \Omega_{\mathrm{T}}, l \in \Omega_{\mathrm{L}}$
$\mathbf{I}_{t,p}^{\mathsf{c}}$	Vector of three-phase currents from the charging point at node p, time t [p.u.]	$\forall t \in \Omega_{\mathrm{T}}, p \in \Omega_{\mathrm{P}}$
$\mathbf{I}_{t,b}^{\mathsf{inflex}}$	Vector of three-phase currents from the non-EV loads and PV at node b, time t [p.u.]	$\forall t \in \Omega_{\mathrm{T}}, b \in \Omega_{\mathrm{B}}$
$\mathbf{I}_{t,b}^{\mathsf{s}}$	Vector of three-phase currents from substation at node b, time t [p.u.]	$\forall t \in \Omega_{\mathrm{T}}, b \in \Omega_{\mathrm{B}}$
$\mathrm{P}_{t,c,\phi}$	Single-phase active power at time t, charging point c [p.u.]	$\forall t \in \Omega_{\mathrm{T}}, c \in \Omega_{\mathrm{C}}, \phi \in \Omega_{\phi}$
$\mathrm{Q}_{t,c,\phi}$	Single-phase reactive power at time t, charging point c [p.u.]	$\forall t \in \Omega_{\mathrm{T}}, c \in \Omega_{\mathrm{C}}, \phi \in \Omega_{\phi}$
$\mathbf{V}_{t,b}$	Vector of phase voltages at node b, time t [p.u.]	$\forall t \in \Omega_{\mathrm{T}}, b \in \Omega_{\mathrm{B}}$
$\mathcal{V}_{t,b,\phi}$	Rotated nodel voltages at time t, node b and phase ϕ [p.u.]	$\forall t \in \Omega_{\mathrm{T}}, b \in \Omega_{\mathrm{B}}$ $\phi \in \Omega_{\phi}$
⋮	⋮	⋮
⋮	⋮	⋮
⋮	⋮	⋮
⋮	⋮	⋮
⋮	⋮	⋮
⋮	⋮	⋮
⋮	⋮	⋮

Symbol	Definition	Set(s)
Parameters related to charging transactions		
Δt	Duration of the time period (0.25 h)	
$\mathrm{c}_t^{\mathsf{DA}}$	Day-ahead price at time t [€/kW/15min]	$\forall t \in \Omega_{\mathrm{T}}$
c^{LL}	Low-Level cost of charging [€/kW/15min]	
c^{ML}	Medium-Level cost of charging [€/kW/15min]	
c^{HL}	High-Level cost of charging [€/kW/15min]	
$\mathrm{c}^{\mathsf{Dis}}$	Discharge price [€/kW/15min]	
m	Weight factor for variable α_c	
η	Charge- and discharge Efficiency	
t_c^{dep}	Departure time at charging point	$\forall c \in \Omega_{\mathrm{C}}$
$\overline{\mathrm{P}}_{t,c}$	Maximum rated active charging power [kW] at charging point	$\forall t \in \Omega_{\mathrm{T}}, c \in \Omega_{\mathrm{C}}$
$\underline{\mathrm{P}}_{t,c}$	Minimum rated active discharging power at charging point [kW]	$\forall t \in \Omega_{\mathrm{T}}, c \in \Omega_{\mathrm{C}}$
$\underline{\mathrm{SOC}}_c^{\mathsf{init}}$	Initial state-of-charge for car at charging point c	$\forall c \in \Omega_{\mathrm{C}}$
$\overline{\mathrm{SOC}}_c$	Maximum SOC for car at charging point c	$\forall c \in \Omega_{\mathrm{C}}$
$\underline{\mathrm{SOC}}_c$	Minimum SOC at charging point	$\forall c \in \Omega_{\mathrm{C}}$
$\overline{\mathrm{SOC}}_c^*$	Desired state-of-charge at charging point	$\forall c \in \Omega_{\mathrm{C}}$
$\overline{\mathrm{E}}_c$	Maximum battery capacity at charging point [kWh]	$\forall c \in \Omega_{\mathrm{C}}$
t_c^{dep}	Departure time at charging point	$\forall c \in \Omega_{\mathrm{C}}$
μ_c^{V2G}	V2G functionality $\in \{0, 1\}$	$\forall c \in \Omega_{\mathrm{C}}$
p^{tf}	Normalised predicted transformer load including PV and non-EV load [p.u.]	$\forall t \in \Omega_{\mathrm{T}}$
$\mathrm{P}_t^{\mathsf{ll*}}$	Available low-cost charging power at time t [kVA]	$\forall t \in \Omega_{\mathrm{T}}$
$\mathrm{P}_t^{\mathsf{ml*}}$	Available medium-cost charging power at time t [kVA]	$\forall t \in \Omega_{\mathrm{T}}$
$\mathrm{P}_t^{\mathsf{hl*}}$	Available high-cost charging power at time t [kVA]	$\forall t \in \Omega_{\mathrm{T}}$
Parameters related to power flow modelling		
pf_c	Powerfactor of each charging point	$\forall c \in \Omega_{\mathrm{C}}$
p^{tf}	Allowed transformer loading percentage	
$\mathrm{V}_t^{\mathsf{tap}}$	Nominal predicted tap position at time t [p.u.]	$\forall t \in \Omega_{\mathrm{T}}$
V_0	Nominal voltage, [kV]	
$\overline{\mathrm{V}}$	Maximum voltage magnitude [V]	
$\underline{\mathrm{V}}$	Minimum voltage magnitude [V]	
$\overline{\mathrm{P}}^{\mathsf{grid}}$	Nominal system power [kVA]	
N	Number of intersecting planes current approximation	
$\mathrm{P}_{t,b,\phi}^{\mathsf{inflex}}$	Consumed or generated power from non-EV loads and PV at time t and node b [kVA]	$\forall t \in \Omega_{\mathrm{T}}, b \in \Omega_{\mathrm{B}}, \phi \in \Omega_{\phi}$
β	Coefficient for voltage magnitude approximation	
λ	Coefficient for voltage magnitude approximation	
Θ	Range angle for voltage magnitude approximation [°]	
$\mathcal{J}_{\phi}$	Rotation coefficient for phase ϕ	$\forall \phi \in \Omega_{\phi}$
$\overline{\mathrm{I}}_l$	Maximum current magnitude at line $l[A]$	$\forall l \in \Omega_{\mathrm{L}}$
$\mathbf{S}_{t,b}^{\mathsf{inflex}}$	Vector of complex loads, pv at node k, period t [p.u.]	$\forall t \in \Omega_{\mathrm{T}}, b \in \Omega_{\mathrm{B}}$
$\mathbf{V}_{t,b}^0$	Vector of estimated phase voltage at node b, time t	$\forall t \in \Omega_{\mathrm{T}}, b \in \Omega_{\mathrm{B}}$
$\mathbf{Y}_{(i,j)}$	Admittance submatrix of line l, with nodes (i,j)	$\forall (i,j) \in \Omega_{\mathrm{L}}$

4-2-2 Objective Function

EVs in the Netherlands are mostly charged using a flat, single or double (day-night) tariff structure. It mainly results in *charge-on-arrival*, or uncontrolled charging. In general, time-varying prices are seen by many authors and institutions as a requirement to unlock the flexibility potential of EVs [3, 35]. In the case of the CPO, this might lower his expenses. Currently, many of these CPOs already contract energy supplying companies to get charged by Day-Ahead (DA) prices. Especially with political and supply instabilities, this particularly becomes interesting. Furthermore, these DA prices somehow reflect how *green* the contracted electricity will be. That is because lower prices are usually accompanied by periods of much wind and solar energy. As a consequence, a lower electricity price is beneficial for the CPO but might also be for the environment. In that way, EVs charging can be scheduled at times of abundant renewable energy generation as long as it complies with the requirements of the EV owner and DSO. Therefore, also stationary grid batteries can be reduced to a bare minimum. Nevertheless, smart charging purely based on day-ahead prices, is not always found to be appealing to the DSO. That was also found by [66]. To better integrate EVs in the LV grid, an adjusted pricing scheme will be needed. **Therefore in this study, after investigating the effect of using DA prices only, a Stacked Tariffs (ST) scheme based on the DA prices was implemented as well.** A similar stacked tariff scheme already runs in the *FLEET* pilot project in Utrecht [1]. On the one hand, the goal is to **reduce congestion and voltage problems in the grid while minimising CPO costs**. For downstream congestion in the feeders as well as voltage problems at the nodes, grid constraints might be needed additionally. On the other hand, the aim is to **balance out the loading at the transformer level**, which should allow for more capacity to be connected to the grid as well as reduce power losses. The stacked tariff structure should help by discouraging loading above a certain level. In fact, the used stacked tariff structure contains the same day-ahead prices with an additional volumetric tariff stacked on top of it that discourages high loading. For the latter, the DSO should be able to apply an additional monetary incentive to the CPO based on the predicted baseload (non-EV load). Related to that, in 2019, the European Commission updated the European Electricity Directive on the Internal Market for Electricity (2019/943). Section 2, Article 18, item 8 states:

> *Charges for access to networks, use of networks and reinforcement:*
>
> *8.* ***Distribution tariff methodologies*** *shall provide incentives to distribution system operators for the most cost-efficient operation and development of their networks including through the procurement of services. For that purpose* ***regulatory authorities shall recognise relevant costs as eligible****, shall include those costs* ***in distribution tariffs, and may introduce performance targets*** *in order to provide incentives to distribution system operators to* ***increase efficiencies*** *in their networks, including through energy efficiency,* ***flexibility and the development of smart grids*** *and intelligent metering systems.* [67]

In principle, together with proper national legislation (Authoriteit Consument en Markt (ACM) in the Netherlands), the DSO should be able to stimulate customers such that congestion is avoided as much as possible. This statement was also the resolution of an extensive study on smart charging in the Netherlands on behalf of Elaad [61]. They advocate financial tariff that encourages more flexibility allocation of loads to avoid congestion and a large mismatch between supply and demand.

Nevertheless, the financial tariff structure applied in this thesis, as derived from [1], is still a proof-of-concept. No further optimisation of the tariff structure is applied. However, the principles are used to compare against the more traditional day-ahead tariff scheme, especially in terms of loading and load fluctuation at transformer level. Furthermore, **the effect of V2G with this new tariff scheme is investigated**, which was not done

before. Table 4-3 gives an overview of the ST scheme. Besides, Figure 4-3 schematises the working principle of the ST. It consists of the DA price and an additional volumetric tariff which is divided into three different cost components: low-level cost for loading up to 60% of transformer-rated power, medium-level costs for loading up to 80% and high-level costs for loading above 80% of transformer rated power. The actual amount of power that can be charged at each level depends on the transformer load predictions of the DSO. Furthermore, the highest power level can be constrained by 100% depending on the selected scenario (see case studies Section 5-2).

Table 4-3: Decomposed stacked tariff structure for the CPO.

Tariff	**Day-ahead electricity tariff component on hourly basis**	**Additional volumetric baseload-based tariff component on 15 minutes basis**
Outgoing party	Contracted energy company	DSO
Goal	Reducing the need for grey electricity	More valley-filling and congestion reduction
Source	ENTSO-E (hourly resolution, day-ahead)	Transformer load predictions DSO (excluding EVs, day-ahead)

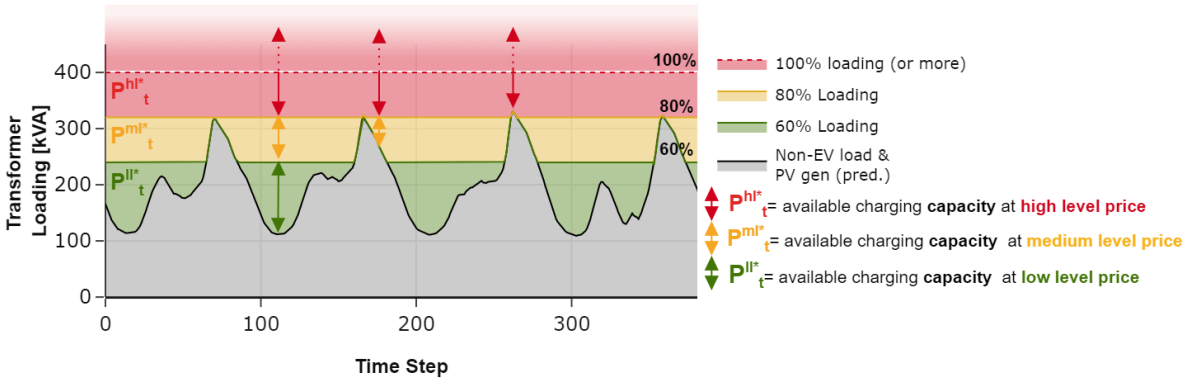

Figure 4-3: Diagram explaining the stacked tariff principle.

The corresponding objective function as in (4-2) entails the integration of the stacked pricing scheme. When only considering day-ahead prices, the first three terms of the sum are omitted. The reader is referred to Table 4-2 to understand all the used symbols.

$$\min \left(\sum_{t \in \Omega_{\mathrm{T}}} \Delta \mathrm{t} (\mathrm{c}^{\mathrm{ll}} \mathrm{P}^{\mathrm{ll}}_t + \mathrm{c}^{\mathrm{ml}} \mathrm{P}^{\mathrm{ml}}_t + \mathrm{c}^{\mathrm{hl}} \mathrm{P}^{\mathrm{hl}}_t + \mathrm{c}^{\mathrm{DA}}_t \sum_{c \in \Omega_{\mathrm{C}}} \mathrm{P}_{t,c}) - \sum_{c \in \Omega_{\mathrm{C}}} m \alpha_c \right) \tag{4-2}$$

The objective is to minimise this function. It contains two main terms, one for the CPO cost optimisation and one for allowing a desired SOC level. The latter is related to the last term in Equation (4-2). m is a constant parameter big enough to ensure that α_c is as close as possible to its upper boundary 1. That leads to the desired SOC level. The meaning of this variable α_c will become more clear in the section below. Logically the following relation holds: $\mathrm{c}^{\mathrm{ll}} < \mathrm{c}^{\mathrm{ml}} < \mathrm{c}^{\mathrm{hl}}$.

4-2-3 Constraints related to the Charging Transactions

When a car enters a particular charging point, the constraints related to the charging transaction are activated until the vehicle leaves again. These constraints are listed in the text below.

Equation (4-3) represents the **lower and upper limits of the SOC** of the EV, these limits are fixed and equal to 20 % and 80 %, respectively. These limits are chosen according to a study that investigates optimal bounds using real-world EV charging data [68]. **Charge power limitations** are included in the model by Equation (4-4). Basically, the charging power is limited by the minimum of the rated power of the charging station or the EV.

$$\underline{\mathrm{SOC}}_c \leq \mathrm{SOC}_{t,c} \leq \overline{\mathrm{SOC}}_c, \quad \forall t \in \Omega_{\mathrm{T}}, c \in \Omega_{\mathrm{C}} \tag{4-3}$$

$$\underline{\mathrm{P}}_{t,c} \leq \mathrm{P}_{t,c} \leq \overline{\mathrm{P}}_{t,c}, \quad \forall t \in \Omega_{\mathrm{T}}, c \in \Omega_{\mathrm{C}} \tag{4-4}$$

Equation (4-5) is used to make sure that the **final SOC is reached** at the end of the charging period. This final SOC is constrained by one of the following parameters: **the departure time, the prediction horizon in case the departure time is larger than 24 hours, or the SOC level of 80$\%$.** In the first case, the battery should be charged continuously on maximum power. The second case for which the SOC is limited by the horizon length, will rarely occur. That is because the longest needed charging time is for the *Tesla Model S - long range* as seen in Table 3-3. The longest charging time corresponds to charging from 20$\%$ to 80$\%$ SOC and equals 24.4 hours. Considering that most cars barely connect for longer than 24 hours, justifies the prediction horizon of 24 hours. Besides, most price, generation and load data are also contained in one entire day, which allows for the best flexibility distribution. In the last case, the connection time of the EV is long enough to reach the maximum SOC of 80$\%$. That means that a vehicle with V2G capability can also discharge a certain amount of its battery capacity during the connection time. EV discharging is enabled by multiplying the minimum power with the parameter $\mu^{V2G} \in \{0, 1\}$. If $\mu_c^{V2G} = 0$, meaning no $V2G$ functionality, then $\underline{\mathrm{P}}_c$ becomes 0. If $\mu_c^{V2G} = 1$, the maximum discharge power becomes equal to minus the maximum charge power: $\underline{\mathrm{P}}_c = -\overline{\mathrm{P}}_c$

$$\mathrm{SOC}_{t,c} = \overline{\mathrm{SOC}}_c^* \alpha_c, \iff \mathrm{t} = \mathrm{t}_{\mathrm{c}}^{\mathsf{dep}}, \forall c \in \Omega_{\mathrm{C}} \tag{4-5}$$

A state-of-charge equality constraint is introduced to update the state of the EV's battery. When an EV connects, the initial SOC is first read by Equation (4-6). The update till the departure time happens by Equation (4-7). The equation is multiplied by the nominal grid power, because $\mathrm{P_{t,c}}$ was initially normalised by $\overline{\mathrm{P}}^{\mathrm{grid}}$. The charging and discharging efficiency (η) was set to 1, because of the linear programming implementation without mixed integers. However, in principle, according to Schram et al. [69], the round-trip efficiency for charging and discharging of EV should be around 87%. This would lead to a charge- or discharge efficiency of $\eta = 93\%$ [69]. They tested this for car types and charging stations, similar to the ones that are or will be installed in the investigated district [69].

$$\begin{cases} \mathrm{SOC_{t,c}} = \mathrm{SOC_c^{init}} \iff \mathrm{t} = 1 & \text{(4-6)} \\ \mathrm{SOC_{t,c}} = \mathrm{SOC_{t-1,c}} + \dfrac{\mathrm{P_{t-1,c}\Delta t}}{\overline{\mathrm{E_c}}}\overline{\mathrm{P}}^{\mathsf{grid}}\eta \quad \forall t : 1 < t < t_c^{\mathsf{dep}} & \text{(4-7)} \end{cases}$$

$$\sum_{c\in\Omega_\mathrm{C}} \mathrm{P}_{t,c} = \mathrm{P}_t^{\mathsf{ll}} + \mathrm{P}_t^{\mathsf{ml}} + \mathrm{P}_t^{\mathsf{hl}} + \mathrm{P}_t^{\mathsf{Dis}} \quad \forall t \in \Omega_\mathrm{T} \tag{4-8}$$

Finally, Equations (4-8) and (4-10) are introduced and relate to the **stacked tariff scheme**. Equation (4-8) makes sure that the stacked power levels equal the sum of all the total aggregated charging powers. In case the net of this aggregated charging power is smaller than zero, the left side of (4-8) becomes equal to $\mathrm{P_t}^{\mathsf{Dis}}$. The other right side terms will become zero due to the following relation (4-9):

$$\mathrm{c}^{\mathsf{Dis}} = 0 < \mathrm{c}^{\mathsf{ll}} < \mathrm{c}^{\mathsf{ml}} < \mathrm{c}^{\mathsf{hl}} \tag{4-9}$$

If the aggregated charging power is negative, the model will automatically assign the total discharge capacity to $\mathrm{P}_t^{\mathsf{Dis}}$. If that is not the case, then at least P_t^{ll} is non-zero implying an additional electricity cost equal to $c^{\mathsf{ll}}\mathrm{P}_t^{\mathsf{ll}}\Delta t$. This would not happen with cost minimisation in the objective function. In the end, this reasoning allows to disregard binary variables which would make the problem a MILP optimisation.

The opposite happens when the aggregated power is net positive. In that case, $\mathrm{P}_t^{\mathsf{Dis}}$ becomes equal to zero and the other terms can take every kind of value that belongs to the intervals as defined in Equation (4-10). Equation (4-10) constraints each power level according to the allowed aggregated charging power in each group. Refer to Figure 4-3, for the correct interpretations of $\mathrm{P}_t^{\mathsf{ll}^*}, \mathrm{P}_t^{\mathsf{ml}^*}, \mathrm{P}_t^{\mathsf{hl}^*}$.

$$0 \le \mathrm{P}_t^{\mathsf{ll}} \le \mathrm{P}_t^{\mathsf{ll}^*}, \quad 0 \le \mathrm{P}_t^{\mathsf{ml}} \le \mathrm{P}_t^{\mathsf{ml}^*}, \quad 0 \le \mathrm{P}_t^{\mathsf{hl}} \le \mathrm{P}_t^{\mathsf{hl}^*}, \quad \mathrm{P}_t^{\mathsf{Dis}} \le 0 \quad \forall t \in \Omega_\mathrm{T} \tag{4-10}$$

4-2-4 Constraints related to Power Flow Modelling

When the objective function fails to allocate EVs properly, causing congestion or voltage problems, extra constraints are needed to avoid these problems. These constraints are listed in Equation (4-11) and Equation (4-12). These two equations are related to current and voltage limitations in the lines and nodes, respectively. The voltage was limited to $\mathrm{V}_0 = 1 \pm 0.05$ [p.u.] as explained in Section 3-1. Constraints related to phase unbalance were not implemented due to the assumed 3-phase nature of the public EV chargers. Nevertheless, a transformer limit was implemented for some of the scenarios by limiting the aggregated sum of loads and generation. No power flow modelling was needed for that.

$$\|\mathbf{I}_{t,l}\|_2 \le \bar{\mathrm{I}}_l, \forall l \in \Omega_\mathrm{L}, t \in \Omega_\mathrm{T} \tag{4-11}$$

$$\underline{\mathrm{V}} \leq \|\mathbf{V}_{b,t}\|_2 \leq \overline{\mathrm{V}}, \forall b \in \Omega_{\mathrm{B}}, t \in \Omega_{\mathrm{T}} \tag{4-12}$$

Although both equations (4-11), (4-12) are non-linear, the aim is to linearise them in order to obtain a linear-AC OPF formulation. That also complies with the linear optimisation model. The problem with the non-linearity in these equations is related to the euclidean norm. Besides, introducing voltage and current constraints requires the introduction of OPF equations to model the LV grid. On its turn, this requires a three-phase linear power flow model. The effectiveness of such a model, can be compared with the Newton-Raphson model used by PowerFactory.

The power flow formulation used for modelling the grid constraints, was derived from a recent paper [4]. Giraldo et al., 2021 [4] published a new AC-linear OPF model, which shows better results both in terms of computational time and accuracy compared to the described bench-marking models in the paper. The OPF model considers three phases, allowing for both single and three-phase loads as is the case in this study. Furthermore, the paper includes a new representation of the Euclidean norm for both nodal voltage and branch current approximations. The voltage magnitudes are approximated by the linear combination of the 1-norm and infinity norm. After linearly rotating the voltages and finding the regression coefficients, an accurate linearised voltage magnitude approximation can be found. The theory and corresponding equations related to the AC-linear OPF model can be found in Appendix D. This also includes the theory behind the euclidean norm approximation of the line currents. This was based on a generalised piece-wise linear approximation used in [70]. It makes use of cutting planes (N). The more cutting planes are used, the better the non-linear line currents can be estimated with a linear formulation. Nevertheless, this is at the expense of computational time.

The voltage at the transformer node, which is used to estimate the other nodal voltages, was derived by running an initial three-phase linear power flow in PowerFactory containing all inflexible loads. Besides, the current, power and voltage variables were normalised to p.u. values using the following formulas (4-13):

$$\mathrm{I}^{\text{p.u.}} = \frac{\mathrm{IV}_0}{(\overline{\mathrm{P}^{\text{grid}}}/3)} \quad , \mathrm{V}^{\text{p.u.}} = \frac{\mathrm{V}}{\mathrm{V}_0} \quad , \mathrm{P}^{\text{p.u.}} = \frac{\mathrm{P}}{(\overline{\mathrm{P}^{\text{grid}}}/3)} \tag{4-13}$$

A first test of the optimisation model including grid constraints was executed on a small-scale model with 17 nodes. After promising results for the current and voltage, the same formulation was transferred to the actual LV grid containing 506 nodes. The error validation related to the LV grid can be found in the next chapter, Section 5-2-4.

Chapter 5

Results & Discussion

This chapter discusses the performance of the applied smart charging model as well as the effect of uncontrolled charging on the discussed LV grid. Several scenarios are investigated and listed below in Table 5-1. Each scenario has a label related to it, which will be used to refer to the respective scenario further down this report. The uncontrolled scenarios were analysed on voltage and congestion problems. The results can be found in Section 5-1. The controlled scenario results can be found Section 5-2. They were compared and assessed based on their adequacy to comply with DSO, CPO and EV-user interests.

Table 5-1: Overview table of the investigated scenarios for both uncontrolled and controlled charging.

Label	Controlled	Price Structure	Grid Constraints	V2G	Period	Thesis Section
1.1-1.8	No	None	None	No	2021, 2025, 2030, 2050 Summer: **1.1 - 1.4** Winter: **1.5 - 1.8**	5-1, 5-2
2.1	Yes	Day-Ahead	None	Yes	2050, winter	5-2
2.2	Yes	Day-Ahead	T-Limit	Yes	2050, winter	5-2
2.3	Yes	Day-Ahead	Sub-grid	Yes	2050, winter	5-2
2.4	Yes	stacked tariffs	T-Limit	No	2050, winter	5-2
2.5	Yes	stacked tariffs	None	Yes	2050, winter	5-2
2.6	Yes	stacked tariffs	T-Limit	Yes	2050, winter	5-2
2.7	Yes	stacked tariffs	Sub-grid	Yes	2050, winter	5-2

5-1 Non-Optimised Charging

The results of the grid impact associated with uncontrolled charging can be found in this section. First of all, with the collected PV, EV and baseload (non-EV load) data from Chapter 3, power flow simulations were run in DIgSILENT PowerFactory 2022 [33]. This was done for eight different cases related to a winter and summer week of the years 2021, 2025, 2030 and 2050. Afterwards, a scenario analysis method was used, containing four important indicators: frequency, concurrency, location and severeness of the events. All these four indicators were introduced to analyse bus voltage and transformer or line loading. The abbreviations Transformer (T), Line of the Transformer (LT) and Lines (L) are used in the text below. The latter denotes all downstream LV lines, excluding the LT. A line forms the interconnection between two nodes, each of which can carry a load (e.g. household connection). The LT, is the line that connects the transformer station with all downstream feeders. Therefore, it contains the aggregated load of the entire LV network. The distinction between LT and L was made, because of the higher importance related to the LT. Congestion in this line is more worrying as the entire LV grid depends on it. The most important results and discussion can be found below.

5-1-1 Frequency of the Events

Event frequency is used to describe how many times during the selected week a certain threshold is exceeded. This frequency was calculated for five classes or sets: transformer congestion (T-CON), congestion in the transformer line (LT-CON), congestion in the other downstream lines (L-CON), as well as overvoltage and undervoltage problems in these lines (L-OV, L-UV respectively). Remark that L-OV and L-UV are defined for the first node of that line in PowerFactory. This is the node closest to the transformer.

Figure 5-1 shows a bar plot containing the frequency analysis of the uncontrolled scenarios. The first four plots correspond to the summer scenarios, the bottom four plots to the winter scenarios. The horizontal axis contains the five classes, the vertical axis the frequency of occurrence γ. That frequency is defined by the following formula (5-1):

$$\gamma = \frac{|\Omega^*|}{|\Omega|}, \quad \text{with} \quad \Omega^* \subset \Omega \wedge |\Omega| = 672 \tag{5-1}$$

The set Ω^* contains all the time points t, with $0 \leq t < 672$, that fulfil a certain class criterion, for instance congestion in the lines (L-CON). For the congestion of T, LT and L, the criterion is 100% loading of the components. The loading percentage is in its turn based on the rated current of the components.

From the barplots, several conclusions can be drawn. It becomes clear that grid problems related to loading and voltage are not frequent during the summer scenarios. Only in scenario 1.4 problems related to congestion begin to form, although the frequency for this summer week is still relatively low. Figure 3-2 and Figure 3-1 in Chapter 3 already indicated a much lower baseload in summer than in winter. Looking at the **winter scenarios, problems already emerge in 2025 at the transformer level. In 2050, all problem classes besides L-OV are detected.** The latter would not make sense during winter, as no V2G was applied yet, and the solar production is only minor. During summer, L-OV was not observed as well. That might be related to the low PV adoption rate assumed in this study.

When focusing on the **worst-case scenario 1.8**, it is important to stress that not all event classes are equally problematic. Line undervoltage does not occur too often to become a problem. Besides, transformers can mostly cope with higher currents than their rating indicates. As a consequence and due to power losses that were not included, for the controlled scenarios a more flexible limit of around 120% was adopted. According to [40] that is a reasonable assumption to implement. The most significant problem is the congestion in the transformer line. As this contains a circuit breaker, it is important to restrict the loading to avoid tripping. That would result in a disconnection and possible black-out of the entire LV grid with the upstream network.

From these barplots **one can conclude that a transformer and transformer line upgrade will be needed towards 2050 if EVs' flexibility is not used optimally.** A transformer upgrade to 630 kVA would be possible [16]. The transformer line can be reinforced from 0.63 kA to 1 kA, for instance.

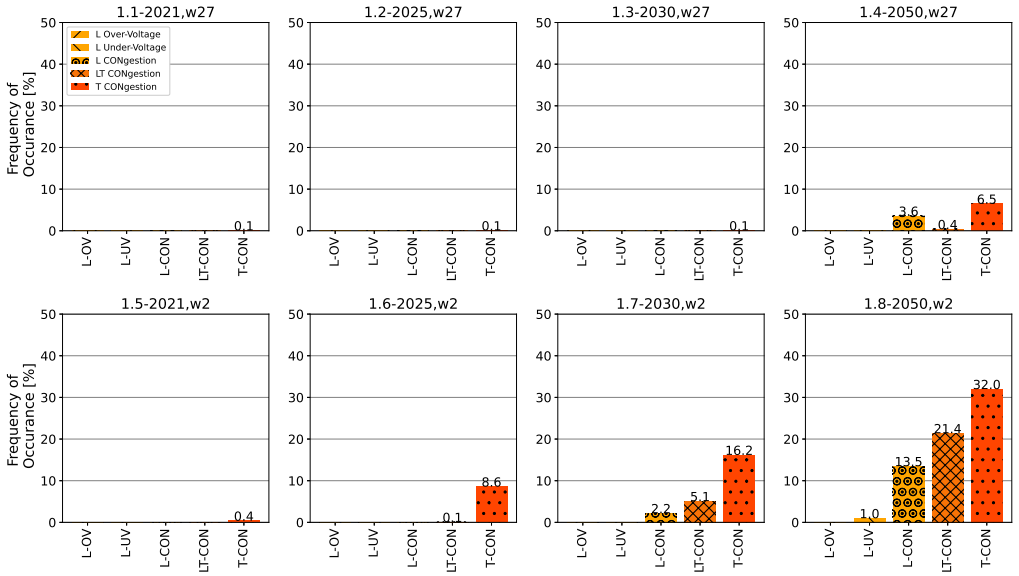

Figure 5-1: Barplot with frequencies of congestion (CON) and under- (UV) or overvoltage (OV) for the uncontrolled scenarios. The first row indicates the frequencies for the summer week, the bottom row for the winter week. The years range from 2021 till 2050.

5-1-2 Concurrency of the Events

Although the frequency of the events is known at this point, it is not clear yet how events correlate with each other. Therefore, event concurrency is discussed in more detail for the two most severe scenarios (1.7 & 1.8). It is important to consider concurrency to investigate the underlying cause of the congestion and voltage problems. In its turn, this can be important to reflect on the relevance of grid constraints.

Event concurrency was defined in two ways: absolute and relative frequency of occurrence. Both describe how two events are interrelated in terms of time. The absolute concurrency (γ_A) is shown in a mathematical way by Equation (5-2).

$$\gamma_A = \frac{|\Omega_{12}|}{|\Omega|}, \quad \text{with} \quad \Omega_{12} \subset \Omega, \quad \Omega_{12} = \Omega_1 \cap \Omega_2, \quad |\Omega| = 672 \tag{5-2}$$

In fact, absolute concurrency is defined as the number of times two classes of sets occur at the same time, divided by the total sample times in one week (672). On the other hand, when divided by the cardinality of the first set, the relative concurrency (γ_R) is obtained. This is represented by formula (5-3).

$$\gamma_R = \frac{|\Omega_{12}|}{|\Omega_1|}, \quad \text{with} \quad \Omega_{12} \subset \Omega, \quad \Omega_{12} = \Omega_1 \cap \Omega_2 \tag{5-3}$$

The result of both concurrency indicators is displayed in two heatmaps. In Figure 5-2 the absolute frequency formulation results in a symmetric heatmap. The diagonal elements correspond with the bars of Figure 5-1. For the sub-diagonal elements, it is easier to read Figure 5-3 first, before interpreting Figure 5-2. In Figure 5-3 it becomes clear that when the LT is congested, the transformer is congested as well, due to a higher rating for the transformer line. On the other hand, it might occur that the transformer is congested while the LT is not. This is the case for both cases as well.

More interesting results are obtained when looking at the downstream lines. In scenario 1.7-2030,w2, line congestion goes hand-in-hand with transformer congestion. That implies that line congestion is more likely to take place closer to the transformer line. Implementing line limitations in an optimisation model would not necessarily be needed after first restricting the transformer loading. Nevertheless, in 2050 (scenario 1.8), this might not be true as 9.9% of the time line congestion occurs while the transformer does not experience congestion. That might indicate the occurrence of local line congestion due to for instance many local charging stations being occupied. In absolute terms, that corresponds to 1.33% of the time during that particular week. **Implementing grid constraints might be valuable to solve local congestion, although only up to minor extent in the case of the uncontrolled scenario (when no price incentives are applied).** Nevertheless, to fully quantify local congestion, a more detailed localisation of the events is needed. That is done in the section below.

Lastly, during the few times line undervoltage occurs, also T and LT congestion is perceived in all cases. To summarise, that would mean that the **following order of events can be expected: transformer congestion, line congestion (both LT and L) due to aggregated peaks, line congestion on local scales and finally, overvoltage problems.**

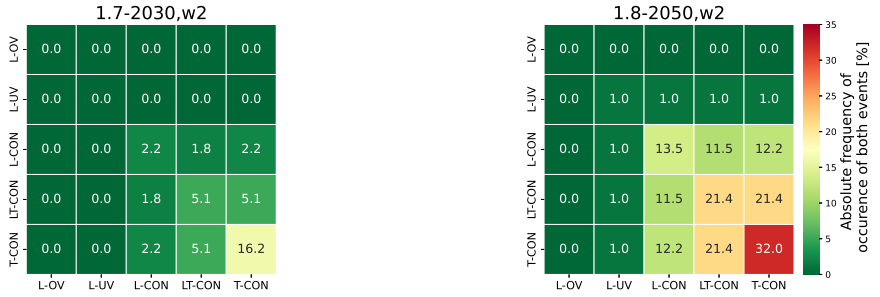

Figure 5-2: Absolute frequency of congestion and voltage problems for the two most severe uncontrolled cases related to week 2 of respectively 2030 and 2050.

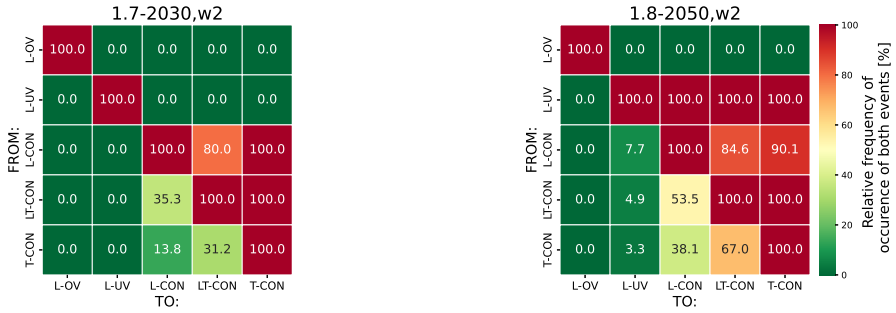

Figure 5-3: Relative frequency of congestion and voltage problems for the two most severe uncontrolled cases related to week 2 of respectively 2030 and 2050.

5-1-3 Location of the Events

It might become important to check which parts of the grid show the earliest signs of congestion and voltage problems. Not only for grid reinforcement and planning, but also when considering grid constraints in a smart charging model, that becomes relevant.

Figure 5-4 shows all the lines and nodes of the LV grid. The light grey lines are the open fuses, to represent the operational radial topology. Furthermore, all charging stations are located on the figure as well to be able to assess on the possible causes of undervoltage and congestion. The colours on the schematic are related to these events and belong to the worst-case scenario discussed so far. This is scenario 1.8-2050, w2.

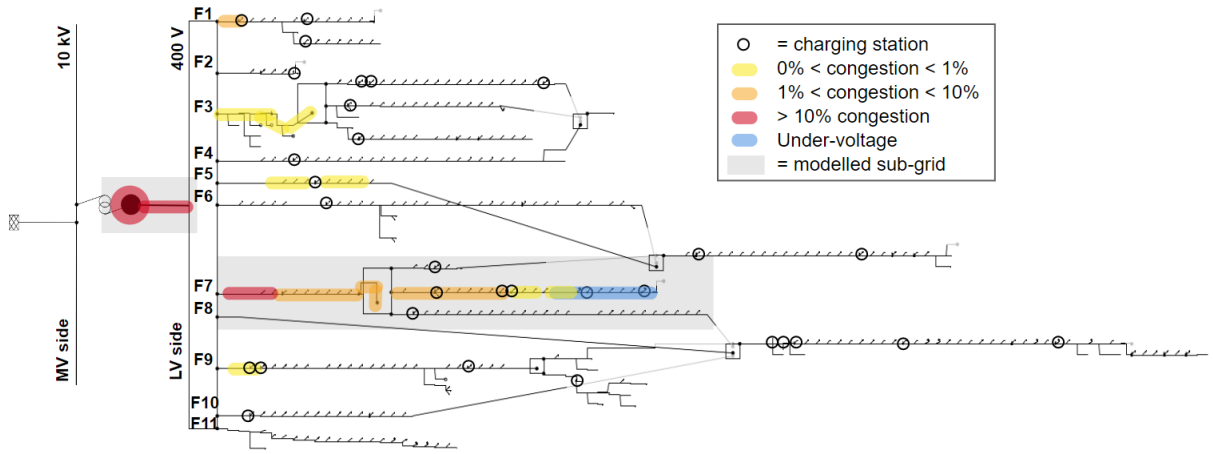

Figure 5-4: PowerFactory model for the LV grid topology with the different feeders indicated. The *grey* boxes indicate the part of the grid modelled in the optimisation. The most problematic areas are indicated with *red* and *orange* meaning overloading issues and *blue* meaning the undervoltage problems.

From Figure 5-4 it becomes apparent that **Feeder 7 (F7) experiences the most problems.** The congestion at the beginning of the feeder line is most likely related to a substantial amount of chargers and other loads resulting in large aggregated load peaks. Furthermore, **low cable ratings** (GPLK 4x25 Curm in Table A-2) amplify congestion in the middle feeder after the distribution substation. **More careful positioning of the EV charging points** might be needed as well to solve the local congestion. Feeder F7 also contains slightly more charging points due to the randomisation process applied in this work. Consequently, due to high loading and low cable ratings, a substantial voltage drop is perceived in that line as well and indicated in *blue*.

The problems in the other lines during the worst-case scenario are negligible. Due to that reason, **it becomes interesting to model only feeder 7 in the optimisation model and see how the rest of the network reacts to that.** In this way, the execution time of finding the optimal solution considering many grid constraints can be reduced drastically. The results of this approach can be found in the next Section 5-2. The modelled (so-called) subgrid is indicated in the grey box. It contains all nodes, lines, loads, PV and EV chargers connected to feeder 7. The analysis in PowerFactory always included the entire grid topology.

5-1-4 Severeness of the Events

Before optimising the charging profiles of the EVs, the event severeness is quantified and qualified as well. Figure 5-5, displays three subplots related to scenario 1.8. The loading levels of most severe lines as well as the lines with overvoltage and undervoltage are plotted, respectively. Again, clear load peaks are perceived in the evening between 6-8 pm.

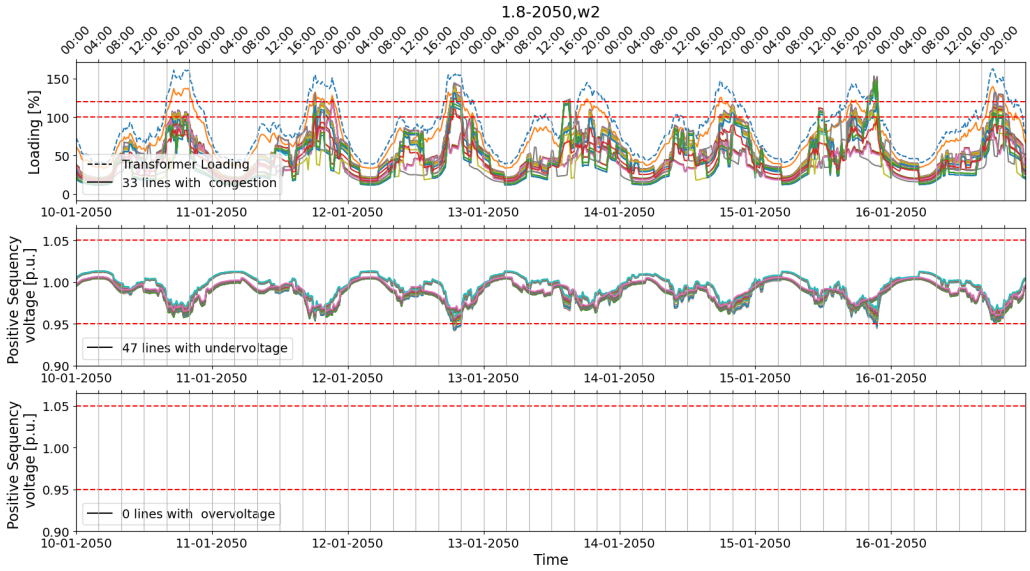

Figure 5-5: Power Flow results: voltage and loading of most severe lines and nodes for week 2, 2050. The top graph plots the lines with more than 100% congestion, the middle graph the lines with voltages under 0.95 p.u. and the bottom graph the lines for which voltages above 1.05 p.u. are perceived (which are not existing).

The **peak transformer and transformer line loading reached 164.0% and 139.8%,respectively**, of their rated current capacities. For the **downstream lines, that value amounted to 153.18%.** Congestion is observed in 48 different lines. Besides that, **the lowest and highest voltage are 0.94 p.u. and 1.02 p.u.** of the nominal, respectively. That explains why no overvoltage is perceived in the bottom plot of Figure 5-5. Undervoltage occurred in 10 different nodes.

5-2 Optimised Charging

In this section, the results of the optimised scenarios are analysed. All scenarios were run for the 2050 winter case (week 2, 2050) due to the relevance of analysing the worst-case scenario.

The results of all the different scenarios are compared based on the parameters listed below.

- Power losses, frequency and statistics of voltage and congestion problems at L, LT and T (5-2-1).
- CPO cost reduction based on day-ahead tariffs (5-2-2).
- User-satisfaction comprising the ability to reach the desired SOC level (5-2-3).
- Model performance in terms of computational time and accuracy of power flow modelling (5-2-4).

These result parameters were also applied to scenario 1.8, which represents the uncontrolled charging scenario (week 2, 2050). Furthermore, section 5-2-5 gives a final overview of the scenario preference of all involved parties, including the DSO, CPO and EV-owners. Refer to Table 5-1 to find the full information related to each scenario label used in this section.

5-2-1 DSO Interest: Grid Impact

Below, the interests of the DSO related to the impact of EV charging on the LV grid are described. First, the aggregated loading profiles are analysed for each scenario. Second, the frequency of the events is discussed. Afterwards, a more detailed statistical analysis is applied to also quantify the severeness of the events. Finally, the power losses are quantified. In the results analysis, favourable outcomes for the DSO are related to more valley-filling reducing power losses and to comply with the grid code in terms of congestion and under- or overvoltage limits. The limits covered in this study correspond to 100% loading for the lines and transformer line, 120% loading of the transformer and voltages between 0.95 and 1.05 p.u. Remark that the actual operational limits can change and depend on the DSO conventions.

Aggregated Loading Profiles

Figures 5-6 to 5-12 in this section contain the first visual representation of the optimisation results. Each figure contains four axes. The horizontal axes indicate the time of the week in terms of days and hours. The left vertical axis indicates the aggregated transformer power (not including power losses). The right axis represents the day-ahead price. Each figure contains four lines. Three of them always stay the same; these represent the day-ahead price profile (*light grey*), the inflexible aggregated loads containing the baseload with PV subtracted (*black*) and the aggregated inflexible loading considering the uncontrolled charging scenario 1.8 (*red*). The most important line is the green one as it contains the optimisation results, which are different for each scenario. The *green* line is the composition of the black line with the addition of the flexible (optimised) EV load.

Looking at scenario 2.1 in Figure 5-6, **it becomes clear that with a large share of V2G and only considering DA prices, more and higher peaks are seen than in the uncontrolled scenario. This results in a non-optimal outcome in terms of the DSO.** Without transformer reinforcement, this would require the need for implementing a transformer constraint. This is done for scenarios 2.2 and 2.3, as can be observed Figure 5-7 and Figure 5-8, respectively. Scenario 2.3 also contains the power flow constraints for feeder 7 (sub-grid). At first glance, not that much difference is perceived between both scenarios. Nevertheless, both scenarios contain an almost continuous high loading at the transformer level, which might involve more power losses.

The visual representation of scenario 2.4 in Figure 5-9 is completely different as it includes a new tariff scheme and only unidirectional charging. The loading is again restricted by a transformer limit and is much more evenly distributed. The latter results in more valley-filling. **At first sight, this ST price scheme that disincentives high load levels succeeds in creating a more balanced load level. That should result in less overall power losses.** A quantification of these power losses can be found at the end of this section.

To really investigate the power of the ST structure, the V2G scenarios were repeated for ST prices as well. Figure 5-10 contains the optimisation results when no grid limitations are applied. It shows that the ST scheme is not fully capable of avoiding load peaks above transformer level. This can be solved by a more careful study

of the adopted price levels or by again adding a transformer limit. The latter solution was applied, because the former falls out of the scope of this work. As a result, Figure 5-11 shows the topped loading at transformer level, including ST and V2G. Less high loading is perceived compared to the equivalent DA scenario. That is quantified in Table 5-2 as well. From this table, it becomes apparent that the DA scenarios have at least three times more loading at transformer level compared to their ST counterparts. As a consequence, it can be concluded that the stacked tariffs effectively discourage high transformer loading.

Again, the scenario including the sub-grid constraints (2.7) in Figure 5-12 almost looks identical to the one with only a transformer limit (2.6) in Figure 5-11. That can be explained by the low amount of line congestion and voltage problems when limiting transformer loading. A more quantitative analysis can be found further down this section.

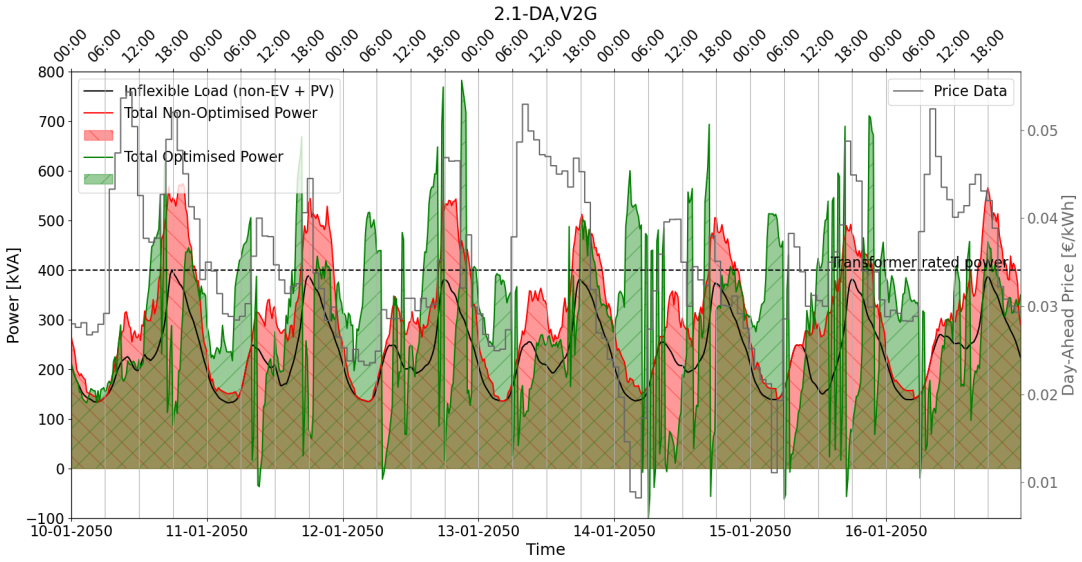

Figure 5-6: Aggregated load (without losses) for scenario 2.1: DA-prices, V2G, no grid constraints.

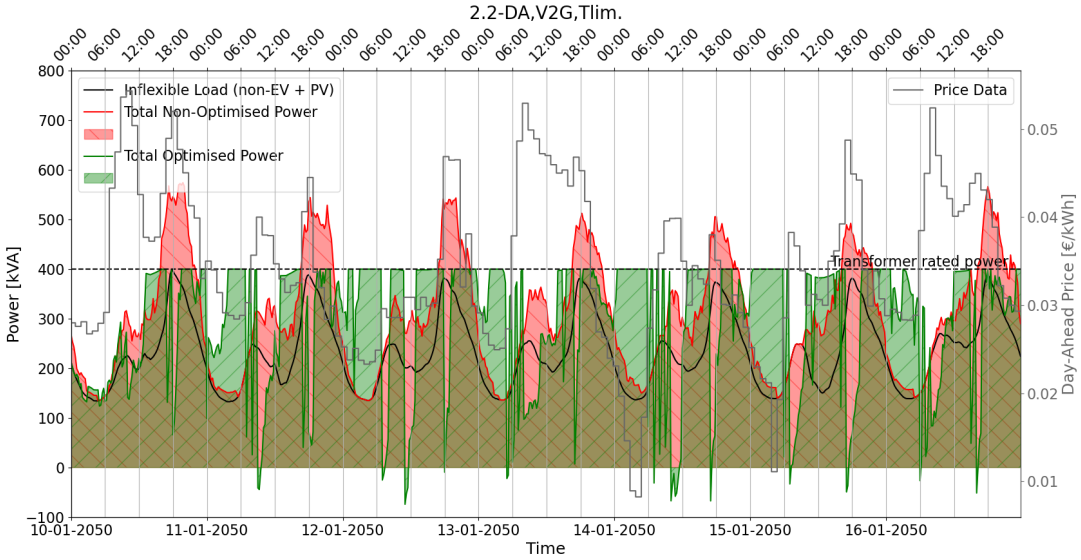

Figure 5-7: Aggregated load (without losses) for scenario 2.2: DA-prices, V2G, transformer limit.

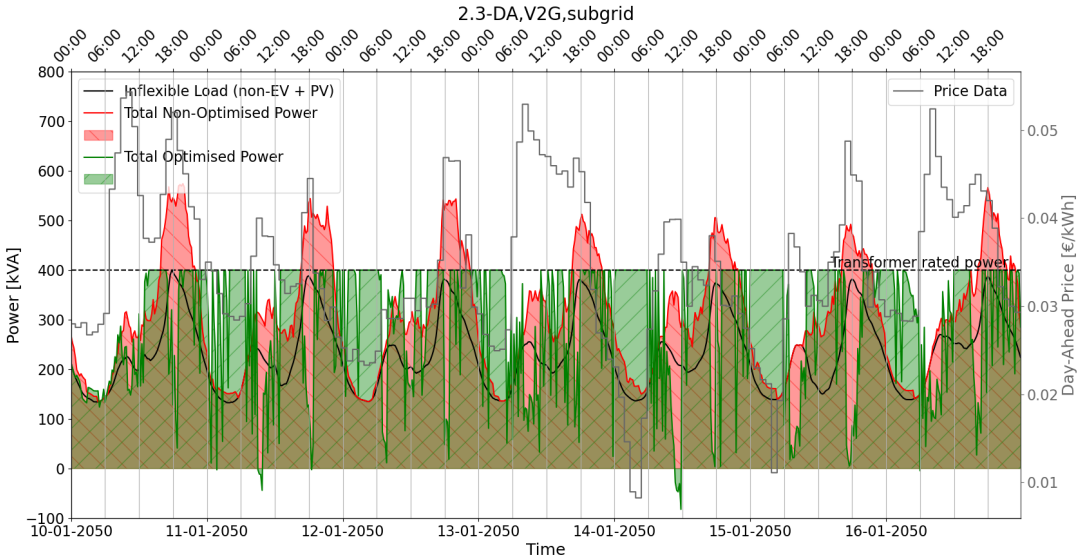

Figure 5-8: Aggregated load (without losses) for scenario 2.3: DA-prices, V2G, sub-grid constraints.

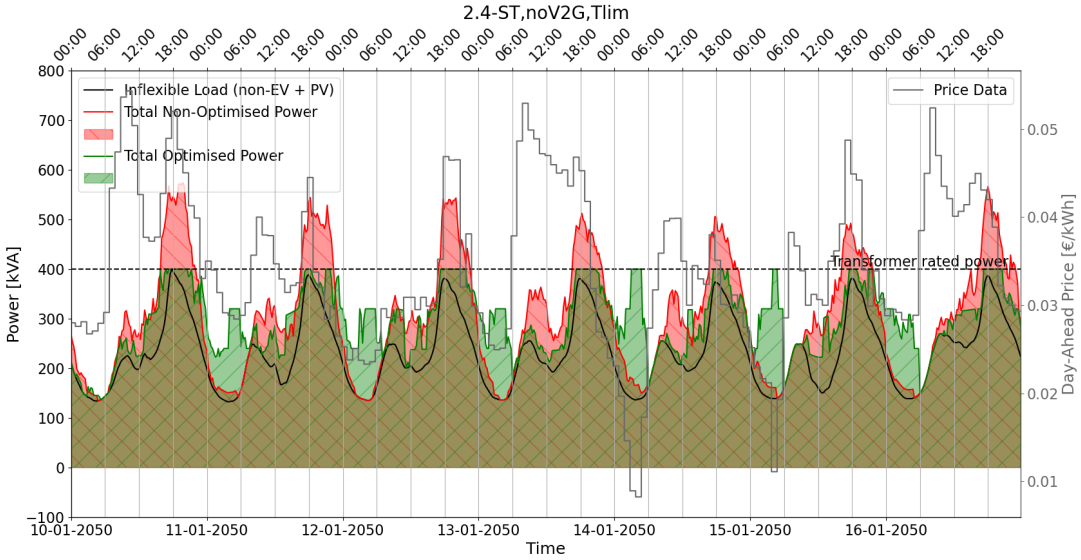

Figure 5-9: Aggregated load (without losses) for scenario 2.4: ST-prices, V1G, transformer limit.

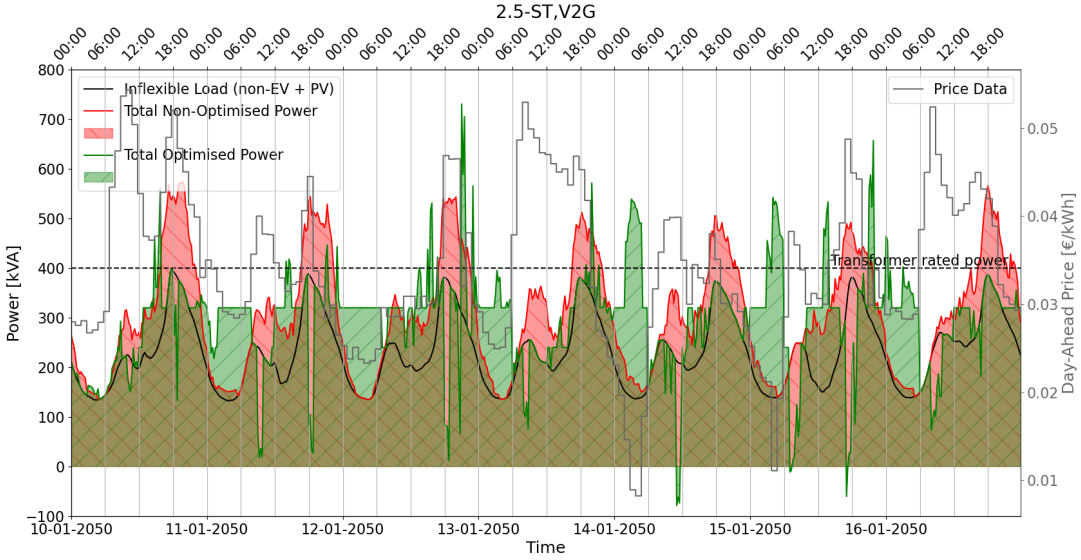

Figure 5-10: Aggregated load (without losses) for scenario 2.5: ST-prices, V2G, no grid constraints.

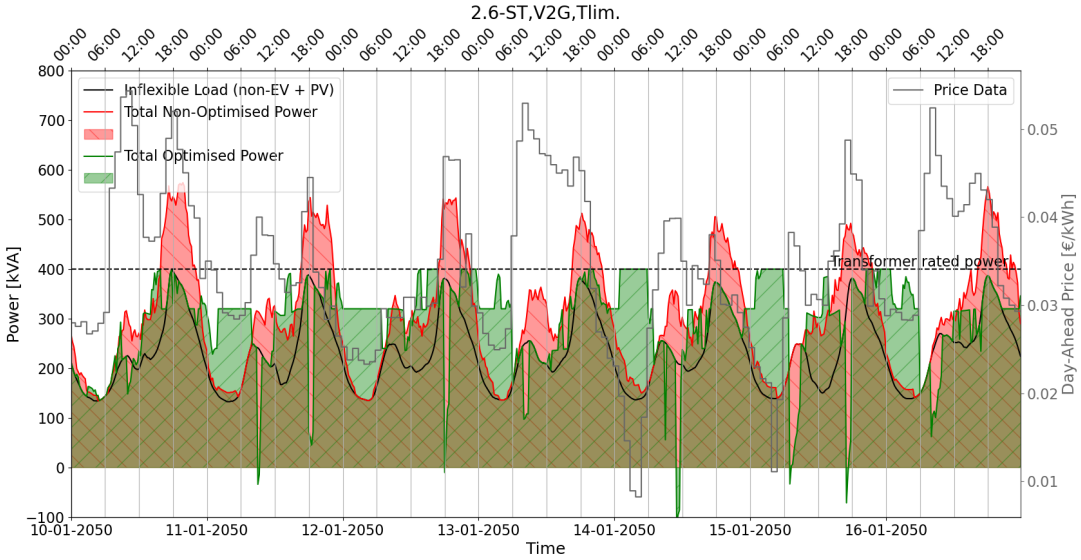

Figure 5-11: Aggregated load (without losses) for scenario 2.6: ST-prices, V2G, transformer limit.

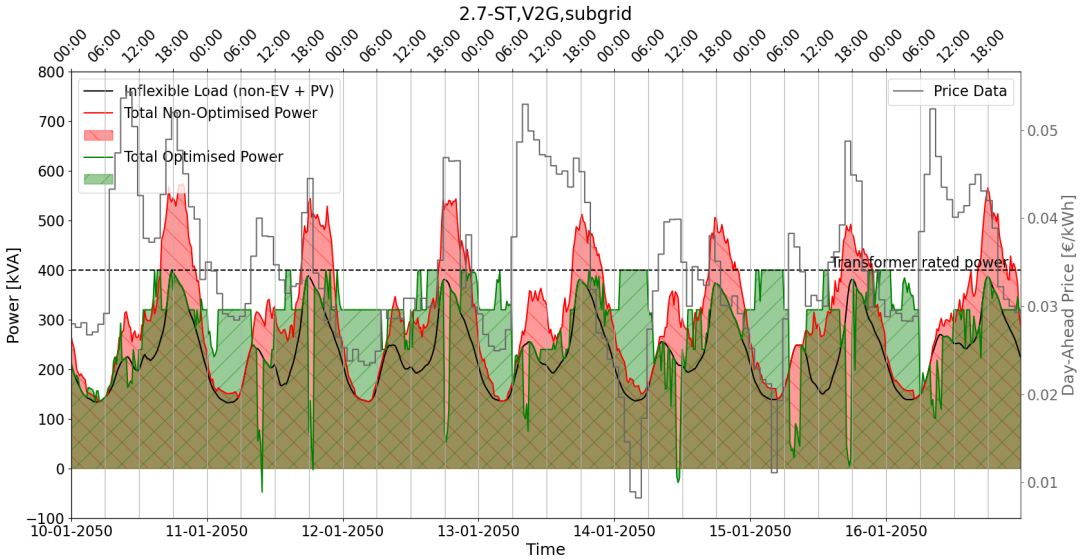

Figure 5-12: Aggregated load (without losses) for scenario 2.7: ST-prices, V2G, subgrid constraints.

Table 5-2: Frequency indicating a loading of at least 400 kVA at transformer level.

	Loading Frequency at T-Lim [%]
1.8-2050,w2	23.96
2.1-DA,V2G,noTlim.	25.15
2.2-DA,V2G,Tlim.	36.16
2.3-DA,V2G,subgrid	47.47
2.4-ST,noV2G,Tlim	15.33
2.5-ST,V2G,noTlim.	8.63
2.6-ST,V2G,Tlim.	11.31
2.7-ST,V2G,subgrid	12.65

Frequency of Voltage and Congestion Events

Figure 5-13 shows the frequencies of all five event classes. The transformer limit was regarded as 120% of the rated current capacity. One can observe that **with DA prices alone, all five event classes contain more events than in the case of uncontrolled charging.** Especially the frequency of line congestion is almost doubled. Congestion at transformer (-line) level and undervoltage in the nodes all increase with a little bit less than 10%. Besides, even line overvoltage is perceived. It again stresses the **need for more regulation.** V1G is regarded as less impacting than V2G.

From scenario 2.2 and 2.6 one can conclude that it would be relevant to include grid constraints downstream the transformer for 14.4% and 8.9% of in the case of DA and ST prices respectively. However, remarkable is that with the line constraints included, the line congestion frequency reaches more than 20%. At first glance, that seems odd because of the inclusion of the feeder constraints. A more careful analysis was performed to check the outputs of the optimisation. First of all, it can be confirmed that all phase current values were topped at their maximum in the optimisation. **Looking at the PowerFactory results, the loading of the modelled feeder lines reached a maximum of 106.5%. This difference can be explained by the errors in the linear AC power flow modelling used in the optimisation.** That can be considered acceptable as PowerFactory makes use of the non-linear Newton-Raphson method for power flow modelling. A complete error analysis can be found in Section 5-2-4. A new simulation was run for scenario 2.7 including an error correction factor of 0.935 multiplied with the rated current of the lines to cope with these differences. The results can be found in Figure 5-14. The line congestion is reduced from 22% to a congestion level of 5.5% only. The remaining 5.5% was afterwards checked on the location of occurrence. It turned out that the concerned lines are all located in feeders other than feeder 7. That validates the effectiveness of the modelled power flow equations and constraints. Moreover, 95% of these congestion occurrences occurred in the same lines that also experienced congestion in the uncontrolled scenario as displayed in Figure 5-4. The exact location of the congestion can be found in Figure B-1.

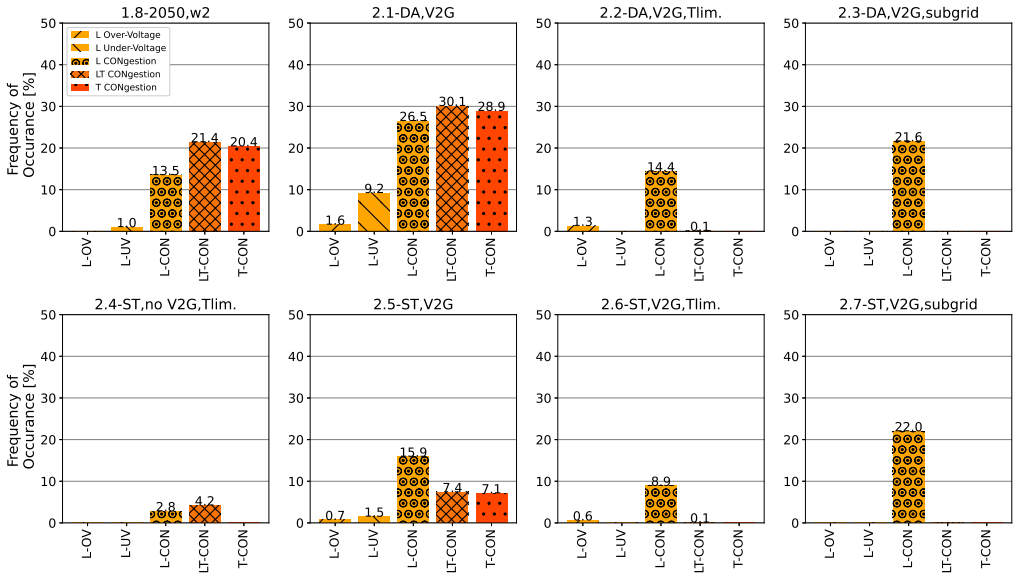

Figure 5-13: Barplot with frequencies of congestion, undervoltage and overvoltage events of the controlled scenarios together with the uncontrolled scenario 1.8.

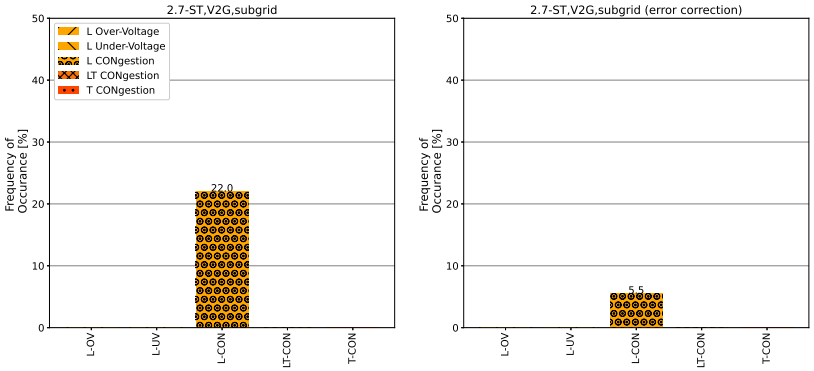

Figure 5-14: Barplot with frequencies of congestion, undervoltage and overvoltage events for scenario 2.7 without and with error correction.

Statistics Congestion & Voltage Events

In this section, statistics related to the grid impact on transformer level (Table 5-3), transformer line (Table 5-4) and the downstream lines (Table 5-5) are schematised. All controlled scenarios are again compared together with scenario 1.8.

Firstly, at the transformer level (see Table 5-3), three different congestion parameters are plotted. The trans-

former peak loading expresses the maximum loading perceived during week 2 of 2050 for each scenario. The lower load peaks are desired to reduce wear and curtailment. For the DA scenario without limitations, loading above 200% of the transformer capacity can be observed. Solving this by implementing grid constraints would avoid load curtailment as much as possible due to flexibility redistribution of EV charging.

Next to congestion, also valley-filling is desirable for the DSO. This is expressed by the remaining two parameters: the Root-Mean-Square (RMS) and the standard deviation of the loading. The lower both values, the better this is in terms of valley-filling. A lower RMS loading is also desired in terms of losses, as these power losses grow quadratic with the loading. **It becomes apparent that for the case with no Vehicle-to-Grid (V2G), best parameters are obtained. Nevertheless, the other ST scenarios also show improved results compared to their DA-based counterparts in terms of valley-filling.** A summary of the DSO benefits related to transformer congestion is provided in the last column of Table 5-3.

Secondly, the transformer line is discussed for which it is important to consider loading below 100% to avoid tripping. As one can see in Table 5-4, the transformer limit should be chosen a bit more tight when the grid is not modelled additionally. As expected, the transformer line peak loading contains similar scenario results as for the transformer peak loading in Table 5-3.

Lastly, five different parameters related to the downstream lines are included in Table 5-5. Line peak loading is for all eight cases higher than 100% even for the scenarios with subgrid constraints. **However, when the feeder constraints are implemented, the peak is reduced by more than 13% and almost 20% for DA and ST, respectively, compared to their counterparts with only a transformer limit.** After a location analysis, these peaks occurred at lines that are not included in the linear OPF. The line RMS loading is the best for the ST scenarios. Furthermore, the variation of the loading is best for scenario 2.6 and 2.7, as well. Especially for GPLK cables, this is favourable, as they cannot withstand high load fluctuations [16]. In terms of line voltage, the scenario that does not include bidirectional charging is the only one besides the ones with grid constraints that shows acceptable voltage limits.

Table 5-3: Congestion statistics at transformer (T) level.

	T peak loading [%]	T loading RMS [%]		T loading stdev. [%]		DSO Benefits
1.8-2050,w2	163.98	94.14	- *	33.19	- *	−−
2.1-DA,noTlim.,V2G	231.58	101.01	(+7.29)	50.69	(+52.72)	− − −
2.2-DA,Tlim.,V2G	117.48	92.43	(-1.81)	32.86	(-1.00)	+
2.3-DA,subgrid,V2G	116.39	91.29	(-3.03)	31.36	(-5.51)	++
2.4-ST,Tlim.,noV2G	117.47	88.26	(-6.24)	19.62	(-40.89)	+++
2.5-ST,noTlim.,V2G	210.50	90.19	(-4.20)	27.02	(-18.59)	−
2.6-ST,Tlim.,V2G	116.95	88.97	(-5.50)	22.59	(-31.94)	++
2.7-ST,subgrid, V2G	116.29	88.70	(-5.78)	22.84	(-31.18)	++

* Reference

Table 5-4: Congestion statistics at the level of the line of the transformer (LT).

	LT peak loading [%]	DSO Benefits
1.8-2050,w2	139.78	−−
2.1-DA,noTlim.,V2G	195.34	− − −
2.2-DA,Tlim.,V2G	100.82	++
2.3-DA,subgrid,V2G	99.54	+++
2.4-ST,Tlim.,noV2G	100.83	++
2.5-ST,noTlim.,V2G	177.74	− − −
2.6-ST,Tlim.,V2G	100.42	++
2.7-ST,subgrid, V2G	99.72	+++

Table 5-5: Congestion and voltage statistics at downstream line (L) level.

	L peak loading [%]	L loading RMS [%]		L loading stdev. [%]	L highest voltage [p.u.]	L lowest voltage [p.u.]	DSO Benefits
1.8-2050,w2	153.18	25.30	-*	6.04	1.018	0.942	−−
2.1-DA,noTlim.,V2G	203.98	27.95	(+10.50)	6.19	1.062	0.913	− − −
2.2-DA,Tlim.,V2G	150.55	25.88	(+2.29)	4.14	1.056	0.951	−−
2.3-DA,subgrid,V2G	130.75	25.99	(+2.71)	3.96	1.048	0.952	+ +
2.4-ST,Tlim.,noV2G	133.87	23.81	(-5.87)	4.11	1.018	0.955	+++
2.5-ST,noTlim.,V2G	199.06	25.80	(+1.97)	4.19	1.058	0.920	− − −
2.6-ST,Tlim.,V2G	148.22	24.87	(-1.68)	3.73	1.059	0.957	−
2.7-ST,subgrid, V2G	119.46	25.87	(+2.27)	3.77	1.046	0.954	+ + +

* Reference

Power Losses

It was hypothesised that the new regime of stacked tariffs should allow for more off-peak charging, which in turn should result in fewer power loss. Table 5-6 indicates the relative increase or decrease of these power losses compared to the uncontrolled scenario. The following conclusions can be drawn from this table. First, **the stacked tariffs give indeed a better outcome compared to their DA-based counterparts.** Nevertheless, the ST-regime is not necessarily always favourable compared to the uncontrolled scenario. **It is mainly the inclusion of subgrid constraints or no V2G implementation that allows for less power losses.** Remark that a relative increase or decrease in the remainder of this work is always defined as the difference between two values divided by the reference value of the two.

Table 5-6: Relative increase or decrease of power losses in the course of one week compared with the uncontrolled scenario. A negative number indicates less power losses compared to the reference scenario.

	Relative Power Loss [%]	DSO Benefits
1.8-2050,w2	0*	++
2.1-DA,V2G,noTlim.	6.08	− − −
2.2-DA,V2G,Tlim.	4.83	−−
2.3-DA,V2G,subgrid	0.02	+
2.4-ST,noV2G,Tlim	-0.48	+++
2.5-ST,V2G,noTlim.	1.55	−
2.6-ST,V2G,Tlim.	1.67	−
2.7-ST,V2G,subgrid	-0.49	+++

* Reference

It can be concluded from these analyses that the DSO would favour grid constraints in case of a large proportion of V2G combined with ST. However, it turned out that with V1G and a transformer limitation, an equally favourable scenario is obtained. This relates to the amount of power losses and severeness of congestion and voltage problems.

As the objective function of the optimisation contains two parts: cost minimisation of the CPO and maximisation of the EV's SOC it is important to look at the results optimality related to CPO and EV-users as well. The next two sections (Section 5-2-2 and 5-2-3) deal with this in more detail.

5-2-2 CPO Interest: Cost Savings

Table 5-7 contains the relative cost savings of the CPO compared to the uncontrolled scenario. These cost savings are calculated based on the difference in DA fraction only. The additional cost in the case of stacked prices is not included as the optimal price selection and price justification are beyond the scope of this work.

Table 5-7: Day-ahead cost fraction reduction to be paid by the CPO for week 2, 2050 compared to the non-optimised charging scenario.

Scenario Label	Cost Savings [%] (DA based)
1.8-2050,w2	-*
2.1-DA,V2G	-50.79
2.2-DA,V2G,Tlim.	-48.03
2.3-DA,V2G,subgrid	-48.46
2.4-ST,noV2G,Tlim	-29.45
2.5-ST,V2G	-46.29
2.6-ST,V2G,Tlim.	-43.34
2.7-ST,V2G,subgrid	-43.30

* Reference

One can conclude from Table 5-7 that **high-cost savings above 25% up to more than 50% are obtained in all controlled cases**. That was expected due to the optimisation objective tailored to minimise CPO costs. As expected, larger cost savings are observed when technical constraints are disregarded. Nevertheless, the inclusion of grid constraints for the DA scenarios only resulted in 5.56% relatively less cost savings compared to the most favourable scenario (2.1).

With **stacked tariffs, around 13% less is saved compared to scenario 2.1.** This concerns the difference in concurrency between favourable DA prices and low transformer loading. The Pearson correlation coefficient that expresses the correlation between both, was calculated as 0.54, for week 2, and 0.49 for 2050 as a whole. A positive correlation is of course justified by the fact that DA prices are greatly influenced by peak loading of the entire network.

Lastly, it becomes clear that the inclusion of **bidirectional charging is favourable from the CPO perspective**. With V2G **more EV flexibility** is obtained, resulting in higher capacities that can be charged at the most favourable moments. With V1G only, cost savings are 13.89% less compared to scenario 2.6, which does include V2G. That involves a relative cost increase of 32.05% compared to its V2G counterpart.

5-2-3 Consumer Interest: SOC-Level

Although the smart charging model tries to minimise the expenses of the CPO in the objective function, the most important objective is to allow users to charge up to their desired battery SOC. This desired SOC was set to 80% [68]. Nevertheless, some EVs do not stay connected long enough to get charged up to 80% meaning that their desired SOC was lowered to the maximum obtainable level ($20\% \leq \overline{\mathrm{SOC_c}}^* \leq 80\%$). If that level is achieved the user-satisfaction is regarded as 100%, indicated by the factor α_c in the objective function (4-2).

In contrast, when the grid limits are too restricting, charging might be delayed. In some cases, this leads to EVs that are not able to charge up to their desired SOC level. In that case, α_c will drop. If α_c is not equal to 1 at the end of charging, the car did not reach its maximum obtainable SOC. In that way, α_c expresses the fraction of this desired SOC level at the end of charging. When too many EVs cannot fully charge, this might be an indication that the constraints of the model are too restricting or that grid reinforcement should take place.

The frequency of events that an EV does not reach its desired SOC is calculated in Table 5-8. Besides, also the minimum, average and standard deviation of these unsatisfied events is displayed by expressing α_c percentage. That gives an idea about the overall dissatisfaction level.

Table 5-8: Statistics related to the level of user-satisfaction for the different scenarios.

Scenario Label	Frequency of Failures [%]	Minimum User Satisfaction [%]	Average Dissatisfied Events [%]	Standard deviation [%]
1.8-2050,w2	0.00	100.00	-	0.00
2.1-DA,V2G	0.00	100.00	-	0.00
2.2-DA,V2G,Tlim.	3.81	71.41	88.98	7.31
2.3-DA,V2G,subgrid	1.75	78.33	90.00	5.72
2.4-ST,noV2G,Tlim	6.67	46.70	87.24	11.92
2.5-ST,V2G	0.00	100.00	-	0.00
2.6-ST,V2G,Tlim.	0.79	90.13	95.64	3.46
2.7-ST,V2G,subgrid	1.11	78.33	91.91	6.36

First of all, it becomes clear that **adding grid limits reduces user-satisfaction. Nevertheless, the level of dissatisfaction stays acceptable.** Strangely, in the case of the DA prices, the feeder constraints allow more satisfied users than with only a transformer limit. A more in-depth analysis would be needed to explain this value. **As one can notify, allowing V2G increases user-satisfaction compared to the V1G scenario.** That makes sense as there is no EV's flexibility to also start discharging without V2G at inflexible load peaks. If the connection time of EV is too short, they would not be able to charge till their desired level during these load peak moments.

5-2-4 Model Performance

The model performance was both assessed in terms of computational time as well as accuracy of the power flow modelling. The results are discussed below.

Computational Time

Table 5-9 contains the performance of the smart charging model in terms of computational time. The average computational time was calculated for the first optimisation step with the CPLEX solver. This includes both parameter and constraint loading as well as the actual solving time. As the horizon contains 96 time steps, the time of computation is rather high and at least 11 seconds. This corresponds to scenario 2.2. Scenario 2.2 was used as a reference to calculate the increase of computational time for the other scenarios as well.

The main conclusion that can be drawn from Table 5-9 is that **the inclusion of grid constraints increases the computational time by around 2000% due to an exponential increase in the number of constraints and variables. In that regard, only considering part of the grid being modelled with power flow equations as adopted in this work, can be seen as an interesting approach to alleviate the most severe problems in power networks when a similar optimisation strategy is applied.** Consequently, a solution can be computed in less than the time window of 15 minutes. The horizon can also be reduced, but that would hypothetically result in less flexibility allocation and therefore reduced CPO and consumer benefits. In the case of grid constraints, including less cutting planes, would imply a reduced calculation time at the cost of accuracy as can be seen in Figure 5-16 below.

The computational results can be compared with the Literature Table 2-2 in Chapter 2. However, due to

different constraints, grid topology and EV fleet size, amongst other, this would not be a fair comparison.

Table 5-9: Computational time for one optimisation step in both absolute and relative terms compared with the number of variables and constraints.

	Absolute Computational 1st Time Step [s]	Relative Computational Time Increase compared to 2.2 [%]	Number of Constraints	Number of Variables
1.8-2050,w2	-	-	-	-
2.1-DA,V2G,noTlim.	13.23	(+20.27)	79937	55361
2.2-DA,V2G,Tlim.	11.00	- *	80129	55361
2.3-DA,V2G,subgrid	245.77	(+2134.27)	1,114,913	520,193
2.4-ST,noV2G,Tlim	12.46	(+13.27)	80513	55745
2.5-ST,V2G,noTlim.	11.38	(+3.45)	80321	55745
2.6-ST,V2G,Tlim.	13.44	(+22.18)	80513	55745
2.7-ST,V2G,subgrid	214.96	(+1854.18)	1,115,297	520,577

Accuracy Power Flow Modelling

In order to justify the correctness of the applied linear optimal power flow model, a sensitivity analysis has been conducted. The results of this sensitivity analysis can be found in Figure 5-15 and Figure 5-16. These figures contain the computational time as well as the maximum and average current and voltage errors in function of the number of cutting planes (N). Figure 5-15 displays the results for the complete modelled topology, Figure 5-16 only for feeder 7. The errors were computed by importing the optimisation results in PowerFactory and comparing phase voltages and currents of both models. The formula for computing these errors can be found in (5-4) for the current. The same formula applies to calculate the voltage errors.

$$\Delta_{I_\phi} = \sum_{\phi} \sum_{t} \left| \frac{I_{t,\phi} - I_{t,\phi}^{\mathrm{PF}}}{I_{t,\phi}^{\mathrm{PF}}} \right| \tag{5-4}$$

It was found that the current errors are strongly dependent on the number of cutting planes. This was also found by [4]. However, on the other hand, the maximum voltage deviations are not dependent on N. That makes somehow sense as the voltage linearisation does not involve the use of N. The size of the errors is higher than in [4], but cannot be compared as this paper used another non-linear model instead of PowerFactory for the error comparison.

An optimal result was found for N=12. For the full grid, this corresponds to a maximal current error of 4.23%, and an average of 1.88%. For the voltage at N=12, the maximum and average errors were perceived as 0.68 and 0.11%, respectively. For the reduced grid topology (subgrid), similar results were found. For the current maximum and average errors values of 4.23 and 1.15% were obtained. For the voltage error, these values reached 0.68 and 0.27%.

Furthermore, both figures prove that the computational time strongly depends both on N as on the size of the modelled grid. This has already been briefly touched upon in the previous points, but proven in the most right plots of Figure 5-15 and Figure 5-16.

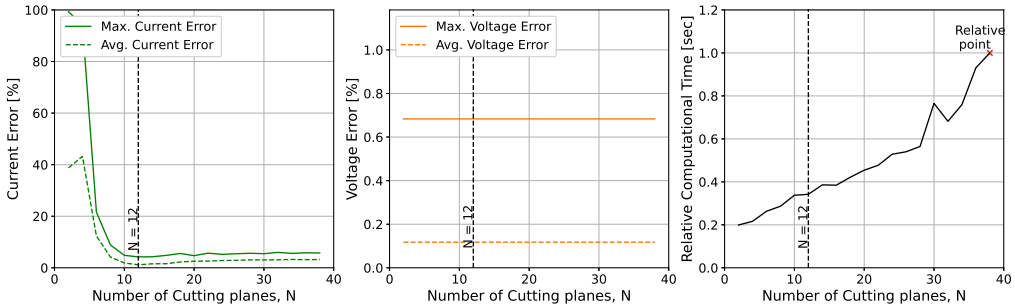

Figure 5-15: Sensitivity analysis on the number of cutting planes for the **entire grid topology**. The left and middle figure represent the current and voltage errors as compared with PowerFactory. The right figure represents the relative computational time of the optimisation model.

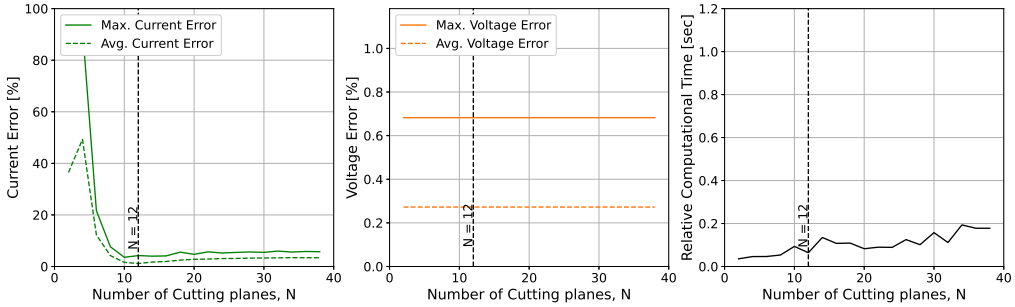

Figure 5-16: Sensitivity analysis on the number of cutting planes for the **partial (sub-)grid topology**. The left and middle figure represent the current and voltage errors as compared with PowerFactory. The right figure represents the relative computational time of the optimisation model.

The preceding graphs, only show the momentary error results for one particular point in time. Figure 5-17 shows the error time series for scenario 2.7. After running the optimisation with power flow constraints, predicted transformer voltage and N=12, the resulting current and voltage values were derived. These values were consecutively validated in PowerFactory over time. Figure 5-17 shows the obtained error fluctuations with intervals of 2.5 hours. As one can see, the voltage maximum error stays bounded at 2%. The current maximum error is always smaller than 12%. That explains why the rated power in PowerFactory was sometimes higher than the allowed implemented congestion levels. Nevertheless, higher current errors were often perceived at the end of the feeder lines due to smaller current flows, resulting in larger error terms in formula (5-4).

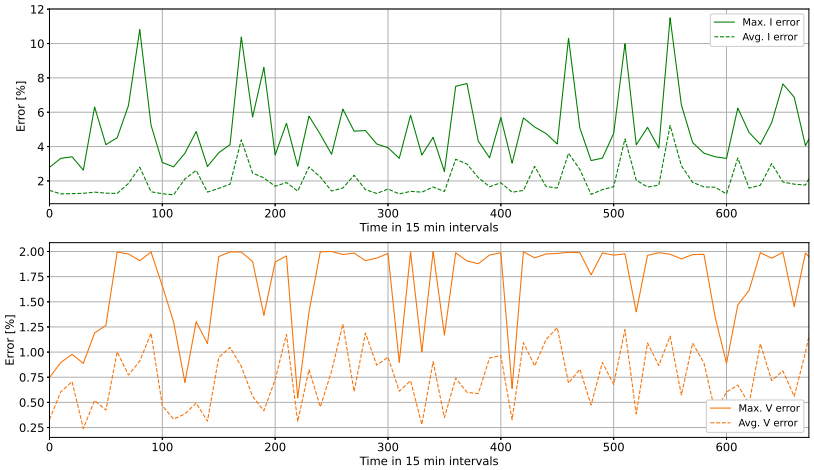

Figure 5-17: Voltage and current error analysis of the sub-grid constraints for one entire week.

5-2-5 Results Summary

To conclude this chapter, Table 5-10 summarises the attractiveness of each scenario to the involved stakeholders. The least attractive scenario is indicated with '$---$', the most attractive scenario with '$+++$'. The assessment was based on the results of Sections 5-2-1, 5-2-2 and 5-2-3. **The conclusion can be made that the most favourable scenarios involve the new ST pricing scheme. Including grid constraints also downstream the transformer turned out to be the most interesting scenario for the DSO when V2G adoption is assumed. Besides, also CPOs and consumers benefit from bidirectional charging. The latter, especially in the case that grid reinforcement cannot keep up with the increasing load demand.** Nevertheless, that would need a careful reflection on the battery degradation as well. Appendix E contains more information about the inclusion of battery degradation in the model and effect this might have on user-satisfaction. So far, the results are not promising, leading to a drastic reduction of user-satisfaction. However, a more thorough investigation is still needed.

Table 5-10: Overview of the attractiveness of each scenario for the three involved stakeholders: DSO, CPO and EV owner.

	DSO Grid Impact	CPO Cost Savings	Consumer SOC Level
1.8-2050,w2	−−	−−−	+++
2.1-DA,V2G,noTlim.	−−−	+++	+++
2.2-DA,V2G,Tlim.	+	++	++
2.3-DA,V2G,subgrid	++	++	+
2.4-ST,noV2G,Tlim	++	−	−
2.5-ST,V2G,noTlim.	−	++	+++
2.6-ST,V2G,Tlim.	++	+	+
2.7-ST,V2G,subgrid	+++	+	+

Chapter 6

Conclusions & Recommendations

6-1 Retrospection of the Thesis

6-1-1 Answer to Research Questions

1. *To what extent do **voltage and congestion problems** manifest in a typical Dutch **LV** grid when **uncontrolled charging** is applied both in winter and summer till 2050?*

   Most problems are experienced during the winter week. For the summer scenarios, no problems are experienced up to 2050 when local line congestion starts to emerge together with transformer congestion. However, the event frequencies are almost negligible and stay far below 10%. In the winter week, problems start to emerge much earlier. In 2025, the transformer gets congestion first. In 2030, also line congestion and transformer line congestion is experienced. However, frequently occurring problems start to form in 2050. The transformer is congested almost one-third of the time in that week. Besides, transformer line and line congestion occur more than 10% of the time. Lastly, also line undervoltage starts to form in 2050 at the end of one of the feeders. The conclusion was made that without optimised charging, the transformer needs to be reinforced first around 2030, quickly followed by the reinforcement of the transformer line. Besides, both with uncontrolled and controlled charging, it would be wise to position the charging points more evenly to avoid local line congestion. In that way, line reinforcement can be avoided as much as possible.

2. *What are **good features of existing optimised charging models** applicable to the studied LV grid to help mitigate grid issues such as congestion and voltage problems?*

   It was found that many of the models in literature make use of the RHO principle. The horizon allows using the EVs' flexibility in an optimal way. That means that the user-satisfaction is maintained at a desired level, while still complying with grid constraints that reduce voltage and congestion problems. RHO was applied in this thesis as well. The side-note should be made that all results are based on perfect

knowledge about the horizon (PV generation, baseload, price data and voltage at the transformer node) and EV characteristics (departure time, SOC). Therefore the results in this thesis should be considered optimal and can be used as a proof of concept.

Another interesting feature is the inclusion of grid constraints to maintain proper thermal and voltage conditions. This can be done on two levels: aggregated or disaggregated. Most existing papers only implement grid constraints on the aggregated level, meaning that only the power at the transformer level is constrained. Some papers looked at the disaggregated level by modelling the entire network topology, including constraints related to line maximum currents and bus voltage limits. In this thesis, both strategies were implemented and assessed on stakeholder interests. A rather new three-phase AC linear power flow model was applied, obtained from [4]. The applicability of this implementation relates to the aim of this thesis of using EVs flexibility to avoid voltage and congestion to maximum extent. This would delay grid reinforcement as much as possible.

Furthermore, literature also indicated that dynamic pricing schemes are most preferred to also comply with grid limitations. Therefore, two dynamic pricing schemes were adopted as well in this thesis.

Lastly, it was found that computational-wise, one should try to avoid non-linear optimisation constraints. Besides that, a linear model is also much more beneficial than a MILP model. Nevertheless, applying linear constraints only does not allow to include some features such as proper battery degradation modelling or discharging and charging efficiencies when V2G is adopted. For the objective function, linearity was maintained by choosing a cost minimisation strategy in the objective function.

3. *In which case is the **integration of grid constraints and power flow modelling relevant** in the optimised charging model?*

   Including grid constraints in a smart charging model is not always that relevant. One should always question three key aspects:

   1. *Where are the main bottlenecks located?*,
   2. *What is the frequency of occurrence?* , and,
   3. *How are different grid bottlenecks interrelated?*.

   The first key question leads to the conclusion that it might be sufficient to include only one feeder in the optimisation model. This is valid as long as the bottlenecks in the rest of the grid are minor, meaning that a few congestion or voltage problems should not be a too big problem. It was proven that this is indeed the case, as congestion in the lines can be reduced to only 5.5%. The third question allows verifying if, for example, transformer congestion goes hand-in-hand with nodal undervoltage and congestion problems. If that is the case, limiting the transformer-rated power, might be enough to solve line problems as well. This only involves one constraint instead of modelling all power flow equations. Nevertheless, if local line congestion occurs, this would not be the case.

   In this study, it was seen that limiting the transformer level did not solve all downstream problems in the 2050 winter scenarios. Therefore it made sense to include grid constraints on a disaggregated level as well. However, it should be mentioned that this would, in principle, only be needed for 8.9% of the time in the case of ST and 14.4% for DA prices during the winter week (see Figure 5-13). That means that this might not be conceived as a too severe problem for the DSO. Nevertheless, it also depends on the line congestion levels the DSO considers to be acceptable. The adopted 100% limit could be even 70% in reality, expressing a higher need for constraining local line loading as well.

4. *To what extent does the developed **optimised charging model** help in mitigating **voltage and congestion** issues in the **LV** grid?*

After applying an error correction factor, to correct for the differences in the linear AC power flow modelling and the results in PowerFactory, congestion was only experienced in some of the other lines then the ones that were included in the power flow modelling. That resulted in line congestion up to 5.5%. However, it was possible to completely eliminate: nodal undervoltage problems, overvoltage problems, as well as transformer and transformer line congestion. Furthermore, it would hypothetically also be possible to completely eliminate line congestion if the entire grid was modelled, but this scenario was not investigated due to the large computational time that would be required.

5. *To what extent does the stacked tariff scheme, V2G and grid constraints affect the **interests of the involved stakeholders** (DSO, CPO and EV owner)*?

   Obviously, it holds that the more grid constraints are include, the better this would be from the DSO perspective. In terms of valley-filling and load fluctuations, the stacked tariff scheme is preferable as well. When only looking at power quality and loading levels, V2G is slightly less preferable than V1G for the DSO. Nevertheless, V2G might provide a lot of other ancillary services and can also reduce curtailment allowing more capacity connected to the electricity grid.

   The CPO benefits in the opposite way. The scenarios in this study proved that less grid constraints and day-ahead prices are more preferable. They also favour a large fraction of V2G. It creates more flexibility, which allows the CPO to charge larger volumes at more favourable moments.

   For consumers it is important that the grid constraints are not too restricting to allow charging in case of lower flexibility provision levels. In that case, grid reinforcement would be needed to allow an acceptable SOC for all vehicles. The conclusion was made that this would not be required with a large share of V2G. Only in maximum 3.8% of all charging sessions, the maximal obtainable SOC was not completely reached. However, a careful analysis on battery degradation due to the extra cycles is required to get the complete picture of the users' benefits of V2G. A start to this analysis was made an can be found in Appendix E. The stacked tariff scheme allowed slightly better user-satisfaction values as well compared to the DA scenarios.

6-1-2 Final Conclusions

This thesis work is concluded by stressing the power of a smart charging model implementation. In this thesis an optimal charging strategy was developed for urban LV grids that can avoid 100% of all voltage and more than 95% of congestion problems without a single need for grid reinforcement till 2050. Moreover, the benefits of all involved parties: DSO, CPO and EV owners can be taken into account in the design of the model. Consequently, as an answer to the main research question:

*How can **EVs' charging flexibility** be **used optimally, to avoid possible grid congestion and voltage problems on a LV grid** due to inflexible loads and non-optimised charging?*

, it can be concluded that an optimum in EV flexibility distribution to avoid grid problems is obtained by using the stacked tariff price scheme (based on [1]), implementing V2G and applying downstream grid constraints in the form of a linear-AC power flow modelling (such as in [4]). This conclusion was derived after assessing DA prices, V1G and a reduced level of grid constraints implementation as well. Although V1G with a transformer limit only, is equally favourable for the DSO, this results in worse outcomes for the EV users and CPO due to less flexibility at peak load hours and high-price moments, respectively. In the end, the scenario with ST, V2G and grid constraints resulted in the best outcomes for the DSO with only 5.5% of line congestion in the most

severe week of 2050. Hypothetically, this can be reduced to 0% when all downstream lines are included in the power flow modelling and when an error correction factor is applied to correct for the linearity of the model. Therefore, it can be concluded that due to the worst week approach, also satisfactory results can be obtained for the other weeks of 2050. Consequently, grid reinforcement can be (almost) completely avoided until at least 2050 when this optimal smart charging strategy is implemented.

The optimally in this work can be regarded both in terms of the joint optimal scenario for all stakeholders but also in terms of a theoretical optimum. The latter relates to the perfect knowledge assumption on SOC, departure time and the horizon forecast applied in this work. Especially the use of the RHO principle allows to better estimate the grid conditions in terms of expected loading, generation and electricity prices. With that information the most optimal real-time charging schedule can be found such that stakeholders benefit the most.

6-2 Highlights & Contributions

The work in this thesis can be used and interpreted in two different ways. First, the methodologies can be used by the DSO of a certain LV grid to identify the future bottlenecks, resulting in efficient grid reinforcement planning. Second, this thesis can be used as a proof of concept, which shows that it is possible to avoid grid reinforcement by applying an optimal smart charging model or similar concepts. The results showed that without grid reinforcements, the interest of all involved parties can still be fulfilled.

Furthermore, this works provides also an assessment on non-optimal strategies such as allowing CPOs to charge on DA prices without grid limitations. Not implementing grid constraints in a model would mean curtailment of the transformer power, leaving behind many unsatisfied consumers. That conclusion resulted from a careful analysis of the relevance of including grid constraints as being adopted in this thesis. This work showed that it might be sufficient to only limit the transformer loading or include downstream power flow modelling only for part of the LV grid feeders. That depends on its turn on the tolerances of the DSO, the LV grid topology, experienced bottlenecks, other scenario assumptions and smart charging model characteristics.

Lastly, the benefits of V2G are also assessed on a broader level for all stakeholders involved in public charging. High adoption rates of V2G cause a greater need for extra grid constraints to be included in a smart charging model.

6-3 Recommendations for future work

Last but not least, the recommendations to future related work are indicated in this section. Due to the limited time and scope of the work, still some improvements and different directions can be investigated.

First, it would be good to include **battery degradation modelling** as well in the developed smart charging model. It would allow for a more careful assessment on the V2G benefits for EV owners. A start was already made by transforming the current model into a MILP model and including both battery degradation and charge and discharge efficiencies. More information about this can be found in Appendix E. It contains some first results which prove that with battery degradation, V2G benefits might diminish drastically. The implementation was

based on [31].

Secondly, the developed model is completely deterministic. Although lots of randomisation was used, each scenario only ran once with the same randomised parameters. **Especially for the part with the uncontrolled scenarios, it would be a good approach to apply a Monte Carlo simulation.** That would assess the effect of uncontrolled charging in a more accurate way. By only applying one randomisation, a biased scenario is easily created. For instance, the location of the chargers might not be very realistic, resulting in unrealistic load results. Nevertheless, although only one randomisation was adopted, the parameters were still checked on reliability to avoid biased results. This method was favoured more due to the fact that simulations in PowerFactory can take quite long when considering the same scenario design as applied in this work. Nevertheless, parallel computing could potentially solve that hurdle as well.

Looking from the optimisation perspective, it would be interesting to include more uncertainty in the model. Investigating the effect of imperfect forecasts and departure times on the optimisation results would be one possibility. It is likely to result in lower user-satisfaction, more CPO costs and more congestion and voltage problems (when no grid constraints are implemented). However, only minor drawbacks for the stakeholders are to be expected according to [71]. This result was obtained after implementing auto-regressive methods in their model to cope with uncertainty in different tariff structures. To mitigate departure-time uncertainty, one could implement a constraint that ensures charging up to a certain percentage during the first time steps. In that way, user-satisfaction can be increased. A similar idea can be found in [46]. Another possibility related to uncertainty modeling, could be the formulation of the optimisation model as a robust optimisation problem. With **robust optimisation, the scenarios can be assessed based on the worst-case point of view.** That would allow to better assess the effect of the smart charging model on all stakeholder interests. Especially for the DSO, it would make sense to plan grid reinforcement according to the worst-case scenario.

Thirdly, the **computational time** of the model can also be tackled. Reducing the horizon is one possibility; changing the horizon time steps to refined steps at the start of the horizon and more coarse towards the end, is another possibility. The latter was applied together with integer relaxation in [47]. Heuristic optimisation methods could also be applied in order to reduce the computational time. Besides, a less constraint-intensive linear OPF model could also be applied, such as the LinDistFlow formulation [45]. However, it is likely that the accuracy will become worse.

The assumption was made as well that only one CPO was involved in EV charging. This roughly corresponds to the situation in the investigated LV grid. Nevertheless, **in reality, also privately owned charging stations or multiple CPOs** are likely to be connected to the same LV grid. In that case, a more decentralised model design can be thought of, as the centralised model developed in this thesis requires perfect knowledge about all cars connected to charging stations.

Another consideration is related to the **flexibility provision** aspect. In April this year, an article appeared in the news [72] in which a car received a fine due to an additional 2 hours of connection time after the battery was full. With smart charging, that regulation should need to be change to allow more flexibility. Besides, reduced flexibility can also be obtained when the EV would have the possibility to participate in smart charging or not. In any case, reduced flexibility would again reduce user-satisfaction if the DSO implements grid constraints.

Lastly, the **newly adopted pricing scheme based on [1], was not yet optimised** in terms of price level, neither are the policies that would allow implementing this tariff change, especially when including V2G. Another study could be devoted to that.

Bibliography

[1] N. B. G. Brinkel, "FLEET: Slim laden met flexibele nettarrieven." [Online]. Available: https://ssc-fleet.nl/

[2] N. Refa, D. Hammer, and J. van Rookhuijzen, "Elektrisch rijden in stroomversnelling - Elektrificatie van personenauto's tot en met 2050, Outlook Q3 2021," ELAAD, Tech. Rep., Oct. 2021. [Online]. Available: 2021Q3_Elaad_Outlook_Personenautos_2050.pdf

[3] IRENA, "Innovation outlook: Smart charging for electric vehicles," International Renewable Energy Agency, Abu Dhabi, Tech. Rep., 2019. [Online]. Available: https://irena.org/-/media/Files/IRENA/Agency/Publication/2019/May/IRENA_Innovation_Outlook_EV_smart_charging_2019.pdf

[4] J. S. Giraldo, P. P. Vergara, J. C. López, P. H. Nguyen, and N. G. Paterakis, "A Linear AC-OPF Formulation for Unbalanced Distribution Networks," *IEEE Transactions on Industry Applications*, vol. 57, no. 5, pp. 4462–4472, Sep. 2021, conference Name: IEEE Transactions on Industry Applications.

[5] Netbeheer Nederland, "Energie in Cijfers | Hoofdstuk 1: Kerngegevens energienetten." [Online]. Available: https://energiecijfers.info/hoofdstuk-1/

[6] A. Amin, W. U. K. Tareen, M. Usman, H. Ali, I. Bari, B. Horan, S. Mekhilef, M. Asif, S. Ahmed, and A. Mahmood, "A Review of Optimal Charging Strategy for Electric Vehicles under Dynamic Pricing Schemes in the Distribution Charging Network," *Sustainability*, vol. 12, no. 23, p. 10160, Jan. 2020, number: 23 Publisher: Multidisciplinary Digital Publishing Institute. [Online]. Available: https://www.mdpi.com/2071-1050/12/23/10160

[7] Y. Zheng, S. Niu, Y. Shang, Z. Shao, and L. Jian, "Integrating plug-in electric vehicles into power grids: A comprehensive review on power interaction mode, scheduling methodology and mathematical foundation," *Renewable and Sustainable Energy Reviews*, vol. 112, pp. 424–439, Sep. 2019. [Online]. Available: https://www.sciencedirect.com/science/article/pii/S136403211930382X

[8] Netherlands Enterprise Agency, "Electric Vehicles Statistics in the Netherlands," Ministry of Infrastructure and Water Management., Tech. Rep., Jan. 2022. [Online]. Available: https://www.rvo.nl/sites/default/files/2022/01/Statistics%20Electric%20Vehicles%20and%20Charging%20in%20The%20Netherlands%20up%20to%20and%20including%20December%202021_0.pdf

[9] ECOMOTORS INC., "EV Compare — Electric car comparison, marketplace and community." [Online]. Available: https://evcompare.io/

[10] A. Klajn and M. Batkiewicz-Pantula, "Voltage characteristics of grid electricity (EN 50160)," Mar. 2017. [Online]. Available: https://www.slideshare.net/sustenergy/voltage-characteristics-of-grid-electricity-en-50160

[11] CEER, "03-Electricity-Voltage Quality," Council of European Energy Regulators, Tech. Rep., 2019.

[12] E. Commission, "2030 Climate Target Plan." [Online]. Available: https://ec.europa.eu/clima/eu-action/european-green-deal/2030-climate-target-plan_en

[13] Rijksoverheid Nederland, "Klimaatakkoord," Rijksoverheid Nederland, Den Haag, Tech. Rep., Jun. 2019.

[14] S. Bhattacharyya, Z. Wang, J. F. G. Cobben, J. M. A. Myrzik, and W. Kling, "Analysis of power quality performance of the dutch medium and low voltage grids," in *2008 13th International Conference on Harmonics and Quality of Power*, Sep. 2008, pp. 1–6, iSSN: 2164-0610.

[15] M. Nijhuis, M. Gibescu, and J. Cobben, "Incorporation of on-load tap changer transformers in low-voltage network planning," in *2016 IEEE PES Innovative Smart Grid Technologies Conference Europe (ISGT-Europe)*, Oct. 2016, pp. 1–6.

[16] Phase to Phase, "Netten voor distributie van elektriciteit," in *Phase to Phase*, 2021. [Online]. Available: https://www.phasetophase.nl/boek/

[17] M. Nijhuis, "Long-term planning of low voltage networks," Phd Thesis 1 (Research TU/e / Graduation TU/e), Technische Universiteit Eindhoven, Eindhoven, Oct. 2017, iSBN: 9789038643519.

[18] B. Bayer, P. Matschoss, H. Thomas, and A. Marian, "The German experience with integrating photovoltaic systems into the low-voltage grids," *Renewable Energy*, vol. 119, pp. 129–141, Apr. 2018. [Online]. Available: https://www.sciencedirect.com/science/article/pii/S0960148117311461

[19] N. B. G. Brinkel, M. K. Gerritsma, T. A. AlSkaif, I. Lampropoulos, A. M. van Voorden, H. A. Fidder, and W. G. J. H. M. van Sark, "Impact of rapid PV fluctuations on power quality in the low-voltage grid and mitigation strategies using electric vehicles," *International Journal of Electrical Power & Energy Systems*, vol. 118, p. 105741, Jun. 2020. [Online]. Available: https://www.sciencedirect.com/science/article/pii/S0142061519319994

[20] Netbeheer Nederland, "Achtergronddocument-Spanningskwaliteit in Nederland," 2019.

[21] M. Verhoog, N. Brinkel, and T. Alskaif, "Congestion Management in LV Grids Using Static and Dynamic EV Smart Charging," in *2020 International Conference on Smart Energy Systems and Technologies (SEST)*, Sep. 2020, pp. 1–6.

[22] M. JUAMPEREZ, G. Yang, and S. KJÆR, "Voltage regulation in LV grids by coordinated volt-var control strategies," *J. Mod. Power Syst. Clean Energy*, vol. 2, pp. 319–328, Dec. 2014.

[23] M. T. Hussain, D. N. B. Sulaiman, M. S. Hussain, and M. Jabir, "Optimal Management strategies to solve issues of grid having Electric Vehicles (EV): A review," *Journal of Energy Storage*, vol. 33, p. 102114, Jan. 2021. [Online]. Available: https://linkinghub.elsevier.com/retrieve/pii/S2352152X20319435

[24] European Automobile Manufacturers' Association, "Risk of two-track Europe for e-mobility with sharp divisions in roll-out of chargers, auto industry warns," Jun. 2021. [Online]. Available: https://www.acea.auto/press-release/risk-of-two-track-europe-for-e-mobility-with-sharp-divisions-in-roll-out-of-chargers-auto-industry-warns/

[25] William Visser, "Laden van elektrische voertuigen," Rijksdienst voor Ondernemend Nederland, Utrecht, Tech. Rep., 2019.

[26] Y. Yu, D. Reihs, S. Wagh, A. Shekhar, D. Stahleder, G. Mouli, F. Lehfuss, and P. Bauer, "Data-Driven Study of LV Distribution Grid Behaviour with Increasing Electric Vehicle Penetration," *IEEE Access*, vol. PP, pp. 1–1, Jan. 2022.

[27] J. Hildermeier, C. Kolokathis, J. Rosenow, M. Hogan, C. Wiese, and A. Jahn, "Start with smart: Promising practices for integrating electric vehicles into the grid," Brussels, Belgium, Regulatory Assistance Project (RAP)®, Apr. 2019.

[28] J. García-Villalobos, I. Zamora, J. I. San Martín, F. J. Asensio, and V. Aperribay, "Plug-in electric vehicles in electric distribution networks: A review of smart charging approaches," *Renewable and Sustainable Energy Reviews*, vol. 38, pp. 717–731, Oct. 2014. [Online]. Available: https://www.sciencedirect.com/science/article/pii/S1364032114004924

[29] Next Kraftwerke, "Next Kraftwerke and Jedlix launch initiative to use electric car batteries for grid stability." [Online]. Available: https://www.next-kraftwerke.be/en/next-kraftwerke-and-jedlix-launch-initiative-to-use-electric-car-batteries-for-grid-stability/

[30] A. Sáez Armenteros, H. de Heer, and M. van der Laan, "Flexibility Deployment in Europe," USEF, White Paper 1, 2021.

[31] N. B. G. Brinkel, W. L. Schram, T. A. AlSkaif, I. Lampropoulos, and W. G. J. H. M. van Sark, "Should we reinforce the grid? Cost and emission optimization of electric vehicle charging under different transformer limits," *Applied Energy*, vol. 276, p. 115285, Oct. 2020. [Online]. Available: https://www.sciencedirect.com/science/article/pii/S0306261920307972

[32] S. Uimonen, "EV Charging Simulator," 2020. [Online]. Available: https://version.aalto.fi/gitlab/power_systems_research_group_aalto

[33] DIgSILENT, "PowerFactory - DIgSILENT." [Online]. Available: https://www.digsilent.de/en/powerfactory.html

[34] Z. Yang, K. Li, and A. Foley, "Computational scheduling methods for integrating plug-in electric vehicles with power systems: A review," *Renewable and Sustainable Energy Reviews*, vol. 51, pp. 396–416, Nov. 2015. [Online]. Available: https://linkinghub.elsevier.com/retrieve/pii/S1364032115005778

[35] S. Limmer, "Dynamic Pricing for Electric Vehicle Charging—A Literature Review," *Energies*, vol. 12, no. 18, p. 3574, Jan. 2019, number: 18 Publisher: Multidisciplinary Digital Publishing Institute. [Online]. Available: https://www.mdpi.com/1996-1073/12/18/3574

[36] N. Leemput, F. Geth, J. Van Roy, J. Büscher, and J. Driesen, "Reactive power support in residential LV distribution grids through electric vehicle charging," *Sustainable Energy, Grids and Networks*, vol. 3, pp. 24–35, Sep. 2015. [Online]. Available: https://linkinghub.elsevier.com/retrieve/pii/S2352467715000375

[37] R. Fachrizal, M. Shepero, D. van der Meer, J. Munkhammar, and J. Widén, "Smart charging of electric vehicles considering photovoltaic power production and electricity consumption: A review," *eTransportation*, vol. 4, p. 100056, 2020. [Online]. Available: https://www.sciencedirect.com/science/article/pii/S2590116820300138

[38] H. Das, M. Rahman, S. Li, and C. Tan, "Electric vehicles standards, charging infrastructure, and impact on grid integration: A technological review," *Renewable and Sustainable Energy Reviews*, vol. 120, p. 109618, Mar. 2020. [Online]. Available: https://linkinghub.elsevier.com/retrieve/pii/S1364032119308251

[39] Y. Wang, T. John, and B. Xiong, "A two-level coordinated voltage control scheme of electric vehicle chargers in low-voltage distribution networks," *Electric Power Systems Research*, vol. 168, pp. 218–227, 2019. [Online]. Available: https://www.sciencedirect.com/science/article/pii/S0378779618304024

[40] J. de Hoog, D. A. Thomas, V. Muenzel, D. C. Jayasuriya, T. Alpcan, M. Brazil, and I. Mareels, "Electric vehicle charging and grid constraints: Comparing distributed and centralized approaches," in *2013 IEEE Power Energy Society General Meeting*, Jul. 2013, pp. 1–5, iSSN: 1932-5517.

[41] N. Nimalsiri, E. Ratnam, D. Smith, C. Mediwaththe, and S. Halgamuge, "Distributed Optimization-based Electric Vehicle Charging and Discharging in Unbalanced Distribution Grids," Nov. 2021, publisher: TechRxiv. [Online]. Available: https://www.techrxiv.org/articles/preprint/Distributed_Optimization-based_Electric_Vehicle_Charging_and_Discharging_in_Unbalanced_Distribution_Grids/16920889/1

[42] N. I. Nimalsiri, E. L. Ratnam, C. P. Mediwaththe, D. B. Smith, and S. K. Halgamuge, "Coordinated charging and discharging control of electric vehicles to manage supply voltages in distribution networks: Assessing the customer benefit," *Applied Energy*, vol. 291, p. 116857, Jun. 2021. [Online]. Available: https://www.sciencedirect.com/science/article/pii/S0306261921003470

[43] Elke Klaassen, M. van der Laan, H. de Heer, J. van Heesbeen, and N. Hubbers, "Case study: practical deployment of electric vehicle flexibility," USEF, Case Study 1, 2020.

[44] A. Goldoust and Masoud Esmaili, "Multi-objective optimal charging of plug-in electric vehicles in unbalanced distribution networks," *International Journal of Electrical Power & Energy Systems*, vol. 73, pp. 644–652, Dec. 2015.

[45] M. Baran and F. Wu, "Optimal sizing of capacitors placed on a radial distribution system," *IEEE Transactions on Power Delivery*, vol. 4, no. 1, pp. 735–743, Jan. 1989, conference Name: IEEE Transactions on Power Delivery.

[46] J. de Hoog, T. Alpcan, M. Brazil, D. A. Thomas, and I. Mareels, "Optimal Charging of Electric Vehicles Taking Distribution Network Constraints Into Account," *IEEE Transactions on Power Systems*, vol. 30, no. 1, pp. 365–375, Jan. 2015, conference Name: IEEE Transactions on Power Systems.

[47] C. Sabillon, J. Franco, M. J. Rider, and R. Romero, "Joint optimal operation of photovoltaic units and electric vehicles in residential networks with storage systems: A dynamic scheduling method," *International Journal of Electrical Power & Energy Systems*, vol. 103, pp. 136–145, Dec. 2018.

[48] F. Carlos, J. Franco, M. J. Rider, and R. Romero, "A MILP model for optimal charging coordination of storage devices and electric vehicles considering V2G technology," *2015 IEEE 15th International Conference on Environment and Electrical Engineering, EEEIC 2015 - Conference Proceedings*, pp. 60–65, Jul. 2015.

[49] Z. Yi, D. Scoffield, J. Smart, A. Meintz, M. Jun, M. Mohanpurkar, and A. Medam, "A highly efficient control framework for centralized residential charging coordination of large electric vehicle populations," *International Journal of Electrical Power & Energy Systems*, vol. 117, p. 105661, May 2020. [Online]. Available: https://linkinghub.elsevier.com/retrieve/pii/S0142061519321775

[50] X. Chen, K.-C. Leung, A. Y. S. Lam, and D. J. Hill, "Online Scheduling for Hierarchical Vehicle-to-Grid System: Design, Formulation, and Algorithm," *IEEE Transactions on Vehicular Technology*, vol. 68, no. 2, pp. 1302–1317, Feb. 2019, conference Name: IEEE Transactions on Vehicular Technology.

[51] S. Zhan, J. Morren, W. v. d. Akker, A. van der Molen, and H. Slootweg, "Optimal Real-time Coordination of Distributed Energy Resources in Low-voltage Grids," *arXiv:2105.01750 [cs, eess]*, May 2021, arXiv: 2105.01750. [Online]. Available: http://arxiv.org/abs/2105.01750

[52] L. Thurner, A. Scheidler, F. Schäfer, J. Menke, J. Dollichon, F. Meier, S. Meinecke, and M. Braun, "pandapower — an open-source python tool for convenient modeling, analysis, and optimization of electric power systems," *IEEE Transactions on Power Systems*, vol. 33, no. 6, pp. 6510–6521, Nov 2018.

[53] J. Quiros-Tortos, L. Ochoa, S. Alnaser, and T. Butler, "Control of EV Charging Points for Thermal and Voltage Management of LV Networks," *IEEE Transactions on Power Systems*, vol. 31, pp. 3028–3039, Jul. 2016.

[54] M. Zhang and X. Fan, "Review on the State of Charge Estimation Methods for Electric Vehicle Battery," *World Electric Vehicle Journal*, vol. 11, no. 1, p. 23, Mar. 2020, number: 1 Publisher: Multidisciplinary Digital Publishing Institute. [Online]. Available: https://www.mdpi.com/2032-6653/11/1/23

[55] N. E. D. Uitwisseling, "Verbruiksprofielen - NEDU," 2021. [Online]. Available: https://www.nedu.nl/documenten/verbruiksprofielen/#

[56] Gemeente Utrecht, "Warmteprofielen." [Online]. Available: https://gemu.maps.arcgis.com/apps/webappviewer/index.html?id=29405f456112454d9312462a84deb81d

[57] Gasunie, "Gasunie Verkenning 2050," Groningen, Tech. Rep., 2018. [Online]. Available: https://www.gasunie.nl/expertise/aardgas/de-energietransitie-en-de-rol-van-aardgas

[58] J. Love, A. Z. P. Smith, S. Watson, E. Oikonomou, A. Summerfield, C. Gleeson, P. Biddulph, L. F. Chiu, J. Wingfield, C. Martin, A. Stone, and R. Lowe, "The addition of heat pump electricity load profiles to GB electricity demand: Evidence from a heat pump field trial," *Applied Energy*, vol. 204, pp. 332–342, Oct. 2017. [Online]. Available: https://www.sciencedirect.com/science/article/pii/S0306261917308954

[59] Western Power Distribution, "Changing Load Profiles," Western Power Distribution, Tech. Rep. [Online]. Available: https://www.westernpower.co.uk/smarter-networks/network-strategy/dsof

[60] NREL, "PVWatts Calculator." [Online]. Available: https://pvwatts.nrel.gov/pvwatts.php

[61] PwC, "Smart Charging of electric vehicles Institutional bottlenecks and possible solutions," Elaad, Tech. Rep., 2017. [Online]. Available: https://www.elaad.nl/uploads/files/201710-_PwC_Smart_Charging_rapport_Final_STC_ENG.pdf

[62] D. Hall and N. Lutsey, "Charging infrastructure in cities: Metrics for evaluating future needs," The International Council on Clean Transportation, Tech. Rep. 17, Aug. 2020. [Online]. Available: https://theicct.org/sites/default/files/publications/EV-charging-metrics-aug2020.pdf

[63] Centraal Bureau voor de Statistiek, "Kerncijfers wijken en buurten 2019," Jul. 2019, last Modified: 2019-07-30T08:11:00+00:00. [Online]. Available: https://www.cbs.nl/nl-nl/maatwerk/2019/31/kerncijfers-wijken-en-buurten-2019

[64] S. Uimonen and M. Lehtonen, "Simulation of Electric Vehicle Charging Stations Load Profiles in Office Buildings Based on Occupancy Data," *Energies*, vol. 13, no. 21, p. 5700, Jan. 2020, number: 21 Publisher: Multidisciplinary Digital Publishing Institute. [Online]. Available: https://www.mdpi.com/1996-1073/13/21/5700

[65] Centraal Bureau voor de Statistiek, "Woon-werkafstanden 2016," Mar. 2018, last Modified: 2018-03-14T23:01:00+00:00. [Online]. Available: https://www.cbs.nl/nl-nl/achtergrond/2018/11/woon-werkafstanden-2016

[66] N. O'Connell, Q. Wu, J. Østergaard, A. H. Nielsen, S. T. Cha, and Y. Ding, "Day-ahead tariffs for the alleviation of distribution grid congestion from electric vehicles," *Electric Power Systems Research*, vol. 92, pp. 106–114, Nov. 2012. [Online]. Available: https://www.sciencedirect.com/science/article/pii/S037877961200168X

[67] European Union, "Regulation (EU) 2019/943 of the European Parliament and of the Council of 5 June 2019 on the internal market for electricity (Text with EEA relevance.)," Jun. 2019, legislative Body: EP, CONSIL. [Online]. Available: http://data.europa.eu/eli/reg/2019/943/oj/eng

[68] E. D. Kostopoulos, G. C. Spyropoulos, and J. K. Kaldellis, "Real-world study for the optimal charging of electric vehicles," *Energy Reports*, vol. 6, pp. 418–426, Nov. 2020. [Online]. Available: https://www.sciencedirect.com/science/article/pii/S2352484719310911

[69] W. Schram, N. Brinkel, G. Smink, T. van Wijk, and W. van Sark, "Empirical Evaluation of V2G Round-trip Efficiency," in *2020 International Conference on Smart Energy Systems and Technologies (SEST)*, Sep. 2020, pp. 1–6.

[70] M. Barni, F. Buti, F. Bartolini, and V. Cappellini, "A quasi-Euclidean norm to speed up vector median filtering," *IEEE Transactions on Image Processing*, vol. 9, no. 10, pp. 1704–1709, Oct. 2000, conference Name: IEEE Transactions on Image Processing.

[71] N. Goedegebure and R. Hennig, "Generating Electricity Price Forecasting Scenarios to Analyze Whether Price Uncertainty Impacts Tariff Performance," in *2022 17th International Conference on Probabilistic Methods Applied to Power Systems (PMAPS)*, Jun. 2022, pp. 1–6, iSSN: 2642-6757.

[72] NOS, "'Laadpaalklevers' riskeren boete van 95 euro," Apr. 2022. [Online]. Available: https://nos.nl/l/2424805

Appendix A

Network Characteristics

Power & voltage quality standards

Table A-1: Power quality standards as defined in EN 50160 during normal operation of the network [10, 11].

Parameter	Limit	Possible Causes of Violation
	Continuous Phenomena	
Supply Voltage	$V_0 \pm 10\%$ *	▪ High cable resistance ▪ High currents
Flicker	$P_{lt} \leq 1$ for 95% of all cases in 1 week	▪ High level of Photovoltaics (PV) combined with cloud transients [19]
Voltage Unbalance	$V_n \ \Delta \max 2$ % of V_p *	▪ Unequal connection of loads and Distributed Generators (DG) to single phase
Voltage harmonics	▪ Each harmonic below predefined relative amplitude * ▪ THD $\leq 8\%$ for harmonics between 2 and 40	▪ Injection by Power Electonic Interfaces (PEI) ▪ Non-linear loads
	Voltage Events	
Voltage dips/ swells	Thresholds: dip at 90% and swell at 110% **	▪ Faults at public network/ user installation
	Other non-voltage related quality issues	
Current Harmonics	Same as with voltage harmonics	▪ Injection by PEI ▪ Non-linear loads
Frequency Deviations	▪ $\pm$ 1% of 50 Hz for 99.9% ▪ -6% - +4% for 100%	▪ Supply-Demand unbalance

* for 95% of all 10 min mean RMS in 1 week. ** Classification depends on time duration and offset.

Cable types

Table A-2: Overview of cable types the investigated Dutch LV grid.

Cable type	Share of Total Cable Length [%]	Max. capacity (in ground) [A]
GPLK 4x6mm Curm	1.02	52
GPLK 4x25mm Curm	32.41	125
GPLK 4x50mm Cusvm	11.42	175
GPLK 4x70mm Cusvm	29.54	220
GPLK 4x95mm Cusvm	5.68	265
4x50mm VVMvKhas/Alk 4x6	7.96	130
4x95mm VVMvKhas/Alk 4x6	2.13	200
4x150mm VVMvKhas/Alk 4x6	9.85	260

Location of PV and Chargers 2050

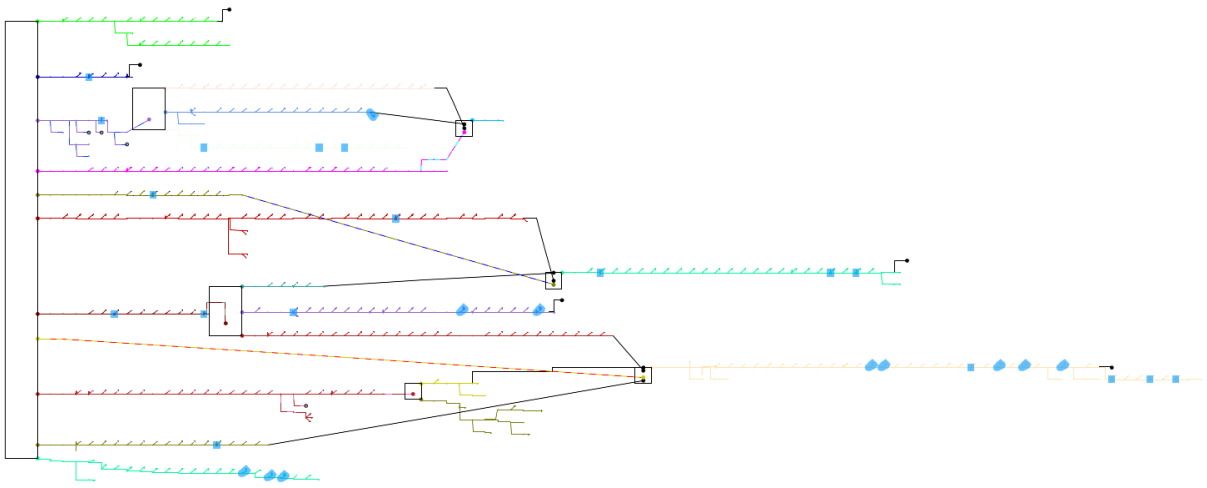

Figure A-1: Position of PV systems 2050 by blue markers.

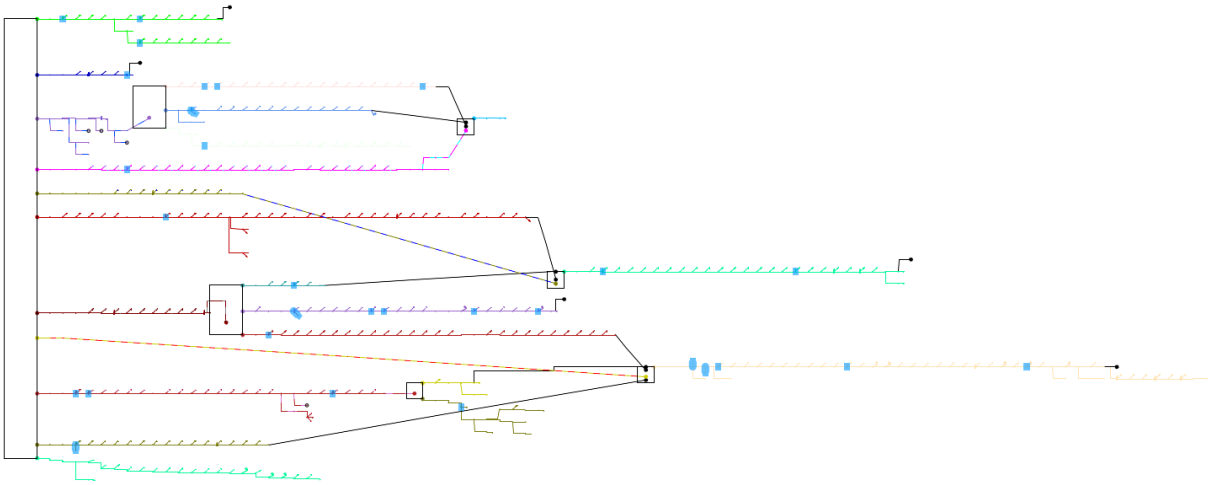

Figure A-2: Position of EV chargers 2050 by blue markers.

Appendix B

Additional Scenario Results

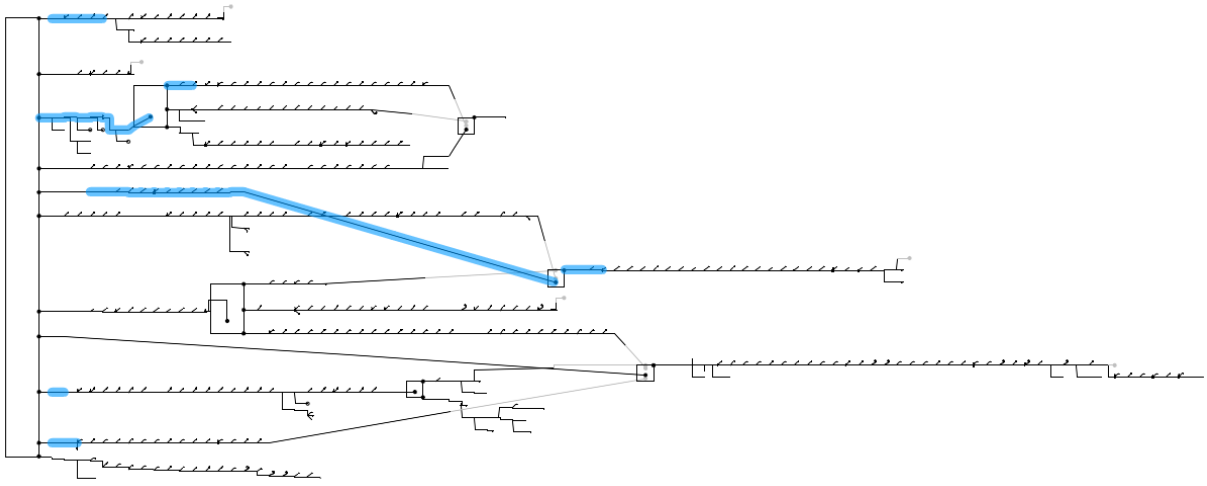

Figure B-1: Lines of the LV grid that experience congestion after the implementation of grid constraints on feeder 7.

Appendix C

Python Project Overview

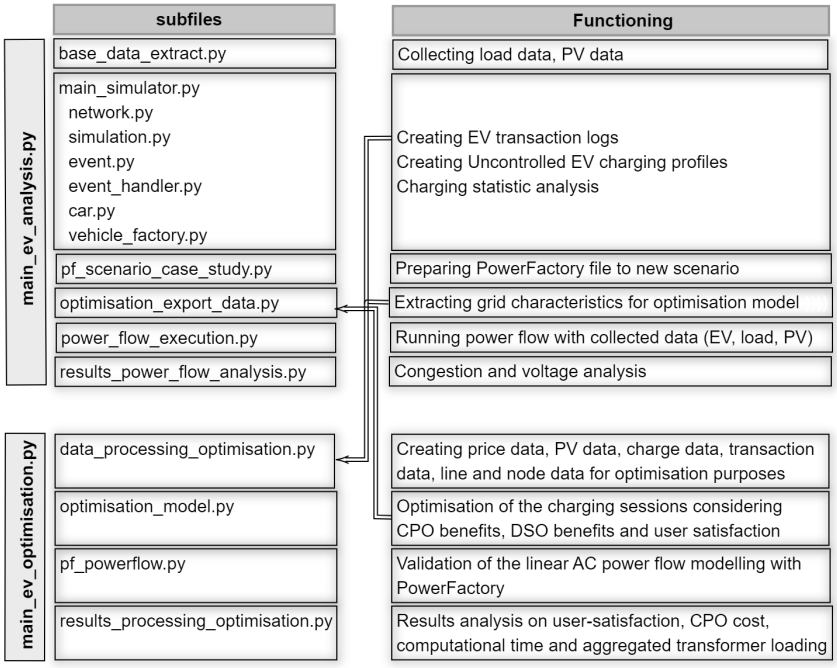

Figure C-1: Overview of the scripts belonging in this thesis work. Two main projects are made, each with a main-file and corresponding sub-files. The interdependencies between the projects are also indicated.

Appendix D

Linear AC- Optimal Power Flow Formulation

The equations below describe the mathematical formulation of the AC-power flow in the grid. All the equations and the theory behind it are based on [4]. Refer again to Table 4-2 to get an overview of the used symbols.

$$\mathbf{I}^{S}_{t,b} - \sum_{p \in \Omega_{\mathrm{P}}: p=b} \mathbf{I}^{c}_{t,p} - \mathbf{I}^{inflex}_{t,b} = \sum_{j \in \Omega_{\mathrm{B}}} \mathbf{Y}_{(b,j)} \mathbf{V}_{t,j} \quad \forall b \in \Omega_{\mathrm{B}}, t \in \Omega_{\mathrm{T}} \tag{D-1}$$

$$P^{S}_{t,b} = \mathfrak{Re}\left\{ \mathbf{V}^{\top}_{t,b} \mathbf{I}^{S*}_{t,b} \right\}, \quad \forall b \in \Omega_{\mathrm{B}}, t \in \Omega_{\mathrm{T}} : b = s \tag{D-2}$$

$$\mathbf{I}^{inflex^{*}}_{t,b} = \mathrm{diag}\left(\mathbf{V}_{t,b}\right)^{-1} \mathbf{S}^{\mathrm{inflex}}_{t,b} \quad \forall b \in \Omega_{\mathrm{B}}, t \in \Omega_{\mathrm{T}} \tag{D-3}$$

$$P_{t,c} = \mathfrak{Re}\left\{ \mathbf{V}^{\top}_{t,p} \mathbf{I}^{c^{*}}_{t,p} \right\}, \quad \forall c \in \Omega_{\mathrm{C}}, t \in \Omega_{\mathrm{T}} \tag{D-4}$$

$$Q_{t,c} = \mathfrak{Im}\left\{ \mathbf{V}^{\top}_{t,p} \mathbf{I}^{c^{*}}_{t,p} \right\}, \quad \forall c \in \Omega_{\mathrm{C}}, t \in \Omega_{\mathrm{T}} \tag{D-5}$$

$$\mathbf{I}_{t,l} = \left[\mathbf{Y}_{(b,j)}\right] \left(\mathbf{V}_{t,b} - \mathbf{V}_{t,j}\right), \quad \forall l \in \Omega_{\mathrm{L}}, \quad (b,j) = l \tag{D-6}$$

$$|Q_{t,c}| \leq P_{t,c} \tan\left(\cos^{-1}\left(\mathrm{pf}_c\right)\right), \forall c \in \Omega_{\mathrm{C}}, t \in \Omega_{\mathrm{T}} \tag{D-7}$$

Due to very slow optimisation related to non-linearities, the OPF is modelled to a linear form with the equations below.

First of all the grid current injected by PV or non-EV loads is approximated by Taylor series expansion as seen in Equation (D-8). To be able to get estimated values for $\mathbf{V}^0_{t,k,\phi}$ historical values can be used with a three-phase power flow analysis. Another option is to use a flat-start, assuming $\mathbf{V}^0_{t,k,\phi}$ to be equal to the nominal tap voltage (eg. 1 p.u.). In this study, the initialised values were derived by running the power flow simulations in PF containing the forecasted non-EV load and PV generation only. With this approximated voltage, also the apparent active and reactive power of the charging points can be linearised. This is shown by Equations (D-9) and (D-10) [4].

$$\mathrm{I}^{inflex}_{t,k,\phi} \approx \mathrm{I}^{inflex}_{t,k,\phi}\Big|_{\mathbf{V}^0_{t,k,\phi}} + \left.\frac{\partial \mathrm{I}^{\mathrm{inflex}}_{t,k,\phi}}{\partial \mathrm{V}_{t,k,\phi}}\right|_{\mathbf{V}^0_{t,k,\phi}} \left(\mathrm{V}_{t,k,\phi} - \mathrm{V}^0_{t,k,\phi}\right) \quad \forall k \in \Omega_{\mathrm{B}}, t \in \Omega_{\mathrm{T}}, \phi \in \Omega_{\Phi} \tag{D-8}$$

$$P_{t,c} \approx \mathfrak{Re}\left\{\mathbf{V}^0_{t,p}\mathbf{I}^{c^*}_{t,p}\right\}, \quad \forall c \in \Omega_{\mathrm{C}}, t \in \Omega_{\mathrm{T}}, p \in \Omega_{\mathrm{P}} \tag{D-9}$$

$$Q_{t,c} \approx \mathfrak{Im}\left\{\mathbf{V}^0_{t,p}\mathbf{I}^{c^*}_{t,p}\right\}, \quad \forall c \in \Omega_{\mathrm{C}}, t \in \Omega_{\mathrm{T}}, p \in \Omega_{\mathrm{P}} \tag{D-10}$$

To derive the **norm of the branch currents**, a new euclidean norm approximation was applied by [4]. The equations related to this norm approximations are (D-11), (D-12). The coefficients A_n, B_n and C_n are given by Equations (D-13), (D-14) and (D-15) respectively. The final euclidean norm of the branch current is approximately equal to the maximum of the parameter ($\Gamma_{t,l,\phi,n}$) as calculated in (D-11) [4].

$$\Gamma_{t,l,\phi,n} = \left(i^{\mathrm{r}}_{t,l,\phi}\mathrm{A}_n + i^{\mathrm{i}}_{t,l,\phi}\mathrm{B}_n\right)/\mathrm{C}_n, \quad \forall l \in \Omega_{\mathrm{L}}, n \in \Omega_{\mathrm{N}}, t \in \Omega_{\mathrm{T}}, \phi \in \Omega_{\Phi} \tag{D-11}$$

$$\Gamma_{t,l,\phi,n} \leq \bar{\mathrm{I}}_l, \quad \forall l \in \Omega_{\mathrm{L}}, n \in \Omega_{\mathrm{N}}, t \in \Omega_{\mathrm{T}}, \phi \in \Omega_{\Phi} \tag{D-12}$$

$$\mathrm{A}_n = \sin(\theta n - \theta) - \sin(n\theta) \tag{D-13}$$

$$\mathrm{B}_n = \cos(n\theta) - \cos(\theta n - \theta) \tag{D-14}$$

$$\mathrm{C}_n = \cos(n\theta)\sin(\theta n - \theta) - \cos(\theta n - \theta)\sin(n\theta) \tag{D-15}$$

$$\left\|\mathrm{I}_{t,l,\phi}\right\|_2 \approx \max_{n\in\Omega_\mathrm{N}} \left\{\Gamma_{t,l,\phi,n}\right\} \tag{D-16}$$

The approximation for the euclidean **norm of the nodal voltages** are approximated by a linear combination of the 1-norm and ∞-norm as seen in formula (D-17) [4].

$$\begin{aligned}\Psi\left(\mathrm{V}_{t,b,\phi}\right) = \lambda_\phi \left\|\mathrm{V}_{t,b,\phi}\right\|_\infty + \beta_\phi \left\|\mathrm{V}_{t,b,\phi}\right\|_1, \quad \forall b \in \Omega_\mathrm{B}, t \in \Omega_\mathrm{T}, \phi \in \Omega_\Phi \\ \text{with} \quad \mathrm{V}_{t,b,\phi} = v^\mathrm{r}_{t,b,\phi} + \mathrm{j}v^\mathrm{i}_{t,b,\phi}\end{aligned} \tag{D-17}$$

The factors λ_ϕ and β_ϕ can be obtained by regression techniques, approximating $\Psi\left(\mathrm{V}_{t,k,\phi}\right)$ properly. To reduce the approximation errors for phases $\phi = \{b, c\}$ (due to its location in the complex plane), the authors of [4] rotated the phases reducing the error significantly. The rotated phases also results in λ_ϕ and β_ϕ to be equal for all phases $\phi = \{a, b, c\}$. The final regression functions of λ_ϕ and β_ϕ are shown in Equations (D-18) and (D-19) [4].

$$\lambda(\Theta) = \frac{-2315 \cdot 10^{-5}}{907}\Theta^2 - \frac{13}{1490}\Theta + 1 \tag{D-18}$$

$$\beta(\Theta) = \frac{819 \cdot 10^{-8}}{394}\Theta^2 + \frac{58}{6647}\Theta + \frac{349 \cdot 10^{-5}}{691} \tag{D-19}$$

As can be derived from Equations (D-18) and (D-19), both of them depend on parameter Θ. This Θ denotes the range angle, which is related to the deviations of the magnitudes of the phase voltages to the nominal voltage. Choosing a proper range angle can tighten up the nodal voltage approximations. Figure D-1 indicates clearly how this range angle can be interpreted and how the rotations are being performed [4].

With the coefficients λ and β defined, the parameter $\Psi\left(\mathcal{V}_{t,b,\phi}\right)$ is the one that is restricted by the minimum and maximum allowed normalised voltages. That is shown by Equation (D-20). The symbol $\mathcal{V}_{t,b,\phi}$ stands for the rotated nodal voltages and equals $\mathcal{V}_{t,b\phi} = \mathrm{V}_{t,b,\phi}\mathcal{J}_\phi$, with $\mathcal{J}_\phi = \left\{1, \alpha, \alpha^2\right\}$ being the rotation coefficients. As a consequence, the real part of $\mathcal{V}_{t,b,\phi}$ is always bigger or equal to zero. This can also be seen in Figure D-1. Furthermore, that allows to reformulate Equation (D-17) as Equation (D-21) [4].

$$\underline{\mathrm{V}} \leq \Psi\left(\mathcal{V}_{t,b,\phi}\right) \leq \overline{\mathrm{V}}, \quad \forall b \in \Omega_\mathrm{B}, t \in \Omega_\mathrm{T}, \phi \in \Omega_\Phi \tag{D-20}$$

$$\begin{aligned}\Psi\left(\mathcal{V}_{t,b,\phi}\right) = \lambda\mathfrak{Re}\left\{\mathcal{V}_{t,b,\phi}\right\} + \beta\left(\mathfrak{Re}\left\{\mathcal{V}_{t,b,\phi}\right\} + \left|\mathfrak{Im}\left\{\mathcal{V}_{t,b,\phi}\right\}\right|\right) \\ \forall b \in \Omega_\mathrm{B}, t \in \Omega_\mathrm{T}, \phi \in \Omega_\Phi\end{aligned} \tag{D-21}$$

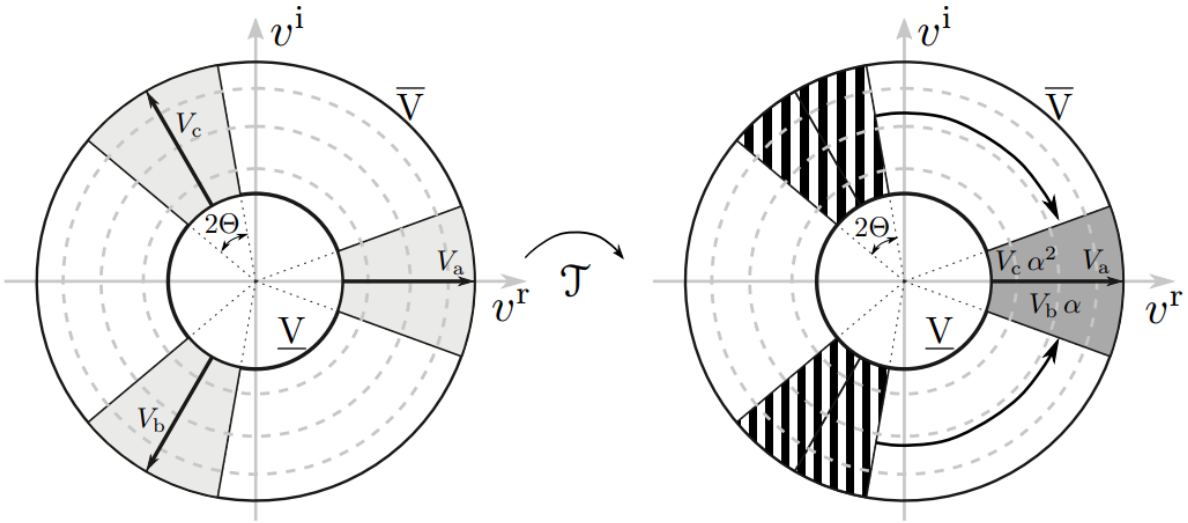

Figure D-1: Representation of rotated voltage magnitudes, limits and range angle Θ [4].

Appendix E

Battery Degradation Modelling

This thesis work contains the benefits of V2G to EV-users in relation to the grid. That means that when grid constraints are becoming more restricting, V2G may help in allowing more users to reach their desired SOC. However, so far no attention was paid at the downsides of V2G. Bidirectional charging may involve more cycles and thus higher degradation rates of the battery. Many papers try to find sophisticated ways to related the cycle effect to battery deterioration; however, few do include this in a smart charging algorithm. To take battery degradation into account in a smart charging model, a penalty term can be included in the objective function. In [31], this was achieved by multiplying the cost of the battery with a dimensionless degradation function. The latter contains the degradation per cycle which depends on the cycle depth. The function was established with the help of previous experimental research found in literature. The degradation function found by [31] including the regression coefficients is shown in Equation (E-1):

$$\Phi(\delta_{t,c}) = \frac{0.5}{b\delta^{m-1}} = \frac{0.5}{4084 \quad \delta^{-0.7514-1}} \tag{E-1}$$

, with δ representing the cycle depth and $\Phi(\delta_{t,c})$ the dimensionless degradation at time t and charging point c. The approach of this paper was applied due to the ease of integration in a smart charging model and the (piece-wise) linearisation of the adopted formula. Due to a lack of time, the formula applied in this work was linearised without piece-wise linearisation. This resulted in the following Equation (E-2). The deviations from the non-linear Equation (E-1) is displayed in Figure E-1.

$$\Phi(\delta_{t,c}) = 9.787 * 10^{-5}\delta \tag{E-2}$$

Next, a new function was implemented in the optimisation model that relates the state-of-charge to the dimensionless degradation. This function is contained in Equation (E-3)

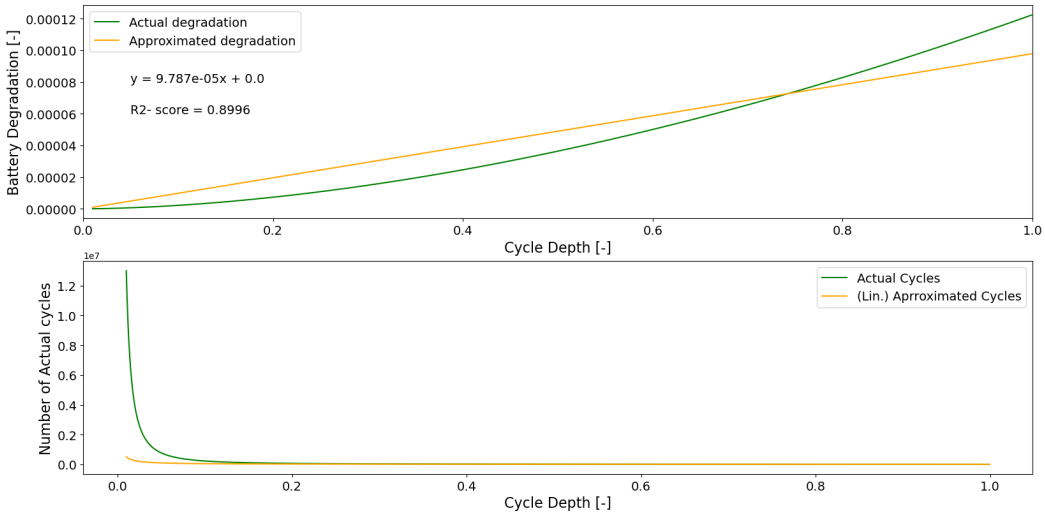

Figure E-1: Linearisation of the battery degradation function (top figure). Corresponding actual cycles for a certain cycle depth (bottom figure).

$$\Phi(\delta_{t,c}) = 9.787 * 10^{-5} \left((SOC_{t,c} - SOC_{t-1,c})\mu^{\text{charge}} + (SOC_{t-1,c} - SOC_{t,c})\mu^{\text{discharge}} \right) \tag{E-3}$$

This function is again linear. Nevertheless, it contains two binary variables μ^{charge} and $\mu^{\text{discharge}}$. Equations (E-4),(E-5) express their relation to each other and to the decision variable, which is split in a charging and discharging term. This transforms the problem into a mixed-integer optimisation problem (MILP). For that reason also discharging and charging efficiencies could be implemented in Equation (4-6). This can be seen in formula (E-7).

$$\mu^{\text{charge}} + \mu^{\text{discharge}} = 1 \tag{E-4}$$

$$P_{t,c}^{\text{charge}} \mu^{\text{charge}} + P_{t,c}^{\text{discharge}} \mu^{\text{discharge}} = P_{t,c} \tag{E-5}$$

$$\begin{cases} \mathrm{SOC_{t,c}} = \mathrm{SOC_c^{init}} \iff \mathrm{t} = 1 & \text{(E-6)} \\ \mathrm{SOC_{t,c}} = \mathrm{SOC_{t-1,c}} + \dfrac{(\mathrm{P_{t-1,c}^{charge}} \mu^{\text{charge}} \eta^{\text{charge}} + \mathrm{P_{t-1,c}^{discharge}} \mu^{\text{discharge}} \eta^{\text{discharge}}) \Delta \mathrm{t}}{\overline{\mathrm{E_c}}} \overline{\mathrm{P}}^{\text{grid}} \quad \forall t : 1 < t < t_c^{\text{dep}} & \text{(E-7)} \end{cases}$$

Eventually, an extra term to discourage too many cycles during a charging session was introduced in the objective function (4-2). This leads to Equation (E-8). However, due to the multi-objective optimisation formulation, a

more careful look should be devoted to find the optimal trade-off between all objective terms. This could be accomplished by analysing the Pareto front [34].

$$\min \left(\sum_{t \in \Omega_{\mathrm{T}}} \Delta \mathrm{t} (\mathrm{c}^{\mathrm{ll}} \mathrm{P}_t^{\mathrm{ll}} + \mathrm{c}^{\mathrm{ml}} \mathrm{P}_t^{\mathrm{ml}} + \mathrm{c}^{\mathrm{hl}} \mathrm{P}_t^{\mathrm{hl}} + \sum_{c \in \Omega_{\mathrm{C}}} \mathrm{c}_t^{\mathrm{DA}} \mathrm{P}_{t,c}) - \sum_{c \in \Omega_{\mathrm{C}}} m \alpha_c + \Phi(\delta_{t,c}) \mathrm{c}^{\mathrm{bat}} \right) \tag{E-8}$$

After running the new MILP formulation for ST, V2G and a transformer limit, the following results were obtained. Figure E-2 contains the aggregated loading at transformer level. It can be compared with Figure E-3 that does not include battery degradation. That corresponds to scenario 2.6 found at Figure 5-11. One can notice that net discharging still takes place but with smaller discharge peaks. This can be explained due the fact that deep discharge cycles are less desired and more gradual charging needs to take place. Consequently, this will result in lower aggregated discharging power. At the single EV level, the charging profiles of charge point 0 and 1 also experience less discharging. This can be seen in Figure E-4 and compared with Figure 4-2.

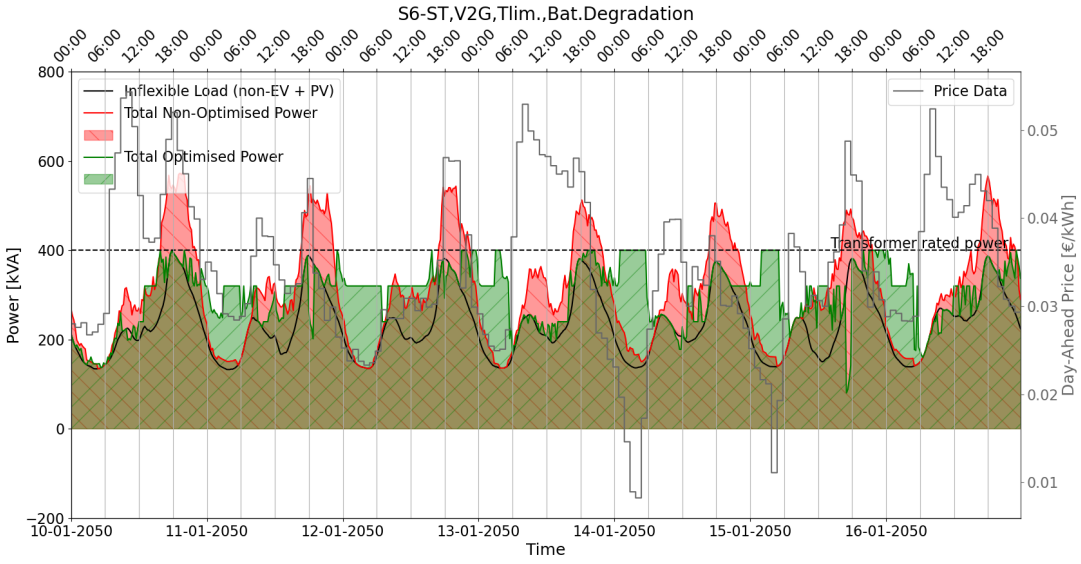

Figure E-2: Aggregated load (without losses) for scenario 2.6: ST-prices, V2G, transformer limit and battery degradation modelling.

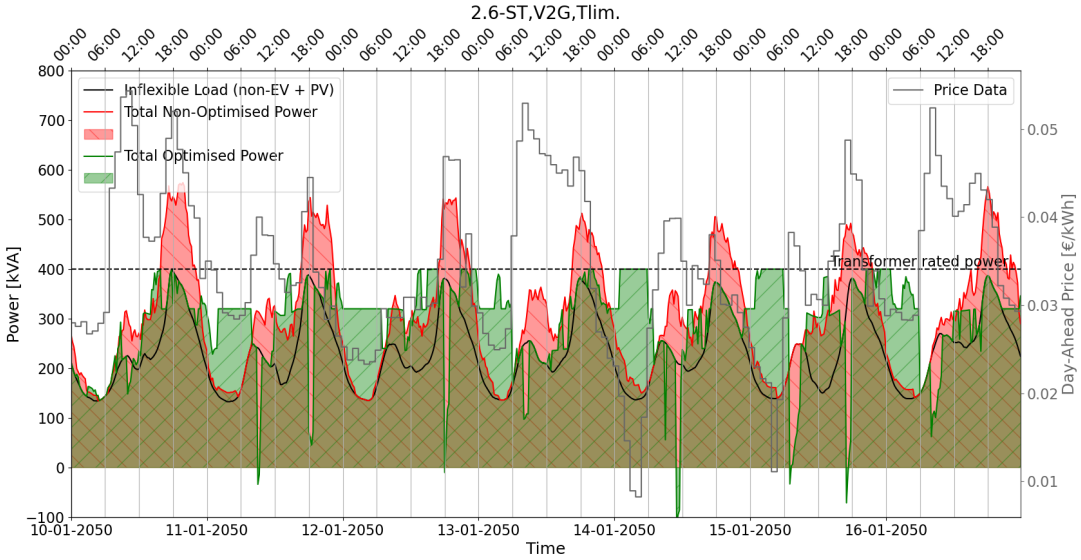

Figure E-3: Aggregated load (without losses) for scenario 2.6: ST-prices, V2G, transformer limit and **no** battery degradation modelling.

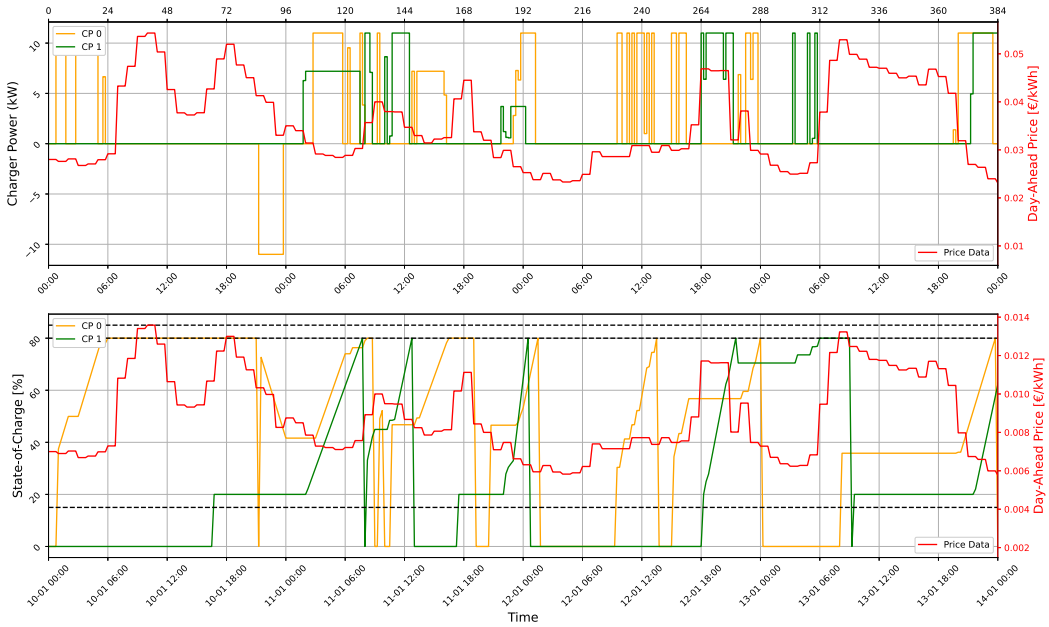

Figure E-4: Charging profiles at the charging points CP0 and CP1 including battery degradation.

The cost of the CPO were reduced with -29.58% (with battery degradation) instead of -43.34% (without battery

degradation) when compared to the uncontrolled scenario. This is slightly better than the scenario with V1G only but the difference is just 0.13%. Consequently, it is less important for a CPO to consider V2G functionality.

In terms of the EV-user, battery degradation modelling results in a dissatisfaction level of 24.92%. This is a drastic increase compared to the 0.79% of the scenario without battery degradation modelling. Nevertheless, the average dissatisfaction is still 92.95% meaning that most charging sessions still reach an acceptable SOC level.

The computational time did not increase drastically. Compared to scenario 2.6, a time increase of 24.40% percent was perceived. However, when allowing grid constraints, this would be 44.19% compared to scenario 2.7. No time was left to also perform the congestion and voltage analysis in PowerFactory to address the benefits for the DSO.

The conclusion can be made that more careful studies are needed to include the battery degradation effect of V2G. So far this section proved that including battery degradation modelling might diminish the benefits of V2G that were mentioned earlier in this work completely.